Author/s:
Xu, SanSan

Title:
Identifying and addressing limitations in deep brain stimulation for Parkinson's disease using novel neuronal biomarkers

Date:
2020

Persistent Link:
https://hdl.handle.net/11343/274847

Title: Identifying and addressing limitations in deep brain stimulation for Parkinson's disease using novel neuronal biomarkers

By

San San Xu, MBBS, FRACP

ORCID ID: orcid.org/0000-0001-5338-5934

Submitted in total fulfilment of the requirements for the degree of Doctor of Philosophy

May 2021

Medical Bionics Department,

The University of Melbourne

Abstract

Deep brain stimulation (DBS) is an effective treatment in Parkinson's disease (PD). DBS is postulated to modulate and restore 'functionality' to the pathological brain networks implicated in PD. DBS therapy improves motor symptoms and quality of life and allows for substantial medication reduction. However, there is little information on the long-term outcomes after DBS implantation including programming rates, battery changes, hardware complication surgeries or the duration of the therapy. This knowledge is crucial to inform on clinical decision making, distribution of healthcare resources and guide research direction for device development.

The first part of this thesis presents a cross-sectional, population-based study of 1849 patients with PD implanted with DBS in Australia over a 15-year period (2002-2016). Individual-level patient data was derived from three linked national government databases and the requirements for DBS care and servicing was evaluated, referenced from the time of surgery. The mean annual programming rate was 6.9 in the first year, and 2.8 annually thereafter. Over 50% of patients required repeat hardware surgery after DBS implantation. 11.3% of patients had repeat intracranial electrode surgery (including 1.1% of patients who were completely explanted). 47.6% of patients had repeat implantable pulse generator/extension-cable surgery including for presumed battery depletion. 6.2% of patients had surgery of the implantable pulse generator /extension-cable surgery within one year of any previous such surgery. 30-day post-operative mortality was 0.3% after initial DBS implantation and 0.6% after any repeat hardware surgery. The median time from DBS surgery to residential care admission was 10.2 years and, to death was 11.4 years. These findings support development of technologies to reduce therapy burden such as enhanced surgical navigation, hardware miniaturisation and improved battery efficiency.

The second part of the thesis focuses on two key contributors to DBS therapy burden, device programming and electrode redo surgery. DBS efficacy relies on the delivery of stimulation to the ideal location to achieve optimal motor benefit. This site is determined by the electrode location and the contact selected to apply DBS by the clinician. DBS programming is an arduous, time-consuming process, and highly dependent on clinician expertise. Neuronal signals have been proposed as biomarkers to assist in DBS programming and guide electrode implantation. The most widely studied signals are local field potentials (LFPs) such as beta

oscillations and high frequency oscillations (HFO). However, LFPs hold recording challenges due to their small size and low signal to noise ratio. More recently, our group has described an evoked potential, elicited by DBS, termed ‘evoked resonant neural activity’ (ERNA). ERNA is a large amplitude signal, with a characteristic decaying oscillation morphology, that is reliably recordable in patients with PD implanted with subthalamic nucleus (STN) DBS. It localises to the postulated ideal anatomical location to apply DBS, in the dorsal STN. However, the clinical relevance of ERNA and its utility compared to LFPs or electrode anatomical location is unknown.

Thus, in 50 (100 hemispheres) consecutive patients with PD implanted with STN DBS, ERNA power, beta power and HFO power was measured from each of the four contacts on the DBS lead during surgery. Neuroimaging was obtained peri-operatively to visualise each contact and determine its proximity to a nominated ideal anatomical location. The four contacts in each hemisphere were ranked from one to four according to neuronal signal power and anatomical location. In 14 patients (28 hemispheres), therapeutic stimulation was applied to each of the four contacts on the DBS lead and the degree of motor benefit measured. ERNA, beta oscillations and the anatomical location of contacts similarly predicted how motor benefit varied across contacts with STN DBS therapy. Combining ERNA, beta and HFO ranking data yielded the strongest predictive model. However, only first-ranked contacts according to ERNA delivered a motor benefit that was significantly better than at the other three contacts on the lead. Furthermore, only first-ranked ERNA contacts delivered a motor benefit that was not significantly less than the maximal available in each hemisphere.

When monopolar configuration was chosen at 6 months after DBS surgery, the clinician-chosen contact corresponded most frequently with the first-ranked ERNA contact in 81% of hemispheres compared to 71% for anatomy and 52% for beta. ERNA performed significantly better than anatomy and beta oscillations and combining data using machine learning algorithms did not improve model performance compared to using ERNA data alone. These results support the role of ERNA in guiding contact selection and assisting intra-operative electrode navigation to ultimately, reduce the treatment burden of DBS therapy.

Declaration

This is to certify that

(i) the thesis comprises only my original work towards the PhD except where indicated in the preface,

(ii) due acknowledgement has been made in the text to all other material used

(iii) the thesis is fewer than 100,000 words in length, exclusive of tables, maps, bibliographies, and appendices

San San Xu

Preface

General statement

The conception and design of the studies were undertaken in collaboration with Associate Professor Wesley Thevathasan and Professor Hugh McDermott with additional guidance from Mr Nicholas Sinclair and Dr Kristian Bulluss. I received invaluable guidance on data processing, analysis, and interpretation from Mr Nicholas Sinclair, Dr Thushara Perera, Associate Professor Tomas Kalincik and Dr Charles Malpas. I would like to acknowledge Dr Wee-Lih Lee, Mr Angus Begg and Ms Nicola Horvath for their assistance in conducting clinical assessments of participants.

I developed the study protocols and was responsible for amendments to existing ethics to conduct the studies, approved by the Human Research Ethics Committees at St Vincent's Public and Private Hospitals, Austin Hospital and Cabrini Hospital. I was responsible for patient enrolment, consent, and evaluation as well as data acquisition, documentation, and statistical analysis. I would like to acknowledge Mr Cameron Patrick from the School of Mathematics and Statistics at The University of Melbourne for his statistical advice. I wrote, revised, and submitted all manuscripts with input as outlined below. All work in this thesis was completed during the time of my candidature.

Contributions to chapters comprised of publications

Chapter 3: *Lesser known aspects of deep brain stimulation for Parkinson's disease: Programming sessions, hardware surgeries, residential care admissions and deaths*
Accepted for publication in Neuromodulation, May 2021.

The study was conceived by Associate Professor Wesley Thevathasan and Dr Kristian Bulluss. With additional guidance from Professor Hugh McDermott, we designed the outline of the study. I was solely responsible for obtaining information from the national databases and performed all data analysis and statistical analysis, with guidance from Associate Professor Tomas Kalincik and Dr Charles Malpas. Interpretation of results were conducted in collaboration with Associate Professor Wesley Thevathasan and Dr Kristian Bulluss. I wrote the first draft of the publication and contributed, in collaboration with Associate Professor

Wesley Thevathasan, to all further revisions. All other authors were involved in the critique of the article. I was responsible for revisions during the submission process. Estimate of my proportion of contributions: 80%.

Chapter 4: *Towards guided and automated programming of subthalamic area stimulation in Parkinson's disease*
Under review, May 2021.

The study was conceived with assistance from Associate Professor Wesley Thevathasan, Professor Hugh McDermott, Dr Kristian Bulluss and Mr Nicholas Sinclair. I developed the study protocol, with reviews and critique from the aforementioned contributors. I wrote and submitted the amendments to existing ethics required to conduct this trial. I was responsible for coordinating participant recruitment, acquisition of imaging data, conducting clinical assessments, documenting study data and the statistical analysis and interpretation of the results. Mr Nicholas Sinclair assisted in signal analysis. Dr Thushara Perera assisted in the analysis of brain imaging. Dr Wee-Lih Lee, Mr Angus Begg and Ms Nicola Horvath aided in the clinical assessments of participants to allow for blinded evaluations. Interpretation of results was conducted in collaboration with Associate Professor Wesley Thevathasan, Professor Hugh McDermott, Mr Nicholas Sinclair and Mr Kristian Bulluss. I wrote the first draft of the publication and contributed, in collaboration with Associate Professor Wesley Thevathasan, to all further revisions. All other authors were involved in the critique of the article. I was responsible for revisions during the submission process. Estimate of my proportion of contributions: 75%.

Chapter 5: *Can brain signals & anatomy refine contact choice for deep brain stimulation in Parkinson's disease?*
Under review, May 2021.

The study was conceived with assistance from Associate Professor Wesley Thevathasan and Professor Hugh McDermott. I wrote and submitted the amendments to existing ethics required to conduct this study. I was responsible for obtaining data, including imaging information from the patient records of Associate Professor Wesley Thevathasan and Mr Kristian Bulluss. I was responsible for the data documentation and analysis, and statistical analysis. Dr Wee-Lih Lee

and Mr Nicholas Sinclair assisted in signal analysis. Dr Thushara Perera assisted in the analysis of brain imaging. Interpretation of results was conducted in collaboration with Associate Professor Wesley Thevathasan, Professor Hugh McDermott and Dr Wee-Lih Lee. I wrote the first draft of the publication and contributed, in collaboration with Associate Professor Wesley Thevathasan, to all further revisions. All other authors were involved in the critique of the article. I was responsible for revisions during the submission process. Estimate of my proportion of contributions: 85%.

Grants

- Personal funding:
    - National Health and Medical Research Council (NHMRC) Postgraduate Scholarship 2016 – 2020
- Project funding:
    - National Health and Medical Research Council Project Grant
    - Colonial Foundation
    - St Vincent's Hospital Research Endowment Fund
    - Victoria government infrastructure program

Acknowledgments

I would like to express my sincerest appreciation and thanks to Wesley Thevathasan for his mentorship, enthusiasm, and unwavering support. I am deeply grateful to Hugh McDermott for his invaluable advice and boundless knowledge.

To Nicholas Sinclair, Thushara Perera, Wee-Lih Lee and the neurobionics team, thank you for your patience, encouragement, and endless generosity in helping me to complete this work.

To Kristian Bulluss, thank you for your guidance and valued insight.

My thanks also to Andrew Hughes, for his valued clinical mentoring, and to Deanne Dawe and the movement disorders department at the Austin Hospital, for their endless encouragement.

To the patients for their generosity and selflessness in participating in these studies.

And finally, to my family, my parents, Ping and Ming, and my friends, for their unconditional love, support and patience throughout this endeavour.

Contents

Abbreviations

ANOVA	Analysis of variance
BDM	Births, Deaths and Marriages
CEP	cortical evoked potentials
CI	confidence interval
CT	computed tomography
CV	cross validation
DBS	deep brain stimulation
ECAP	evoked compound action potentials
ERNA	evoked resonant neural activity
ET	essential tremor
FLAIR	Fluid attenuation inversion recovery
GABA	gamma-aminobutyric acid
GPe	globus pallidus pars externa
GPi	globus pallidus pars interna
HFO	high frequency oscillations
HR	hazard ratio
IPG	Implantable pulse generator
IQR	interquartile range
LED	Levodopa equivalent dose
LFP	local field potentials
LR	logisitic regression classification
LRRK2	leucine-rich repeat kinase 2
MBS	Medicare Benefits Scheme
MEM	mixed effect model
MER	microelectrode recordings
MF	motor fluctuations
MNI	Montreal Neurological Institute (referring to a standard stereotactic space)

MRI	magnetic resonance imaging
NSQIP	National Surgical Quality Improvement Program
PBS	Pharmaceutical Benefits Scheme
PD	Parkinson's disease
PPN	pedunculopontine nucleus
RF	random forest classification
RN	red nucleus
SD	standard deviation
SMD	standardised mean difference
SMR	standardised mortality ratio
SNc	substantia nigra pars compacta
SNr	substantia nigra pars reticularis
STN	subthalamic nucleus
SVM	support vector machine classification
SyN	symmetric image normalisation method
UPDRS	Unified Parkinson’s disease rating scale

List of Figures

1 Introduction and Background

1.1 Introduction

Parkinson's disease (PD) is a common neurodegenerative movement disorder with clinical features of bradykinesia, rigidity, tremor, and postural instability. Oral dopaminergic replacement therapy is the cornerstone of early symptomatic treatment. However, as the condition advances, these medications become inadequate to control the motor state. Therapies including deep brain stimulation (DBS) are introduced to address fluctuations in motor symptoms which emerge with PD progression.

DBS involves the implantation of electrodes into the deep nuclei of the brain, most commonly, the subthalamic nucleus (STN) or globus pallidus interna (GPi). Recordings in the parkinsonian brain have revealed evidence of aberrant neuronal activity and pathological synchronisation of the cortico-basal-ganglia-thalamic circuits. DBS is hypothesised to modulate this neuronal activity locally, and with downstream effects that aim to restore 'functionality' in the affected neural networks.

DBS has been shown to improve motor scores and quality of life in patients with PD. DBS is a permanent therapy, active for the duration of the patient's life, yet there are few studies that characterise the long-term outcomes after DBS implantation. Most longitudinal studies have focused on hardware complication rates in large, experienced centres. Thus, the published data is susceptible to the intrinsic biases of high volume, academic DBS services and may not accurately reflect broader DBS outcomes. Furthermore, there is a paucity of data on routine DBS maintenance (e.g. programming encounters) and the duration of community living and survival in this unique cohort of patients with PD. This is critical to guide clinical practice and inform on research priorities for device development.

The available data has highlighted weaknesses in DBS devices. The efficacy of DBS is highly contingent on the application of stimulation to an ideal location that will deliver maximal clinical benefit. This relies on the accurate implantation of electrodes during surgery, and appropriate selection of the ideal contact to apply stimulation. At present, DBS surgery utilises techniques including stereotactic guidance, intra-operative clinical assessment, and

microelectrode recordings of single cell activity to optimise surgical targeting. Despite these strategies, poorly placed electrodes account for over 40% of patients with a suboptimal response to therapy. After surgery, the clinician identifies the ideal location to apply stimulation. Optimal motor outcomes rely heavily on the quality of programming and are limited by clinician experience and time. Indeed, 40-55% of patients achieve better outcomes with expert reprogramming.

Neuronal signals measured from DBS electrodes have been proposed as a potential biomarker to guide electrode implantation and assist in DBS programming. The most widely studied are local field potentials (LFPs) such as beta oscillations or high frequency oscillations (HFO), which represent spontaneous electrical discharges from the neuronal population. More recently, our group has reported on a novel neuronal signal, elicited by DBS pulses, termed evoked resonant neural activity (ERNA). ERNA is reliably recordable in the STN region of patients with PD during DBS surgery. It localises anatomically to the ideal location to apply stimulation, in the dorsal STN, and is modulated by DBS. However, the clinical relevance of ERNA remains unexplored.

This thesis characterises DBS services in PD patients in Australia and the long-term outcomes over a 15-year period. In Chapter 3, an analysis of national databases illustrates the cost of continuing care in this cohort, highlighting the burden of electrode complication surgery and programming over the duration of DBS therapy. Chapters 4 and 5 investigate the role of neuronal signals, including ERNA, in simplifying programming and improving the accuracy of electrode placement.

1.1.1 Hypothesis

1. The burden of therapy after DBS surgery in patients with PD is high due to:
    a. Routine device maintenance requirements e.g. DBS programming, battery depletion
    b. DBS hardware complications
    c. The duration of community living and survival in PD patients after DBS surgery

2. An electrophysiological neuronal signal could reduce the burden of DBS therapy by:
    a. Guiding clinicians in DBS programming
    b. Improving the accuracy of electrode placement during DBS implantation surgery

1.1.2 Aims

Chapter 3:

a. To establish the requirements for device maintenance in patients with PD implanted with DBS
b. To establish the frequency and type of DBS hardware related complications
c. To determine the duration of community living and survival of patients with PD after DBS surgery

Chapter 4 and Chapter 5:

d. To examine the correlation between ERNA power and motor benefit with DBS in patients with PD
e. To evaluate the utility of ERNA power in guiding contact selection during DBS programming
f. To compare the utility of ERNA power in guiding contact selection during DBS programming with existing neuronal signals (beta and HFO)
g. To compare the utility of ERNA power in guiding contact selection during DBS programming with anatomical guidance

1.2 Parkinson's disease

PD is a common neurodegenerative condition, affecting over 70,000 Australians (Deloitte, 2014). The estimated worldwide prevalence is 0.3% and this increases to 1% in those over the age of 60 years (de Lau and Breteler, 2006).

The condition was first described in 1817 by James Parkinson in 'An essay on the shaking palsy'. He reported on six patients with an "*involuntary tremulous motion, with lessened muscular power, in parts not in action and even when supported; with a propensity to bend the trunk forwards, and to pass from a walking to a running pace: the senses and intellects being uninjured*" (Parkinson, 2002). The portrayal of the motor deficit remains markedly accurate, though there is now increasing recognition of the many complex facets of PD.

1.2.1 Pathology

PD is characterised by the abnormal deposition of α-synuclein, a naturally occurring pre-synaptic neuronal protein (Lewy, 1912; Spillantini et al., 1997). Cellular and biochemical factors such as mitochondrial dysfunction (Park et al., 2018), calcium homeostasis (Surmeier et al., 2010) and failure of protein degradation pathways (Obeso et al., 2010) are implicated in aberrant accumulation of α-synuclein. Collectively, this protein deposition is termed 'Lewy pathology' and is typified by intracytoplasmic eosinophilic inclusions called Lewy bodies, which can also be present in neuritic processes (Figure 1.1) (Braak *et al.*, 2003; Dickson *et al.*, 2009). Current neuropathological criteria for PD requires loss of dopaminergic neurons in the substantia nigra pars compacta (SNc), with accompanying gliosis, in combination with Lewy pathology (Fearnley and Lees, 1991; Gelb et al., 1999; Dickson et al., 2009). Up to 50-80% of dopaminergic neurons can be lost prior to the emergence of the motor phenotype of PD (Bernheimer et al., 1973). Lewy pathology has also been found outside the SNc in the central and peripheral nervous systems and gastrointestinal system (Orimo et al., 2007; Ikemura et al., 2008; Beach et al., 2010). The Braak staging system proposes that deposition of α-synuclein occurs in a stepwise manner from the enteric and peripheral autonomic nervous system and spinal cord, to the brainstem and ascends the neuroaxis to ultimately include the neocortex (

Figure 1.2) (Braak *et al.*, 2003; Braak and Del Tredici, 2008). The significance of Lewy pathology in the absence of SNc neuronal loss is unclear and is postulated to reflect preclinical or pre-symptomatic PD (Gibb and Lees, 1988b; Markesbery *et al.*, 2009).

1.2.2 Aetiology

Idiopathic or sporadic Parkinson's disease is likely due to a complex combination of environmental and genetic factors. Age is the most strongly correlated risk factor (Nussbaum and Ellis, 2003). Ageing dopaminergic neurons with failing physiological and biochemical processes are postulated to be more susceptible to toxic insult (Schapira and Jenner, 2011). Environmental exposure to neurotoxins (1-methyl-4-phenyl-1,2,3,6-tetrahydropyridine, 6-hydroxydopamine), and agrochemical exposure result in mitochondrial dysfunction and nigrostriatal degeneration (Ungerstedt et al., 1973; Betarbet et al., 2000; Tanner et al., 2011). Cigarette smoking and caffeine are protective in PD (Hernán et al., 2002; Abbott et al., 2003), with both agents hypothesised to potentiate dopamine transmission and increase levodopa bioavailability and effect duration (Quik, 2004; Deleu et al., 2006; Postuma et al., 2012b). An alternative hypothesis is that due to variations in dopamine modulation in the reward pathway, PD patients have reduced sensation seeking and are less vulnerable to substance addiction (Evans et al., 2006).

PD was traditionally thought to be the archetypal non-heritable condition. However, the discovery of an α-synuclein mutation in an Italian kindred, the Contursi family, heralded the beginning of the genetic era in PD (Polymeropoulos et al., 1997). Since then, multiple genes and risk loci have been associated with PD and informed on molecular pathogenesis and novel therapeutic targets. Autosomal dominant forms of mutations in the α-synuclein (PARK1) gene and the leucine-rich repeat kinase 2 (LRRK2/PARK8) gene cause autosomal dominant forms of PD and are usually associated with classical Lewy bodies (Healy et al., 2008; Singleton et al., 2013). The more common autosomal recessive forms of PD are due to mutations in PRKN (parkin, PARK2), PINK1 (PARK6) and DJ-1 (PARK7), with PRKN accounting for up to 50% of recessive cases (Kitada et al., 1998; Bonifati et al., 2003; Valente et al., 2004). Recently, mutations in the glucocerebrosidase gene have been found in 5.5% of PD patients and 15% of Ashkenazi Jewish PD patients (Aharon-Peretz et al., 2004; Sidransky et al., 2009; McNeill et al., 2012). Autosomal recessive mutations in this gene result in Gaucher disease, a lysosomal storage disorder, with neurological sequalae of Parkinsonism (Neumann et al., 2009). The

phenotype of glucocerebrosidase mutation positive PD is often identical to sporadic PD with subtle differences in age of onset and rate of cognitive decline and disease progression (Neumann et al., 2009; Beavan and Schapira, 2013).

1.2.3 Clinical features

PD is characterised by a combination of motor and non-motor features. Diagnosis relies on motor clinical criteria, outlined in the UK Parkinson's Disease Society Brain Bank (Gibb and Lees, 1988b). The critical feature is bradykinesia; a slowness of initiation of movement with progressive decrementation in the speed and amplitude of subsequent repetitive movements (Fahn, 2003). The other cardinal features are tremor, rigidity and postural instability. Rest tremor, classically of the hands, is the most well recognised symptom of PD and is present in 69% of patients at diagnosis, and affects 75% of patients during the course of the illness (Hughes *et al.*, 1993b). Postural instability emerges later in the disease course due to loss of postural reflexes (Jankovic, 2008). Supportive diagnostic features include unilateral onset with persistent asymmetry, a progressive course (>10 years) and good levodopa response, though this may be absent in 30% of patients (Gibb and Lees, 1988b).

Non-motor symptoms are also common. Prodromal PD is increasingly recognised and characterised by olfactory dysfunction, rapid eye movement sleep behaviour disorder, constipation, depression and anxiety (Abbott *et al.*, 2003; Postuma *et al.*, 2012a). These are likely clinical manifestations of the early pathologic changes outside of the SNc (Section 1.2.1) (Braak *et al.*, 2003).

1.2.4 Diagnosis

Definitive diagnosis of PD is established post mortem, with neuropathological confirmation of Lewy bodies and nigrostriatal degeneration (Gibb and Lees, 1988b; Fearnley and Lees, 1991). In practice, diagnosis relies on the identification of the cardinal clinical features (Gibb and Lees, 1988b; Gelb *et al.*, 1999; Suchowersky *et al.*, 2006) and the diagnostic acumen of movement disorders neurologist is high at over 95% (Hughes et al., 2002). Neuroimaging with magnetic resonance imaging (MRI), nuclear medicine scans and transcranial ultrasound can

improve diagnostic accuracy and assist in the differentiation of PD from non-neurodegenerative conditions and atypical Parkinsonian syndromes (Politis, 2014).

Figure 1.1: Lewy pathology in the brain of PD patients.
(a), (b) and (f) (arrows) shows intracytoplasmic Lewy bodies. (c) (arrow), (d), (e), (f) shows α-synuclein deposition in neuritic processes termed Lewy neurites.

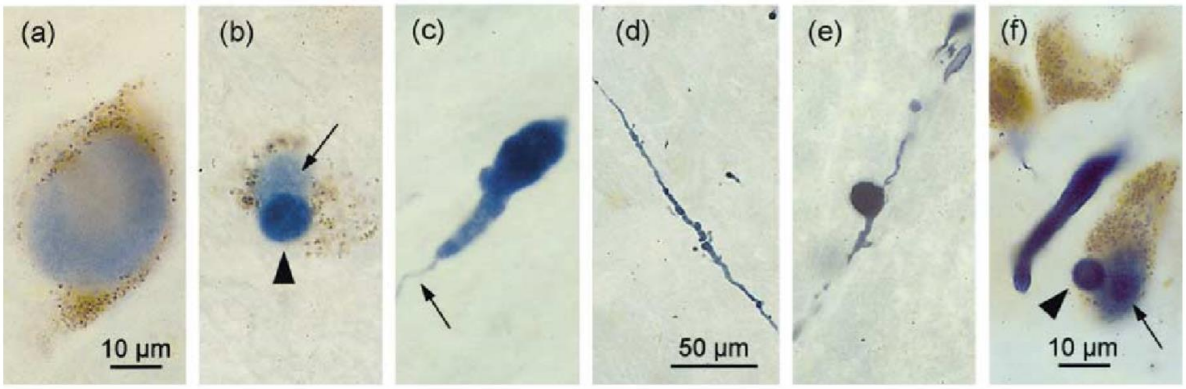

Images courtesy of *Braak H et al. Staging of brain pathology related to sporadic Parkinson's disease. Neurobiology of aging 2003; 24(2): 197-211.*

Figure 1.2: Progression of Lewy pathology in the brain in PD.

Lewy pathology ascends with disease progression from the brainstem structures to the basal ganglia and cortex. (b) – (e) demonstrates upward ascension of pathology from the medulla oblongata, pontine tegmentum, and olfactory nucleus (b, d), to the basal ganglia and temporal mesocortex (c, d) and neocortex (e). White arrows depict the gradual spread of Lewy pathology to susceptible adjacent structures.

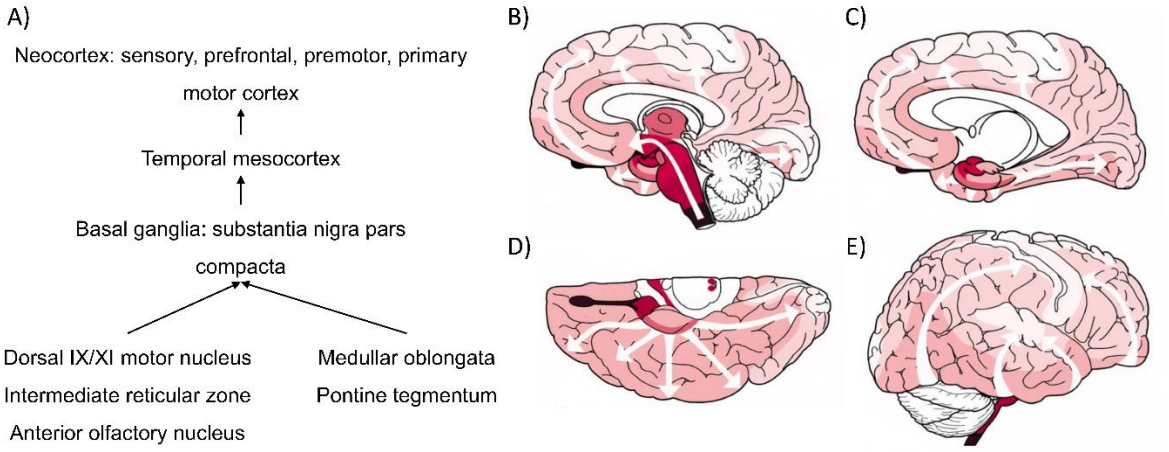

Images (b)-(e) courtesy *of Braak H et al. Staging of brain pathology related to sporadic Parkinson's disease. Neurobiology of aging 2003; 24(2): 197-211.*

1.2.5 Motor scales

Several clinical rating scales have been developed to stratify disease severity and monitor disease progression and response to therapy. The Hoehn and Yahr scale (Hoehn and Yahr, 1967; Goetz et al., 2004), first developed in 1967, focuses on the degree of appendicular and axial motor involvement with an emphasis on postural instability as a marker of disability. The Unified Parkinson's disease rating scale (UPDRS) is a more comprehensive assessment involving clinical motor evaluation (part III, Figure 1.3) and patient questionnaires to assess motor complications and non-motor features (Fahn, 1987; Goetz et al., 2008).

1.2.6 Prognosis

PD is a heterogenous condition, with a natural history that varies between patients. It is postulated that the phenotypic variations in PD (e.g. early onset, tremor dominant, postural instability gait difficulty) may determine the therapeutic response and natural history of the condition (Jankovic et al., 1990; Lewis et al., 2005; Selikhova et al., 2009). The mean age of disease onset is 62 years old and mean duration of disease is 15 years (Hughes et al., 2001). Younger age at diagnosis is associated with longer duration of disease (Selikhova et al., 2009; Kempster et al., 2010). Median time from diagnosis to death is 12 years, with 40-55% of patients losing functional independence and 25% requiring residential facility admission after a decade of disease (Lees et al., 2001; Hely et al., 2005; Kempster et al., 2010; Macleod et al., 2016). Most studies have reported a higher mortality rate in PD patients compared to the general population with a standardised mortality ratio between 1.58-1.78 at 10 years (Hely et al., 1999; Lees et al., 2001; Marras et al., 2005). Cognitive impairment, neuropsychiatric symptoms, autonomic instability and falls are the major cause of disability in later disease (Hely et al., 2005; Kempster et al., 2010).

Figure 1.3: Unified Parkinson's disease rating scale Part III motor subscore (UPDRS).

III. MOTOR EXAMINATION

18. Speech
0 = Normal.
1 = Slight loss of expression, diction and/or volume.
2 = Monotone, slurred but understandable; moderately impaired.
3 = Marked impairment, difficult to understand.
4 = Unintelligible.

19. Facial Expression
0 = Normal.
1 = Minimal hypomimia, could be normal "Poker Face".
2 = Slight but definitely abnormal diminution of facial expression
3 = Moderate hypomimia; lips parted some of the time.
4 = Masked or fixed facies with severe or complete loss of facial expression; lips parted 1/4 inch or more.

20. Tremor at rest (head, upper and lower extremities)
0 = Absent.
1 = Slight and infrequently present.
2 = Mild in amplitude and persistent. Or moderate in amplitude, but only intermittently present.
3 = Moderate in amplitude and present most of the time.
4 = Marked in amplitude and present most of the time.

21. Action or Postural Tremor of hands
0 = Absent.
1 = Slight; present with action.
2 = Moderate in amplitude, present with action.
3 = Moderate in amplitude with posture holding as well as action.
4 = Marked in amplitude; interferes with feeding.

22. Rigidity (Judged on passive movement of major joints with patient relaxed in sitting position. Cogwheeling to be ignored.)
0 = Absent.
1 = Slight or detectable only when activated by mirror or other movements.
2 = Mild to moderate.
3 = Marked, but full range of motion easily achieved.
4 = Severe, range of motion achieved with difficulty.

23. Finger Taps (Patient taps thumb with index finger in rapid succession.)
0 = Normal.
1 = Mild slowing and/or reduction in amplitude.
2 = Moderately impaired. Definite and early fatiguing. May have occasional arrests in movement.
3 = Severely impaired. Frequent hesitation in initiating movements or arrests in ongoing movement.
4 = Can barely perform the task.

24. Hand Movements (Patient opens and closes hands in rapid succesion.)
0 = Normal.
1 = Mild slowing and/or reduction in amplitude.
2 = Moderately impaired. Definite and early fatiguing. May have occasional arrests in movement.
3 = Severely impaired. Frequent hesitation in initiating movements or arrests in ongoing movement.
4 = Can barely perform the task.

25. Rapid Alternating Movements of Hands (Pronation-supination movements of hands, vertically and horizontally, with as large an amplitude as possible, both hands simultaneously.)
0 = Normal.
1 = Mild slowing and/or reduction in amplitude.
2 = Moderately impaired. Definite and early fatiguing. May have occasional arrests in movement.
3 = Severely impaired. Frequent hesitation in initiating movements or arrests in ongoing movement.
4 = Can barely perform the task.

26. Leg Agility (Patient taps heel on the ground in rapid succession picking up entire leg. Amplitude should be at least 3 inches.)
0 = Normal.
1 = Mild slowing and/or reduction in amplitude.
2 = Moderately impaired. Definite and early fatiguing. May have occasional arrests in movement.
3 = Severely impaired. Frequent hesitation in initiating movements or arrests in ongoing movement.
4 = Can barely perform the task.

27. Arising from Chair (Patient attempts to rise from a straightbacked chair, with arms folded across chest.)
0 = Normal.
1 = Slow; or may need more than one attempt.
2 = Pushes self up from arms of seat.
3 = Tends to fall back and may have to try more than one time, but can get up without help.
4 = Unable to arise without help.

28. Posture
0 = Normal erect.
1 = Not quite erect, slightly stooped posture; could be normal for older person.
2 = Moderately stooped posture, definitely abnormal; can be slightly leaning to one side.
3 = Severely stooped posture with kyphosis; can be moderately leaning to one side.
4 = Marked flexion with extreme abnormality of posture.

29. Gait
0 = Normal.
1 = Walks slowly, may shuffle with short steps, but no festination (hastening steps) or propulsion.
2 = Walks with difficulty, but requires little or no assistance; may have some festination, short steps, or propulsion.
3 = Severe disturbance of gait, requiring assistance.
4 = Cannot walk at all, even with assistance.

30. Postural Stability (Response to sudden, strong posterior displacement produced by pull on shoulders while patient erect with eyes open and feet slightly apart. Patient is prepared.)
0 = Normal.
1 = Retropulsion, but recovers unaided.
2 = Absence of postural response; would fall if not caught by examiner.
3 = Very unstable, tends to lose balance spontaneously.
4 = Unable to stand without assistance.

31. Body Bradykinesia and Hypokinesia (Combining slowness, hesitancy, decreased armswing, small amplitude, and poverty of movement in general.)
0 = None.
1 = Minimal slowness, giving movement a deliberate character; could be normal for some persons. Possibly reduced amplitude.
2 = Mild degree of slowness and poverty of movement which is definitely abnormal. Alternatively, some reduced amplitude.
3 = Moderate slowness, poverty or small amplitude of movement.
4 = Marked slowness, poverty or small amplitude of movement.

1.2.7 Management

There are no disease modifying agents for PD and the goal of treatment is symptom improvement. Patient and carer education and support and rehabilitation programs delivered by PD trained therapists (Canning *et al.*, 2015; Schenkman *et al.*, 2018; van der Kolk *et al.*, 2019) are a crucial aspects of management given the heterogeneity of the disease and the absence of neuroprotective therapies.

Dopaminergic replacement therapy

Dopamine replacement therapy remains the cornerstone of PD treatment and levodopa endures as the most effective agent (Rascol *et al.*, 2002). Adjuvant agents such as dopa decarboxylase inhibitor and catechol-O-methyl transferase inhibitors can reduce peripheral side effects and/or prolong levodopa action (Nutt and Wooten, 2005). Dopamine agonists (e.g. pramipexole and ropinirole, transdermal rotigotine) and monoamine oxidase B inhibitors (e.g. rasagiline, selegiline, safinamide) are less efficacious than levodopa, but can be used as an alternative or adjuvant agent (Fox *et al.*, 2018). Amantadine and anti-cholinergic agents such as trihexylphenidyl are occasionally employed to improve dyskinesia and tremor (Katzenschlager *et al.*, 2002; Hubsher *et al.*, 2012).

Treatment and disease complications

As PD progresses, patients develop motor fluctuations and drug related side effects including dyskinesias, neuropsychiatric complications (Dewey and O'Suilleabhain, 2000), dopamine dysregulation syndrome (O'Sullivan et al., 2009) and impulse control disorders (Weintraub *et al.*, 2006; Weintraub *et al.*, 2010).

Motor fluctuations (fluctuations in motor control) and dyskinesias (abnormal involuntary movements) emerge after a mean duration of disease of 6-7 years (Schrag and Quinn, 2000; Evans et al., 2011; Cilia et al., 2014) and occur in 40-60% of patients after 5 years of levodopa therapy (Ahlskog and Muenter, 2001). Progressive nigrostriatal degeneration and dopamine depletion combined with the short half-life of dopaminergic agents results in pulsatile stimulation of striatal dopamine receptors leading to fluctuations in motor state and dyskinesias (Obeso et al., 2004). Risk factors for the development of motor fluctuations include younger age, longer duration of disease and levodopa dose, though duration of levodopa exposure may

not confer a higher risk (Schrag and Quinn, 2000; Jankovic, 2005; Cilia et al., 2014; Group, 2014).. Initial treatment of motor fluctuations involves adjustments in dopaminergic medication dosage and frequency and the introduction of adjuvant agents such as dopamine agonists, monoamine oxidase B inhibitors, catechol-O-methyl transferase inhibitors and amantadine (Metman et al., 1998; Pahwa et al., 2006).

Device assisted therapies

Device assisted therapies such as DBS, subcutaneous apomorphine and levodopa/carbidopa intestinal gel are introduced when troublesome motor fluctuations and dyskinesia persist despite optimisation of oral therapies (Volkmann et al., 2013). Subcutaneous apomorphine is a dopamine agonist that can be given as intermittent injections or a continuous infusion (Hughes *et al.*, 1993a; Katzenschlager *et al.*, 2018). Levodopa/carbidopa intestinal gel is administered continuously via a percutaneous endoscopic gastrostomy tube with a jejunal extension (Olanow *et al.*, 2014). DBS (Section 1.4) involves the insertion of electrodes into deep nuclei of the brain including the STN and GPi with continuous stimulation administered by an implantable pulse generator (IPG). There have been no randomised controlled trials directly comparing the device assisted therapies, though the efficacy is thought to be similar (Odin et al., 2015). The improvement in motor fluctuations and reduction in dyskinesia is reported to be between 25-85% and 25-65% respectively in all therapies (Pietz *et al.*, 1998; Manson *et al.*, 2002; Katzenschlager *et al.*, 2005; Deuschl and Agid, 2013; Fernandez *et al.*, 2015; Martinez-Martin *et al.*, 2015).

1.3 Neuroanatomy and neurophysiology in Parkinson's disease

1.3.1 Basal ganglia

The motor manifestations of PD are thought to arise from abnormalities in the cortico-basal-ganglia-thalamic network (DeLong, 1990) (Section Disease mechanisms in Parkinson's disease). The basal ganglia can be separated into striatal and extra-striatal components. The striatum is divided into the ventral (nucleus accumbens, olfactory bulb) and dorsal (caudate, putamen) structures and is the major input nucleus of the basal ganglia, receiving and

processing afferents from the cortex. The striatum contains gamma-aminobutyric acid (GABA)-ergic and cholinergic interneurons and GABA-ergic output projection neurons called medium spiny neurons (Hammond *et al.*, 2007). Discharges from the medium spiny neurons are highly regulated by intrinsic inhibitory control and cortical inputs. Conversely, the extra-striatal neurons in the STN, globus pallidus pars externa (GPe), GPi and the substantia nigra pars reticularis (SNr) have spontaneous, intrinsic, tonic neuronal cell activity.

The two traditional pathways of the basal ganglia are the monosynaptic 'direct' pathway involving the putamen and GPi/SNr and the tri-synaptic 'indirect' pathway involving the putamen, GPe, STN and GPi/SNr (Figure 1.4A) (Obeso *et al.*, 2000). STN glutamatergic neurons also receive direct, independent cortical input through the 'hyperdirect' pathway (Obeso *et al.*, 2000). Dopamine from the SNc acts on the putamen, potentiating neurons in the direct circuit and inhibiting neurons in the indirect circuit. Activation of the direct pathway results in reduced GPi/SNr firing and reduced inhibition of the ventrolateral nucleus of the motor thalamus, allowing for downstream activation of cortical and brainstem motor regions that facilitate movement. Conversely, the indirect and hyperdirect pathways increase GPi/SNr firing and suppress movement.

1.3.2 Subthalamic nucleus

The STN is a critical component of the indirect and hyperdirect pathways of the basal ganglia and is one of the common anatomical targets for DBS in the treatment of PD (Okun, 2012). The observation of altered neuronal activity recorded from the STN of 1-methyl-4-phenyl-1,2,3,6-tetrahydropyridine primate models by Miller *et al* in 1987 highlighted the importance of this structure in PD (Miller and DeLong, 1987). Shortly afterwards, Bergman *et al* lesioned the STN in primates resulting in reversal of parkinsonism in the contralateral limb (Bergman et al., 1990), further cementing the STN's pivotal role in the cortico-basal-ganglia-thalamic network (DeLong, 1990; Bevan, 2017).

Anatomy

The STN is a small paired structure, measuring less than 10 millimetres, located ventral to the thalamus, dorsal to the substantia nigra and medial to the internal capsule. Traditionally, the STN was thought to be a relay nucleus to facilitate suppression of unwanted motor programs.

More recently, the STN has been shown to integrate motor, cognitive and limbic components of behaviour. The various pathways are arranged topographically with a motor gradient, which is most concentrated in the dorsolateral STN (Haynes and Haber, 2013). Conversely, the cognitive and limbic terminals are positioned within the central and ventromedial regions, respectively. Accordingly, DBS of the dorsolateral STN produce motor effects, while central and ventromedial stimulation precipitate attentional dysfunction and mania (Mallet et al., 2007).

STN neurons

The STN neurons contain autonomous firing activity, discharging spontaneously in the absence of external input (Bevan, 2017). They receive glutamatergic afferent inputs from the cortex, parafascicular thalamic nucleus, superior collicus and pedunculopontine nucleus. The GPe neurons project to the STN via GABA-ergic inputs. Cholinergic neurons from the pedunculopontine nucleus, serotonergic neurons from the dorsal raphe and dopaminergic neurons from the midbrain all play a role in STN neuromodulation (Bevan, 2017). Specifically, dopamine induces STN neuron membrane depolarisation and increases autonomous firing in the STN (Loucif et al., 2008).

Normal STN activity in movement

The STN receives cortical information directly via the hyperdirect pathway and via the indirect pathway from the striatum and GPe (Figure 1.4A). This information is relayed to the basal ganglia output nuclei, the GPi and SNr, resulting in movement, thought and emotional suppression (Bevan, 2017). Cortical stimulation precipitates a triphasic response in STN neurons with initial excitation, then a 5 millisecond period of inhibition, followed by a prolonged period of increased activity due to GPe inhibition by the striatum (Fujimoto and Kita, 1993; Maurice et al., 1998). A sustained increase in STN firing occurs at the time of or shortly after skeletomotor and oculomotor movements suggesting a role in movement suppression (Matsumura et al., 1992; Wichmann et al., 1994). The STN may also assist in switching from automatic to voluntary movements (Isoda and Hikosaka, 2008) and in modulating the reward pathway (Baunez et al., 2005; Lardeux et al., 2009).

1.3.3 Disease mechanisms in Parkinson's disease

Traditional anatomical model

The traditional model of cortico-basal-ganglia-thalamic dysfunction in PD relies on the critical and discrepant role of dopamine on the direct, indirect and hyperdirect pathways. SNc degeneration results in a dopamine deplete state with loss of inhibition of the striatal neurons that give rise to the indirect pathway. In turn, disinhibition of the indirect and hyperdirect GPe and STN mediated circuits with concurrent hypoactivity of the direct circuit results in GPi/SNr activation (Figure 1.4B). Downstream, there is increased inhibition of the ventrolateral thalamus and reduced activation of cortical and brainstem motor regions (Albin et al., 1989; DeLong, 1990). Thus, this model supports the hypothesis that greater GPi inhibition of the ventrolateral thalamus produces the cardinal hypokinetic features of PD, while a reduction in GPi inhibition, with resultant thalamic activation, yields hyperkinetic movements such as dyskinesia. Indeed, lesioning of the GPi and STN ameliorates PD symptoms (Bergman et al., 1990; Fine et al., 2000; Alvarez et al., 2005), while subthalamotomy can produce contralateral hemiballismus and dyskinesia (Hamada and DeLong, 1992b; Lee and Marsden, 1994) and inhibition of GPi neuronal activity (Hamada and DeLong, 1992a). However, contradictory to this traditional anatomical model, lesioning of the thalamus or GPe does not produce parkinsonism (Matsumoto et al., 1984; Soares et al., 2004) and GPi pallidotomy reduces dyskinesia in PD patients (Lozano et al., 1995).

Updated neurophysiological model

The inconsistencies of the traditional anatomical model have prompted growing interest in the neural networks implicated in PD and their relevance to the therapeutic mechanisms of DBS (Section 1.4). The insertion of electrodes into the deep brain structures allows for recording of spontaneous electrical discharges from the neuronal population termed local field potentials (LFPs) (Priori *et al.*, 2013) (Section 1.5). While not inherently pathological, abnormal LFP firing patterns and synchronisation is observed in disease states such as PD (Hammond *et al.*, 2007). Indeed, it is hypothesised that the therapeutic effects of DBS are related to modulation of aberrant neural activity with downstream effects on the entire cortico-basal-ganglia-thalamic network (Hashimoto *et al.*, 2003).

Figure 1.4: Traditional anatomical pathway of the cortical-basal-ganglia-thalamic network in the normal state and Parkinsonian state.

Green arrows represent excitatory pathways. Red arrows represent inhibitory pathways. In (b), dashed arrows represent reduced activity and thickened arrows represent increased activity. In the normal state (a), activation of D1-dopamine receptors potentiates direct pathway inhibition of GPi/SNr and inhibition of D2-dopamine receptors reduces indirect pathway activation of the GPi/SNr. Ultimately, this results in disinhibition of the ventrolateral thalamus and activation of the cortical and brainstem motor regions. In the dopamine deplete Parkinsonian state (b), there is disinhibition of the D2-dopamine receptors in the striatum, resulting in increased GPe inhibition and disinhibition of the STN. Furthermore, reduced activation of D1-dopamine receptors decreases direct pathway activity. Ultimately, this results in activation of the GPi/SNr, over-inhibition of the ventrolateral thalamus and reduced activation of the cortical and brainstem motor regions. GPe, globus pallidus externa; GPi, globus pallidus interna; SNc, substantia nigra pars compacta; SNr, substantia nigra pars reticularis; STN, subthalamic nucleus; VL, ventrolateral; D1, D1-dopamine-receptors; D2, D2-dopamine-receptors.

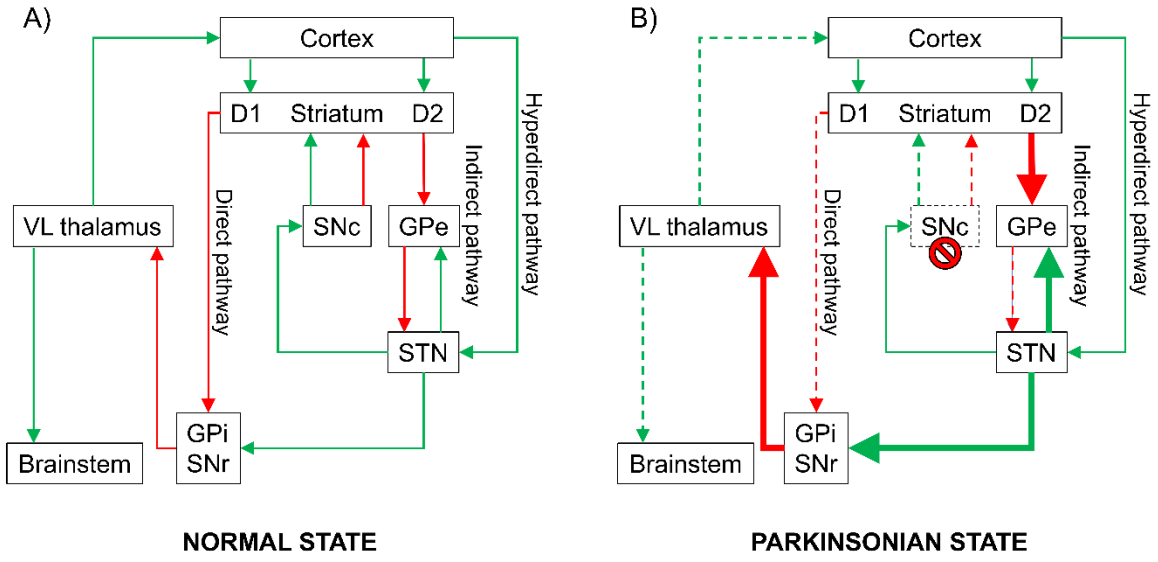

Images adapted from *Obeso JA, et al. Pathophysiology of the basal ganglia in Parkinson's disease. Trends in neurosciences 2000; 23: S8-S19* and *Bevan MD. Chapter 14 - The Subthalamic Nucleus. In: Steiner H, Tseng KY, editors. Handbook of Behavioural Neuroscience: Elsevier; 2017. p. 277-91.*

1.4 Deep brain stimulation in Parkinson's disease

In the 1960s, chronically implanted electrodes were stimulated to assist in targeting of surgical lesions in neurological conditions such as PD (Sem-Jacobsen, 1966). Two decades later, Benabid and colleagues demonstrated the therapeutic effect of chronic high frequency stimulation of the ventral intermediate nuclei of the thalamus on tremor in PD and essential tremor (Benabid et al., 1987; Benabid et al., 1991). Since then, DBS has been used in the management of a number of neurological and psychiatric conditions (Mayberg et al., 2005; Vidailhet et al., 2005; Kupsch et al., 2006; Boon et al., 2007). DBS is now an established therapy for PD, with more than 150,000 people having had surgery worldwide (Hariz, 2017).

1.4.1 Short term outcomes of DBS

The primary indications for DBS in PD are motor fluctuations, medication induced dyskinesia and drug refractory tremor (Okun, 2012). The therapeutic impact of DBS is well characterised with multicentre trials demonstrating reduction in motor off time and increase in motor on time without dyskinesia, coinciding with a substantial reduction in dopaminergic medications (Deuschl et al., 2006; Weaver et al., 2009; Williams et al., 2010). Patients with DBS report improvements in quality of life and activities of daily living (Deuschl and Agid, 2013; Schuepbach et al., 2013). The common surgical targets for DBS in PD are the STN and GPi for motor fluctuations and the thalamus or posterior subthalamic area for tremor control alone (Ondo *et al.*, 1998; Barbe *et al.*, 2018). Randomised control trials have not revealed a significant difference in motor outcomes between STN or GPi DBS. STN DBS may offer superior off-medication motor scores, allowing for greater medication reduction (Odekerken et al., 2013; Odekerken et al., 2016), while GPi DBS may deliver direct dyskinesia suppression (Oyama et al., 2012). Greater cognitive and mood changes have been observed with STN DBS, though the overall difference is likely small (Okun et al., 2009; Follett et al., 2010; Odekerken et al., 2015).

1.4.2 Long term outcomes of DBS

DBS is a life-long therapy for patients with PD, yet surprisingly, there are few longitudinal studies of this unique cohort. The available studies report a sustained benefit on motor function, albeit with therapy efficacy waning over time due to disease progression and emergence of DBS unresponsive PD features (Fasano et al., 2010; Castrioto et al., 2011; Zibetti et al., 2011; Aviles-Olmos et al., 2014; Limousin and Foltynie, 2019). There is a paucity of data on the life-time servicing requirements of DBS and the community and survival outcomes after DBS implantation. For example, though clinician programming is a major component of DBS maintenance, there is no published data on programming rates. Furthermore, the existing data on DBS servicing, largely pertaining to hardware complications, is derived from single centres and a handful of healthcare systems. The published results vary greatly due to a lack of standardised reporting (Videnovic and Metman, 2008) and there are sampling biases inherent to individual institutions and specialised healthcare databases. Case series have reported a broad electrode complication rate of between 1% to 12.5% (Joint et al., 2002; Oh et al., 2002; Vergani et al., 2010). Conversely, an analysis of two American databases, the Medicare and Medicaid database and the National Surgical Quality Improvement Program (NSQIP) database, revealed a markedly higher rate of brain electrode revision surgery of 15% and 34% respectively (Rolston et al., 2016). Importantly, these databases only reported on the number of events, as a proportion of total procedures and lacked individual patient level information. There is also scarce data on the duration of community living and survival in PD patients after DBS surgery. Two single centre studies reported quite different rates of residential care admission at 42% ten years after DBS (Bang Henriksen *et al.*, 2016) and 6% after a median follow-up over seven years (Ngoga *et al.*, 2014). Similarly, ten year survival rates vary greatly, ranging from 50% to 80% (Lilleeng et al., 2014; Ngoga et al., 2014; Rocha et al., 2014; Bang Henriksen et al., 2016; Cubo et al., 2018). Greater knowledge of these underexplored DBS outcomes is vital to accurately inform patients and health care services and identify research priorities to improve DBS devices.

1.4.3 Limitations in DBS systems

The limited longitudinal data has highlighted several weaknesses in existing DBS devices. For example, the suboptimal response to DBS therapy in 45% of patients can be accounted for by poorly placed electrodes (Okun et al., 2005). DBS efficacy is highly dependent on the application of stimulation at the ideal location or ‘sweet spot’ to achieve maximal clinical

benefit. This relies on the accurate implantation of the electrode during surgery and the appropriate selection of the contact to apply DBS by clinicians post-operatively. A variety of anatomical, clinical, and neurophysiological methods are employed to assist localisation of the surgical target. Firstly, the surgery is performed under stereotactic guidance, with the optimal anatomical target and trajectory identified on a high-resolution pre-operative MRI brain scan (Starr, 2002). Secondly, the patient is often awake during electrode implantation to allow for assessment of the clinical response to electrode stimulation (Mehanna *et al.*, 2017; Geraedts *et al.*, 2019). Finally, some centres perform intra-operative microelectrode recordings (MER) to help localise the STN or GPi (Bour *et al.*, 2010; Montgomery Jr, 2012). Despite these techniques, electrode revision and replacement surgeries are not uncommon (Rolston *et al.*, 2016). One consideration is that the postulated ideal location to apply stimulation in the STN is in the dorsolateral motor region (Herzog *et al.*, 2004; Horn *et al.*, 2017b). However, there is significant inter-patient heterogeneity in STN size, morphology and location, which limits accuracy of atlas-based targeting (Richter et al., 2004; Ashkan et al., 2007; Daniluk et al., 2010; Nestor et al., 2014). Even amongst DBS experts, there is disagreement on the optimal anatomic target for STN stimulation (Hamel et al., 2017). Moreover, there is growing evidence that anatomical networks are inferior to functional networks in predicting clinical benefit with DBS (Horn *et al.*, 2017c). However, existing neurophysiological guidance methods also have limitations. The STN and GPi possess a 'physiological signature' and MER aims to measure single cell activity to determine the span of these structures (Montgomery Jr, 2012). Yet MER findings are not always reliable and in up to 60% of cases, do not coincide with the location that delivers best clinical benefit with DBS intra-operatively (Bour et al., 2010). Finally, awake surgery remains a valuable tool to guide electrode navigation and are associated with lower rates of therapy related side effects and superior axial outcomes compared to asleep procedures (Blasberg et al., 2018; Ho et al., 2018). However, an awake procedure can be daunting and uncomfortable, with up to 40% of patients experiencing significant pain during the operation (Mulroy et al., 2017). Furthermore, clinical evaluation during surgery is not always reliable and therapeutic thresholds established by intra-operative stimulation do not always coincide with chronic stimulation findings (Blume *et al.*, 2017).

Post-operatively, the optimal DBS parameters for the patient need to be identified. This involves manual adjustments by the clinician over multiple programming sessions, which can be time consuming and laborious. Initially, the clinician must identify the ideal location to apply DBS. Traditionally, this involves a 'contact screen', where stimulation is applied to each

contact on the array in a monopolar configuration and the resultant clinical benefit is measured (Volkmann et al., 2006). Determining DBS benefit can be particularly challenging in the weeks after DBS surgery with factors such as the stun effect (the therapeutic micro-lesioning effect related to lead implantation) and medication wash-out confounding the patient motor state (Mestre *et al.*, 2016). Therefore, additional information including anatomy is also employed to assist in contact selection (Hamel et al., 2003). This requires acquisition of pre-operative and post-operative images and expert analysis, a process which can take days. After selection of the active contact, the clinician determines the appropriate amplitude, pulse width and frequency to apply DBS (Volkmann et al., 2006). This heuristic has grown exponentially more complex with the introduction of directional contacts (Figure 1.5) and stimulation that can be delivered via independent current control (Timmermann *et al.*, 2015; Dembek *et al.*, 2017; Schüpbach *et al.*, 2017). Accordingly, emerging technologies aim to simplify this process, by automating post-operative lead localization and providing probabilistic algorithms to predict the ideal anatomical location to apply DBS across groups (Horn and Kühn, 2015; Anderson et al., 2018; Dembek et al., 2019).

Finally, DBS devices deliver 'open loop', continuous, high frequency stimulation. However, PD symptoms vary greatly between patients and within patients. Therefore, fixed stimulation can be insufficient to relieve symptoms, or excessive, impairing physiological networks (Chen et al., 2006a) and draining battery life (Little and Brown, 2012). DBS efficacy could be substantially improved if stimulation parameters was tailored to the individual or ideally, automatically adjusted according to the patient's requirements in a closed-loop system (Meidahl *et al.*, 2017; Weiss and Massano, 2018). Indeed, closed-loop DBS using LFPs as a feedback signal suggest that this system could offer superior motor outcomes, minimise stimulation related side effects and increase energy efficiency compared to conventional open loop devices (Little et al., 2013; Little et al., 2016; Rosa et al., 2017; Arlotti et al., 2018).

Figure 1.5: Different DBS electrode designs.

Traditional, omnidirectional DBS leads have four cylindric contacts. Newer, directional DBS leads have eight contacts, including six segmented contacts in the two central tiers. Each segmented contact spans a circumference of approximately 120°. At the top of the lead, there is a radiopaque marker, which assists in confirming orientation of the contacts.

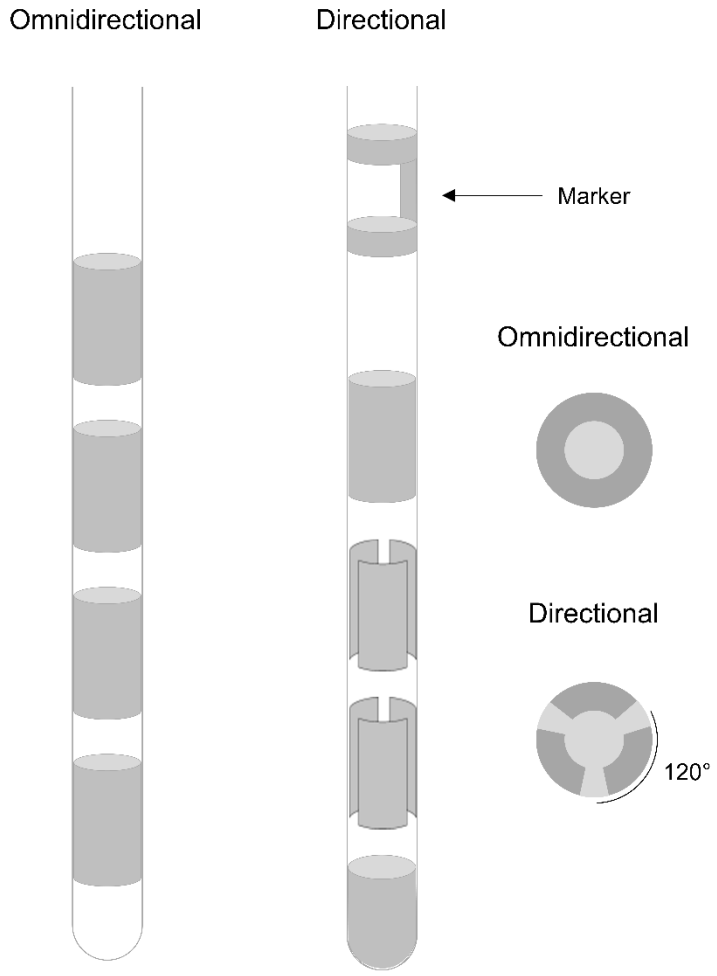

Adapted from *Steigerwald F, Matthies C, Volkmann J. Directional Deep Brain Stimulation. Neurotherapeutics : the journal of the American Society for Experimental NeuroTherapeutics 2019; 16(1): 100-4.*

1.5 Neurophysiological biomarkers in deep brain stimulation

Our understanding of the therapeutic mechanisms of DBS continues to evolve. The classic 'rate model' hypothesised that DBS locally inhibits overactive neurons in the STN and GPi, coinciding with the traditional anatomical paradigm of PD (Albin et al., 1989; DeLong, 1990). However, high quality recordings employing superior artefact filtering algorithms demonstrate an increase in STN activity at the time of therapeutic DBS (Montgomery Jr *et al.*, 2005). Furthermore, there is growing evidence that DBS modulates abnormal synchronisation of both local and distant neural networks to restore 'functionality' in the cortico-basal-ganglia-thalamic network (Section 1.3.1) (Ashkan et al., 2017). Neurophysiological signals recorded from the deep nuclei and cortex are intrinsic to this hypothesis and could play a crucial role in addressing the limitations of existing DBS systems. These neurophysiological signals could act as a 'biomarker', informing us on the electrophysiological state of the neural networks and the clinical efficacy of DBS. Thus, these signals could assist intra-operative navigation, guide DBS programming in individual patients and deliver information to alter DBS parameters in a closed-loop system. A feasible biomarker requires several key characteristics (Little and Brown, 2012; Priori *et al.*, 2013; Little and Brown, 2020):

1. Reliable recordability with a high signal-to-noise ratio, even after chronic DBS implantation
2. Localisation to the ideal position to apply stimulation
3. Accurate reflection of the clinical state with high temporal resolution
4. Modulation by DBS in a predictable manner

LFPs are recordable in normal neural networks and represent the summation of spontaneous electrical activity from the neuronal population. These oscillations are dependent on the cellular-synaptic spatial architecture and temporal fluctuations in synchrony (Buzsáki et al., 2012) and are thought to enable dynamic communication between different neuronal populations (Brown and Williams, 2005). Thus, LFP power reflects the degree of synchronisation, the density and area of the local neuronal population and the changes in activity over time (Little and Brown, 2014). In the disease state, there is evidence of pathologic oscillatory activity, which can be modulated by therapeutic DBS. The oscillatory activities of LFPs are a composite of different frequency bands; 0-3 Hz (delta), 4-7 Hz (theta), 7-12 Hz

(alpha), 13-30 Hz (beta), 31- 200 Hz (gamma) and >200 Hz (high frequency) (Thompson et al., 2014). In PD, the most well studied LFPs are beta oscillations and more recently, high frequency oscillations (HFO).

1.5.1 Beta oscillations

Physiological beta activity

Beta oscillations occupy the frequency range of 13-30 Hz and modulates with movement in healthy individuals. It is more pronounced during steady-state contractions, suppressed and replaced by faster gamma band activity prior to and during movement and rebounds after movement (Baker, 2007; Engel and Fries, 2010; Little and Brown, 2014). Consequently, beta oscillations are postulated to play an integral role in maintaining the 'status quo' in the motor system.

Pathological beta activity in Parkinson's disease

Beta oscillations can be recorded from intracranial electrodes intra-operatively or post-operatively during periods of lead externalisation (Figure 1.6). In the dopamine depleted Parkinsonian state, recordings from the STN, GPi and cortex have revealed excessive synchronisation of beta activity in the cortico-basal ganglia-thalamic network (Bergman et al., 1994; Nini et al., 1995; Gatev et al., 2006; Mallet et al., 2008). Beta activity is enhanced with dopamine withdrawal, and levodopa and DBS attenuates pathological beta band synchronisation (Brown et al., 2001; Silberstein et al., 2005; Bronte-Stewart et al., 2009; Eusebio et al., 2011). Modulation of beta oscillations by therapeutic DBS and medication coincides with clinical improvement in bradykinesia and rigidity (Kühn et al., 2006; Hammond et al., 2007; Ray et al., 2008; Kühn et al., 2009). However, the correlation between beta activity at rest and the patient's clinical state is less clear with only some groups demonstrating an association between beta activity and rigidity and bradykinesia (Weinberger *et al.*, 2006; Chen *et al.*, 2010; Little *et al.*, 2012; Neumann *et al.*, 2016a). A recent study has proposed that excessive beta bursts could disrupt the basal ganglia's ability to encode information on intended limb movements, resulting in a pathological state (Khawaldeh *et al.*, 2020).

To refine the clinical relevance of beta, other temporo-spatial features of beta have been explored. A spectral division of beta band into lower (<20 Hz) and higher (>20 Hz) frequency bands has been proposed. Low frequency beta could have greater clinical relevance, with high frequency activity possibly representing a harmonic distortion of the lower spectral band (Marceglia et al., 2006). Therapeutic DBS has been shown to selectively suppress the low frequency beta band and correlate with contralateral clinical improvement (Oswal et al., 2016). Recent work has proposed a somatotopic related spectral difference, with both lower and upper limb activation modulating low frequency beta but a far greater correlation between lower limb movements and high frequency beta desynchronization (Tinkhauser et al., 2019). The duration of beta bursts also alters motor function. Short bursts are thought to be physiological and long bursts have been correlated with motor impairment (Murthy and Fetz, 1992; Feingold et al., 2015; Torrecillos et al., 2018). In PD patients, levodopa administration changes the distribution of STN beta bursts, from long to short duration and reduces beta amplitude, coinciding with clinical improvement (Tinkhauser et al., 2017b). The spatial distribution of beta is also relevant. Greatest beta activity has been recorded in the dorsolateral STN and the span of these oscillations may coincide with DBS efficacy (Kühn et al., 2005; Zaidel et al., 2010).

Clinical application of beta oscillations

Beta oscillations have been proposed as a potential neurophysiological signal to improve DBS systems. Greater beta activity is recorded in the postulated 'sweet spot' to apply stimulation, in the dorsolateral STN, and intra-operative beta recordings may assist in STN localisation during surgery (Chen *et al.*, 2006b; Telkes *et al.*, 2016; Horn *et al.*, 2017b). Selection of an active contact based on beta power recordings has been explored, though this beta metric alone is insufficient to identify the optimal contact in every patient (Ince et al., 2010; Tinkhauser et al., 2018). Closed-loop DBS systems using beta amplitude as a feedback signal for on-off strategies or voltage adjustments have been evaluated (Figure 1.7) (Little et al., 2013; Rosa et al., 2015). These adaptive models conferred better motor scores, reduced stimulation related side effects, decreased power usage and selectively modulated the duration of beta bursts compared to conventional DBS (Little et al., 2016; Rosa et al., 2017; Tinkhauser et al., 2017a). However, the ubiquitous use of beta in clinical practice has been limited by several factors. Firstly, there is a variable correlation between beta amplitude and resting motor state (Weinberger *et al.*, 2006; Chen *et al.*, 2010; Little *et al.*, 2012; Neumann *et al.*, 2016a). Secondly, beta band activity is small (measured in microvolts) with a low signal-to-noise ratio.

It is not reliably detectable in all patients and attenuated by movement and stun effect (Chen et al., 2006b; Giannicola et al., 2010). Identification of beta oscillations in freely moving patients using IPGs has proven challenging due to stimulation and cardioballistic artefact (Quinn *et al.*, 2015; Neumann *et al.*, 2016b; Steiner *et al.*, 2017). The shortcomings of beta oscillations have prompted researchers to explore the utility of alternative neurophysiological signals such as HFO and evoked potentials (Section 1.5.3).

1.5.2 High frequency oscillations

Physiological HFO activity

HFO occupy the frequency range of 200-400 Hz and are measurable in the STN of parkinsonian and non-parkinsonian patients, suggesting a broader physiological function in STN related networks (Foffani et al., 2003; Danish et al., 2007). HFO is postulated to have a prokinetic role and in the parkinsonian state, is enhanced with voluntary movement and dopaminergic medication (Foffani *et al.*, 2003; López-Azcárate *et al.*, 2010).

Pathological HFO activity in Parkinson's disease

HFO has been recorded from the STN and GPi of patients with PD (Figure 1.6) (Foffani et al., 2003; Danish et al., 2007; López-Azcárate et al., 2010), with greater HFO power measured in the dorsal STN (Wang et al., 2014). The correlation between HFO power and motor scores is inconsistent, with some studies demonstrating a negative relationship between the magnitude of HFO power and the severity of bradykinesia and rigidity scores (López-Azcárate et al., 2010; Wang et al., 2014; van Wijk et al., 2016). Spectral divisions of HFO and its correlation with beta oscillations has also been explored. Levodopa administration precipitates a spectral shift in HFO frequency from slow HFO (200 – 300 Hz) to fast HFO (300 – 400 Hz) and the ratio of slow and fast HFO positively correlates with severity of motor scores (Özkurt et al., 2011). Further analysis has revealed coupling between HFO amplitude and the phase of beta oscillations, with the degree of coupling associated with motor impairment (Özkurt *et al.*, 2011; van Wijk *et al.*, 2016). Beta HFO phase-amplitude coupling is stronger in the 50% of cases where HFO and beta co-localise to the same region of the STN (van Wijk *et al.*, 2017). However, HFO is susceptible to similar recording limitations as beta. It is not reliably detectable in all patients with PD and HFO measurements may vary between different electrode

types, with spectral divisions difficult to record on microelectrodes (López-Azcárate *et al.*, 2010; Wang *et al.*, 2014).

1.5.3 Evoked potentials

To date, the search for a neurophysiological biomarker for DBS has largely focused on LFPs, with little exploration of the neural potentials evoked by DBS pulses.

Cortical evoked potentials

In a variety of movement disorders, STN, GPi and thalamic stimulation produce cortical evoked potentials (CEPs) recordable on electroencephalography and electrocorticography (Ashby *et al.*, 2001; Baker *et al.*, 2002; Tisch *et al.*, 2008; Eusebio *et al.*, 2009; Walker *et al.*, 2012). In PD, the characteristics of these multi-phasic cortical waveforms, including latency and amplitude, vary across patients with different stimulation locations and DBS parameters (Limousin *et al.*, 1998; MacKinnon *et al.*, 2005; Eusebio *et al.*, 2009). High frequency therapeutic STN stimulation evokes short latency CEPs that coincide with attenuation of beta oscillation and therapeutic effect (Dejean *et al.*, 2009; Walker *et al.*, 2012). In dystonia, larger CEPs are measured at clinically effective contacts in the GPi, suggesting a potential role in intra-operative navigation and contact selection (Tisch *et al.*, 2008). However, previous evaluation of CEPs in PD suggested great variation across clinically effective contacts (MacKinnon *et al.*, 2005; Devergnas and Wichmann, 2011). Furthermore, the clinical feasibility of CEPs is limited by the need to implant additional electrodes near the cortex, introducing greater surgical and infection risk, particularly with monitoring in the chronic setting.

Evoked compound action potentials

Evoked compound action potentials (ECAPs) can also be measured from DBS electrodes implanted into the deep nuclei of the brain. Small, short latency ECAPs have been measured in the thalamus of tremor patients (Kent and Grill, 2013) and though their characteristics are altered by adjustments in stimulation parameters, there is great inter-participant variability and no compelling correlation with clinical efficacy (Kent *et al.*, 2015). ECAPs characterised by an early response and late response have also been recorded from electrodes implanted into the

STN of two patients with PD (Gmel *et al.*, 2015). The early response was detectable directly after the DBS is delivered, lasting 2 milliseconds, while the late response occurred 0.5-1 millisecond later (~3 milliseconds after the early response onset). The late response morphology varied with delivery of therapeutic DBS, though the nature of this change differed between the two patients measured.

Evoked resonant neural activity

More recently, our group described a large amplitude (hundreds of microvolts) evoked response, termed evoked resonant neural activity (ERNA), recorded from the STN electrodes of patients with PD (Sinclair *et al.*, 2018; Sinclair *et al.*, 2019a). ERNA has a highly characteristic, readily identifiably, decaying oscillation morphology of 200-500 Hz that is time locked to DBS pulses (Figure 1.8A). Peak ERNA amplitude is usually recorded ~4 milliseconds following each pulse, and the response can last for tens of milliseconds. ERNA is localised to the dorsal subregion of the STN (Sinclair *et al.*, 2018). Therapeutic 130 Hz DBS modulates ERNA, with greater stimulation amplitude associated with lower ERNA frequency and higher ERNA amplitude (Figure 1.8B), coinciding with intra-operative measures of bradykinesia and rigidity. The modulation of ERNA with therapeutic DBS also corresponded with beta band suppression. Furthermore, ERNA and HFO occupy comparable frequency bands and are similarly modulated by therapeutic DBS to approximately twice the stimulation rate (Sinclair *et al.*, 2019b). However, what remains unexplored is the correlation between ERNA features, the patient motor state and the clinical response to DBS therapy. Assessment of this correlation is critical to establishing the clinical utility of ERNA as a neural biomarker in DBS for PD.

Figure 1.6: STN beta oscillations and HFO in the rest state from a patient.

The thin horizontal lines at 50 Hz, 150 Hz, 250 Hz and 350 Hz are artefacts at the mains frequency and their harmonics. (c) represents the mean power spectrum of beta and HFO on a logarithmic scale recorded from 22 STN in patients with PD. In the off-motor state, there is prominent beta oscillations and HFO activity at a peak frequency of 250-260 Hz. In the on-motor state, there is attenuation of beta oscillations in the low-frequency spectral band (12-20Hz) and a short period of HFO attenuation followed by higher frequency HFO activity (300-350 Hz) with a broad spectral distribution.

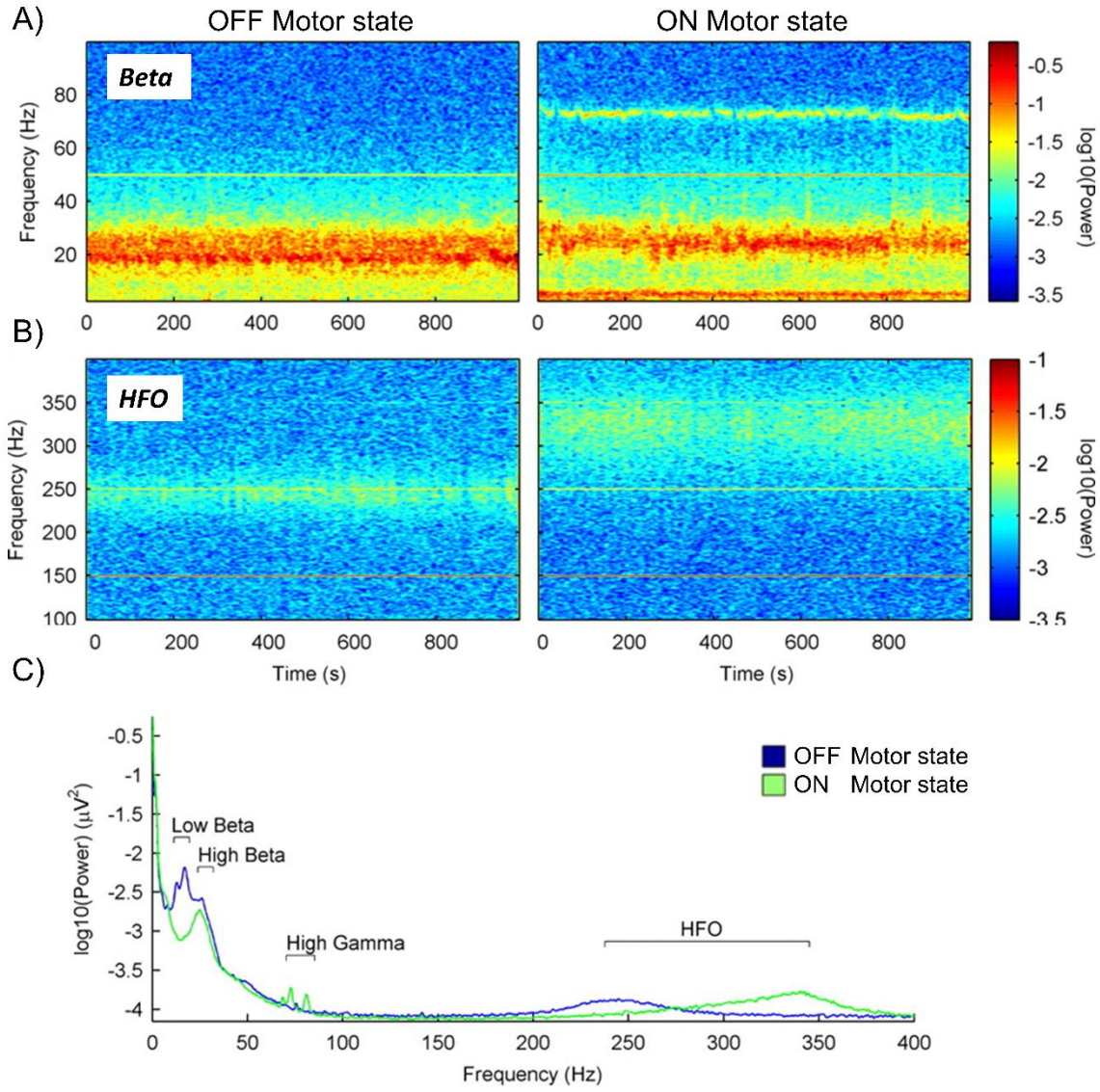

Adapted from *López-Azcárate J et al. Coupling between beta and high-frequency activity in the human subthalamic nucleus may be a pathophysiological mechanism in Parkinson's disease. Journal of Neuroscience. 2010;30(19):6667-77.*

Figure 1.7: Sample of adaptive DBS recordings using a beta amplitude threshold to trigger on-off stimulation.

Channels from bottom to top are: digitally filtered LFPs around the beta peak; running average of filtered beta with the blue horizontal line representing the amplitude threshold that triggers stimulation; stimulation trigger signal; adaptive DBS stimulation pattern. The red box shows a beta burst, resulting in a rise in beta amplitude that triggers stimulation.

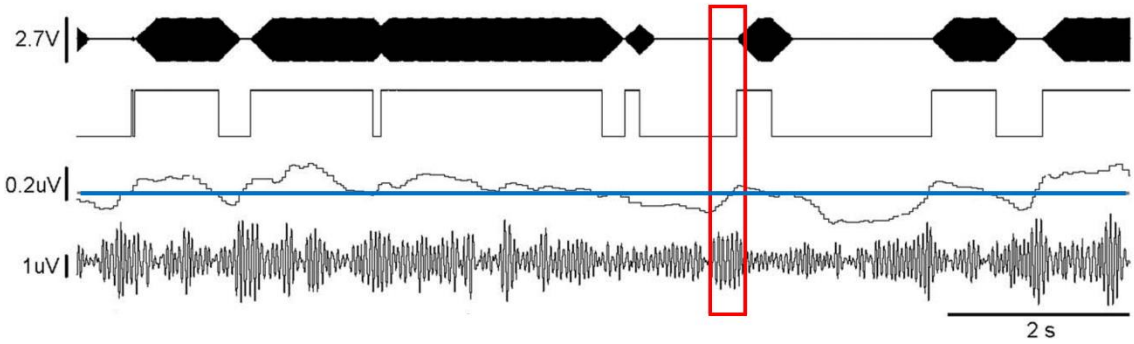

Images courtesy of *Little et al. Adaptive deep brain stimulation in advanced Parkinson disease. Annals of neurology. 2013;74(3):449-57.*

Figure 1.8: Evoked resonant neural activity (ERNA) morphology (a) and modulation by therapeutic DBS (b) recorded from the STN of a PD patient.

(a) ERNA evoked by a 10-pulse burst of stimulation delivered at 3.38 mA, 60 µs and 130 Hz. The red waveform indicates the pulses delivered, black arrows indicate the peak observed between pulses and the green arrows indicate the resonant peaks observed at the end of a burst, with a characteristic decaying amplitude over time. (b) ERNA recorded during DBS delivered at different amplitudes (indicated at top of each plot) at 60 µs and 130 Hz. Amplitude is depicted by colour, with yellow representing ERNA peaks. The x-axis represents the overall stimulation time for each condition and the y-axis represents the time window between pulses in which ERNA can be measured. ERNA frequency decreases and ERNA amplitude increases with higher stimulation amplitudes.

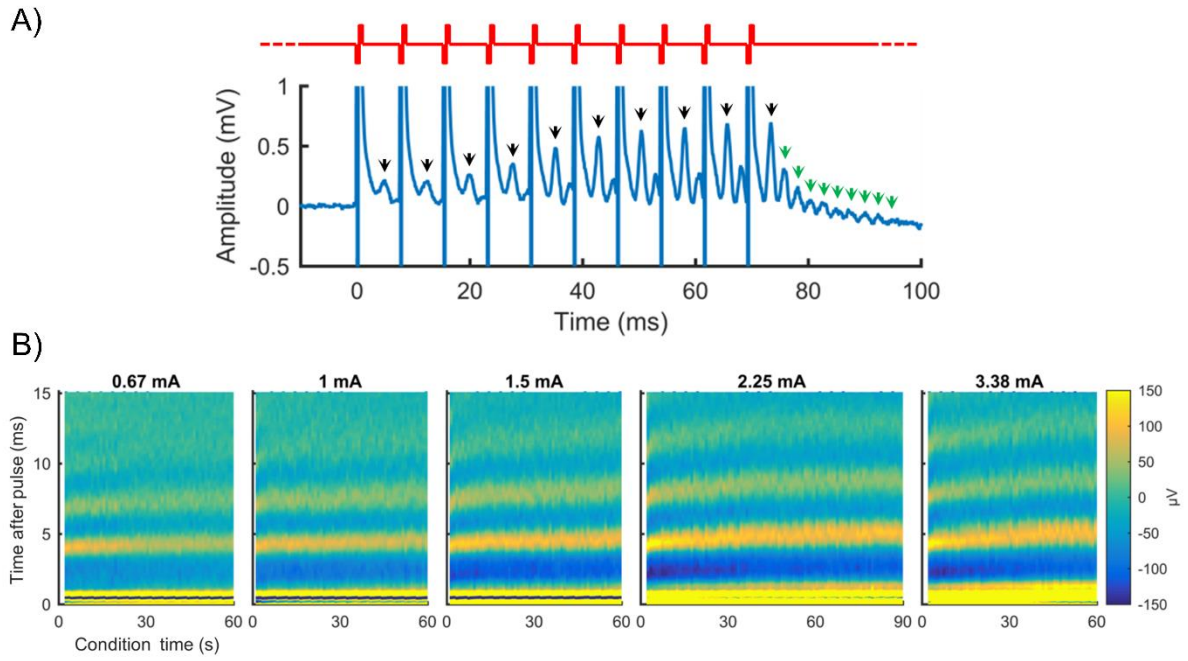

Images courtesy of *Sinclair NC, et al. Subthalamic nucleus deep brain stimulation evokes resonant neural activity. Annals of neurology 2018; 83(5)* and *Sinclair NC, et al. Deep brain stimulation for Parkinson's disease modulates high-frequency evoked and spontaneous neural activity. Neurobiology of Disease 2019b: 104522.*

2 Materials and Methods

The following chapter will outline general materials and methods. Detailed information on the methods for each study are discussed in the subsequent chapters.

2.1 DBS database analysis (Chapter 3)

2.1.1 Cohort derivation

De-identified individualised data on patients with DBS was requested from three linked national databases held by the Australian Federal Government; the Medicare Benefits Schedule (MBS), Pharmaceutical Benefits Scheme (PBS) and the register of the Births, Deaths and Marriages (BDM). The MBS and PBS are publicly funded, national healthcare schemes which subsidise medical services and certain medications for all Australians. DBS surgery for PD has been funded by the federal government since 2002 and for dystonia and essential tremor since 2009. The MBS subsidises all DBS outpatient services such as programming encounters. Inpatient DBS services including implantation surgery and other DBS related surgeries (IPG, extension cable and lead procedures) are subsidised by the MBS for patients who utilise private health insurance. Inpatient DBS related services are also available to the 40% of Australians (ABS, 2017) without private health insurance in state government-funded public hospitals. This information is not captured by the MBS database. However, the proportion DBS procedures undertaken in these state government-funded public hospitals is thought to be small (MSAC, 2006).

The MBS encompasses eight DBS item numbers relating to implantation surgery, programming and hardware maintenance and complication surgery (Table 3.1). Information on all patients recording a DBS related item in the MBS database from 1st January 2002 to the nominated end point of 31st December 2016 was obtained. The medical indication for DBS surgery was not listed (PD, dystonia or essential tremor). Medication prescribing information was obtained from the PBS database. Levodopa responsiveness is a strong predictor of DBS efficacy in PD (Charles *et al.*, 2002; Okun, 2012) so patients were deemed to have a diagnosis

of PD if they had been prescribed levodopa for over one year. A flowchart of the cohort derivation process is shown in Figure 3.1.

2.1.2 Characterisation of cohort and DBS implantation surgery

The demographic details of the cohort including gender and age at time of DBS implantation or other DBS related encounters was collected from the MBS database. Precise details of the DBS implantation procedure could be deduced from the database. For example, specific MBS item numbers fund the neurosurgeon to perform ipsilateral or bilateral electrode implantation surgery. The attendance of a neurologist to assist surgical navigation is also recorded by the MBS (Table 3.1).

2.1.3 DBS maintenance and hardware related complications

The documentation of DBS programming item numbers in the MBS database enabled an estimation of programming frequency. The nature of DBS procedures after the initial DBS implantation surgery was deduced by the combination of DBS related item numbers recorded on the day of surgery (Supplementary table 3.1). Distinctions could therefore be made between routine DBS maintenance procedures (IPG surgery for battery depletion) and hardware complication surgeries involving the intracranial electrodes, extension cables and IPG. All DBS encounters were referenced back to the date of DBS implantation surgery.

2.1.4 Community living and survival

A medical evaluation and admission by a family physician is standard practice for patients entering a residential facility in Australia (Reed, 2015). Medical visits by the family physician into a residential facility are funded by the federal government and recorded in the MBS database. All patients in the study cohort with a residential care related MBS item numbers were identified. The earliest documented residential care related item number was deemed as the date of admission into the care facility.

The date of death of any patients who died during the study period was identified using linked data from the BDM registry. The duration of time from DBS implantation to date of death was calculated to determine survival after DBS surgery.

2.1.5 Statistical analysis

For descriptive statistics, mean and standard deviation and median and interquartile range was used, dependant on data distribution, determined by the Shapiro Wilk test. Sociodemographic and clinical determinants of hardware complication surgery (age, gender, residential care admission) were explored using a univariate logistic regression model and multivariable Cox proportional hazards regression model. The association between the number of IPG changes and the risk of IPG complications was analysed using an Andersen-Gill recurrent events model and adjusted for gender and age at the time of IPG surgery. The sociodemographic and clinical determinants of time from DBS implantation to residential care and death (age, gender, hardware complication surgery, residential care admission) was investigated using a univariate logistic regression model and multivariable Cox proportional hazards regression model. A standardised mortality ratio (SMR) adjusted for gender and age, was calculated using the Poisson regression. Data processing and statistical analysis were performed using R Project 3.4.3 (R core team, Vienna, Austria).

2.2 Neuronal signals, anatomy, and DBS clinical outcomes analysis (Chapters 4 and 5)

2.2.1 Patient selection and surgical technique

We enrolled 50 consecutive patients with PD who had STN DBS for motor fluctuations from the practice registry of neurologist Associate Professor Wesley Thevathasan and neurosurgeon Dr Kristian Bulluss. An additional comprehensive post-operative clinical evaluation was completed on a subset of 14 patients. The studies were conducted in accordance with local and international standards and approved by the St Vincent's Public (HREC-D 071/14 and

HREC/17/SVHM/81), St Vincent's Private (R0236-15), Cabrini Hospital Malvern (02-15-02-16) and Austin Health (SSA/15/Austin/266) Human Research Ethics Committees.

Quadripolar leads (Medtronic, model 3387, 1.5 mm contact spacing) were implanted bilaterally into the STN during awake neurosurgery. Stereotactic surgery was performed using a CRW frame (Integra Lifesciences Corporation, Plainsboro, NJ) and co-registration of a pre-operative 3-dimensional volumetric MRI with a computed tomography (CT) scan. Microelectrode recordings and clinical evaluation were both employed to guide surgical navigation. The middle two contacts of the lead targeted the STN, with the dorsal contact targeting the zona incerta and the ventral contact targeting the substantia nigra pars reticulata (Figure 2.1). Intra-operatively, the lead was attached to an extension cable, externalised through the scalp and connected to a highly configurable, customised neurostimulator (Figure 2.2) (Slater *et al.*, 2015). The neuronal signals were recorded on a biosignal amplifier with a 38.4 kHz sampling rate (g.USBamp, g.tec medical engineering GmbH, Schiedlberg, Austria). After the experimental period, the extension cable was connected to the subcutaneous IPG under general anaesthetic.

2.2.2 Neurophysiological recordings

Neural activity was recorded from each contact in a hemisphere in a monopolar configuration with recordings re-referenced to an average of the four unstimulated contacts in the contralateral hemisphere. LFPs were recorded during an off-stimulation period of 15 seconds, prior to application of burst stimulation. To elicit ERNA, each contact was stimulated sequentially with a ten second burst of stimulation. Each second of stimulation was comprised of ten symmetric 60 μs biphasic pulses delivered at 3.375 mA and 130 Hz.

2.2.3 ERNA signal analysis

Evoked potentials were filtered using a 2^{nd}-order Butterworth high-pass (f_c = 2 Hz) and band-stop filter (f_c = 49-51 Hz) and subsequently processed using a 21-point centered moving-average filter. ERNA signal was recorded after the last pulse of each burst of stimulation. In Chapter 4, the amplitude at the contact of interest was calculated as the average of the root mean square amplitude between 4 to 20 milliseconds measured after stimulation at the three

other contacts on the electrode array (Figure 2.1). The ERNA power was derived by squaring the ERNA amplitude. In Chapter 5, the signal processing and analysis of ERNA was refined. ERNA was recorded from the stimulating contact after the last pulse of each burst. ERNA amplitude was measured by averaging the root mean square amplitude from 3.5 to 20 milliseconds after the onset of the last pulse of each burst and squared to calculate power.

2.2.4 LFP signal analysis

For beta analysis, Blackman-Harris windowed epochs of one second were processed using short-time Fourier transformation with beta power estimated over the 13-30 Hz frequency band (Sinclair *et al.*, 2019b). For HFO analysis, sharp spikes from power line interference was filtered using 2nd-order Butterworth bandstop filters with cutoff frequencies set to +/- 0.5 Hz of the spike frequency based on visual inspection. Thompson's multi-taper spectral estimates (20 tapers) were used to process one second epochs and HFO power was estimated over the 200-400 Hz frequency band (Sinclair *et al.*, 2019b).

Figure 2.1: Intra-operative ERNA recordings from quadripolar DBS leads implanted into the region of the STN.

The four contacts targeted the following structures: inferior – substantia nigra pars compacta, ventral – ventral subthalamic nucleus, dorsal – dorsal subthalamic nucleus, superior - zona incerta. For ERNA recordings, monopolar stimulation was applied to each of the four contacts sequentially (crossed axes indicate stimulated electrode and dashed lines separate stimulation conditions). The panel below represents the ERNA recorded at each contact from 0 to 20 milliseconds after the last pulse of a ten second burst of stimulation.

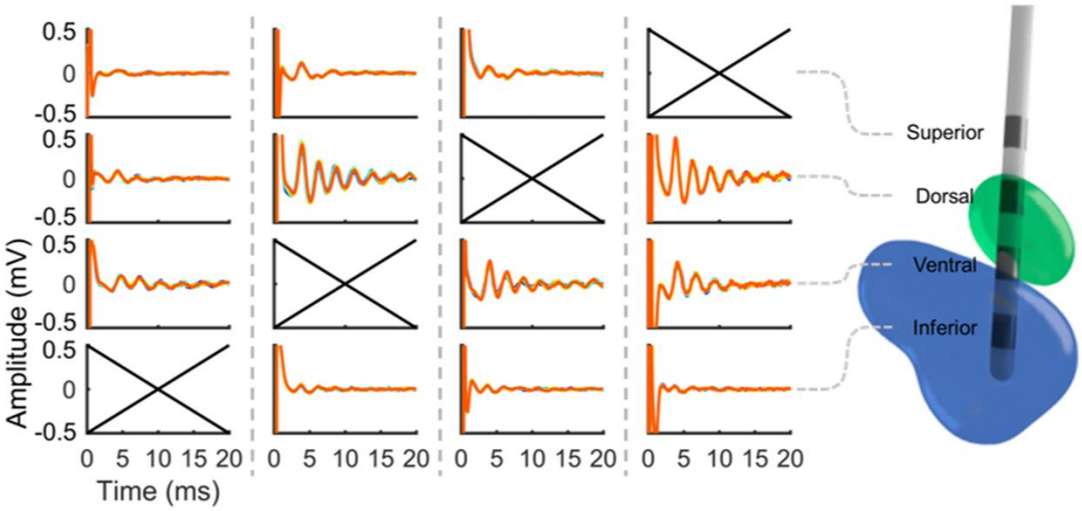

mV = millivolts, ms = milliseconds

Images courtesy of *Sinclair NC, et al. Subthalamic nucleus deep brain stimulation evokes resonant neural activity. Annals of neurology 2018; 83(5)*

Figure 2.2: The intra-operative stimulation and recording system.

The intracranial lead is implanted, externalised and plugged into a patient connector. The patient connector is linked to a relay box which is connected to a customised neurostimulator (neuroBi stimulator) and a biosignal amplifier (g.USBamp amplifier). LFP signals, measured spontaneously, and ERNA signals, elicited with stimulation delivered from the neurostimulator, are recorded by the biosignal amplifier and exported to a laptop for analysis.

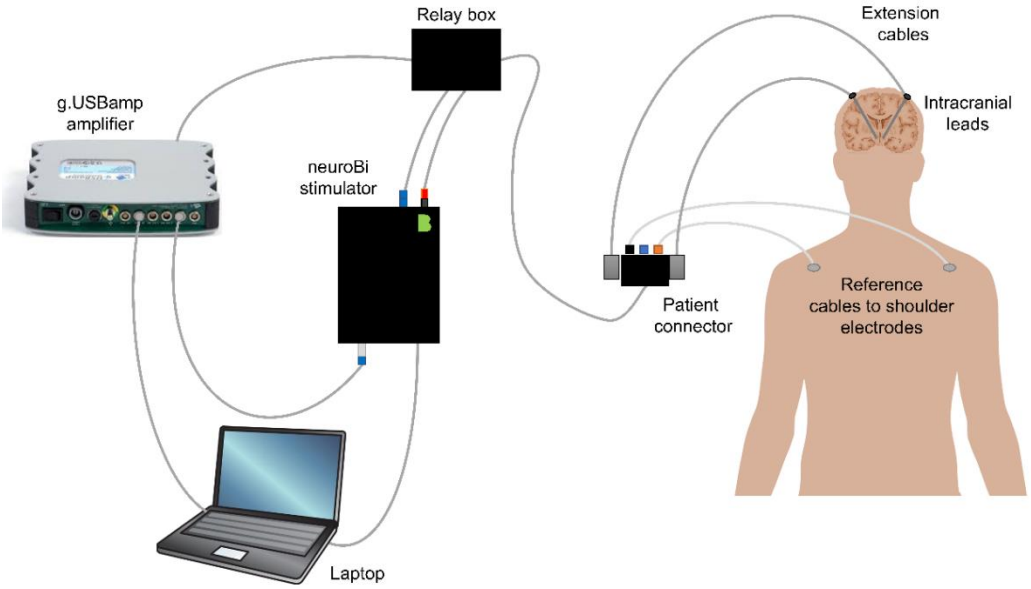

Adapted from image courtesy of Nicholas Sinclair.

2.2.5 Anatomical localisation of electrodes

Post-operative CT were obtained within three days of DBS implantation surgery and co-registered to each patient's pre-operative volumetric MRI Brain scan (BRAINSFit, 3D Slicer). A custom Python script was used for image processing (Python Software Foundation, Python Language Reference, v3.7).

Method 1 (Chapter 4)

Contact location was determined by visually identifying the relevant artefact. The contacts were ranked from one to four according to proximity to a nominated ideal anatomical location to apply DBS. The methodology to identify this ideal anatomical location is described below.

Initially, a local landmark-based targeting technique was employed to identify a putative ideal STN location referenced to the red nucleus, along the anterior border ('Bejjani line'), 2 mm inferior to the superior border and 3 mm from the lateral border (Bejjani *et al.*, 2000). This method has been shown to closely approximate the clinically effective stimulation location (Andrade-Souza *et al.*, 2005; Houshmand *et al.*, 2014). The Euclidean distance from each contact in a hemisphere to the ideal anatomical location derived from the red nucleus-based targeting technique was calculated using a dedicated script on MATLAB R2017a. This technique may not always account for inter-patient variability in size, shape, and position of the STN. As such, each contact location was also visually inspected using the Fluid attenuation inversion recovery (FLAIR) sequence on the pre-operative MRI to confirm the centrality of the contact within the STN and the STN width at that location (ideally > 2mm) (Tripoliti *et al.*, 2008; Hershey *et al.*, 2010). During visual inspection, the clinician was blinded to the clinical and neuronal signal data of the patient. Thirty of 111 rankings using Euclidean distance alone, were adjusted after visual inspection due to the location of the contact within the STN. The four contacts in each hemisphere were ranked according to proximity to the nominated ideal anatomical location to apply DBS.

Method 2 (Chapter 5)

The pre-operative volumetric MRI Brain scan was reorientated to align the anterior and posterior commissures using an automated utility (NITRC, acpcdetect, v2.0). The reoriented MRI and post-operative CT scans were co-registered with BRAINSFit (Fedorov *et al.*, 2012)

(v4.11) and normalized into the Montreal Neurological Institute (MNI) 152 2009b (Collins *et al.*, 1999; Fonov *et al.*, 2011) space using Advanced Normalization Tools SyN (Avants *et al.*, 2008). A PaCER toolbox (Husch *et al.*, 2018) was used to localise DBS leads on the CT with the resultant contact coordinates transformed into MNI space. The ideal location to apply STN-DBS in PD was identified using MNI coordinates provided by Horn et al (Horn *et al.*, 2017a). The Euclidean distance between this location and each contact was calculated using a custom Python script. The DISTAL atlas (Ewert *et al.*, 2018) was used to segment the STN and surrounding structures for 3D visualization. The four contacts in each hemisphere were ranked according to proximity to the nominated ideal anatomical location to apply DBS.

2.2.6 DBS programming

Patients were reviewed by two experienced DBS neurologists after surgery (Associate Professor Wesley Thevathasan and Dr San San Xu). The frequency of programming sessions varied according to clinical need. On average, patients were reviewed, weekly or fortnightly in the first two months after DBS implantation and at one to three-month intervals thereafter. During the programming sessions, clinicians were blinded to the neuronal signal data but had access to the anatomical location of the electrodes. Monopolar configuration was preferentially selected initially. If symptom control was suboptimal or intolerable stimulation side effects emerged, the electrode configuration would at times be adjusted to bipolar or interleave. The clinician programming data 12 months after DBS surgery was obtained from automatically generated reports from the DBS programmer and cross-referenced to patient records.

2.2.7 Post-operative clinical evaluation

A subset of 14 patients underwent a comprehensive motor evaluation (part III, items 20 – 26 of the UPDRS) with a movement disorders neurologist (Dr San San Xu) after surgery. A follow-up period of at least 3 months was implemented to minimise the impact of stun effect on parkinsonian symptoms (Mestre *et al.*, 2016). All patients had an overnight withdrawal of dopaminergic medications. On arrival, the DBS was switched off for 45 minutes and the UPDRS was measured ‘off medication’ and ‘off stimulation’. Thereafter, bilateral monopolar stimulation was delivered through each of the four contacts in a counterbalanced order. If the clinician chosen configuration was not tested in this standard protocol (e.g. clinician selected

bipolar configuration), the chronic stimulation settings were included as an additional condition in the counterbalanced design. The clinician selected chronic stimulation parameters (amplitude, pulse width, frequency) were used for all conditions with the following exceptions:

- When the clinician selected configuration was bipolar, the amplitude selected for monopolar stimulation was reduced by 10%

- The test amplitude was reduced by 25%, 50% or 75% in the presence of stimulation related side effects such as capsular side effects, visual change, nausea or paraesthesia.

The patient and movement disorders neurologist were blinded to the stimulation conditions during clinical evaluations.

2.2.8 Statistical analysis

In each hemisphere, the four contacts on the DBS lead were ranked according to ERNA power, beta power, HFO power or proximity to the nominated ideal anatomical location to apply DBS. In Chapter 4, the degree of acute UPDRS benefit with DBS was calculated according to the following equation:

$$Motor\ benefit\ (\%) = \frac{Off\ DBS\ UDPRS\ score - \ On\ DBS\ UPDRS\ score}{Off\ DBS\ UPDRS\ score} \times 100$$

A mixed effects model (MEM) was applied to evaluate the correlation between neuronal signal power and the acute motor benefit of DBS. A fundamental advantage of the MEM is that it enables simultaneous evaluation of variation due to independent factors of interest (fixed effects) and due to uncontrollable factors (random effects) (McCulloch and Neuhaus, 2005; Baayen *et al.*, 2008). Participants were included as random effects for the model. Hemisphere was not a significant random effect in the model and removed from the final analysis. The order of conditions and the stimulation level tolerated at the given contact (25%, 50%, 75% or 100% of chronic amplitude) were assessed as fixed effects. Only stimulation level correlated with the acute motor benefit from DBS and was therefore retained in the model. The four contacts in each hemisphere, ranked according to the various factors of interest (ERNA, beta,

HFO, anatomy) were assigned as fixed effects to build the final MEM. The MEMs were compared using ANOVA with Bonferroni-holm method employed for post-hoc analysis.

A repeated-measures analysis of variance (ANOVA) was employed to compare the maximal UPDRS DBS benefit in each hemisphere, the UPDRS DBS benefit at the clinician-chosen contact and the UPDRS DBS benefit at the contact ranked first according to neuronal signal power (ERNA, beta, HFO) and anatomy. A repeated-measures ANOVA was also utilised to evaluate 1) the variation in UPDRS DBS benefit across the four contacts in each hemisphere, 2) the variation in neuronal signal power (ERNA, beta, HFO) across the four contacts in each hemisphere, 3) the variation in neuronal signal power across the four contacts in each hemisphere ranked according to proximity to the nominated ideal anatomical location to apply DBS. Tukey's method was used to correct for multiple comparisons (Cooley and Tukey, 1965).

Chapter 5 evaluated all hemispheres where monopolar configuration was employed at 6 months after DBS implantation surgery. In a simple-ranking method, the four contacts on the DBS lead, ranked according to ERNA power, beta power and proximity to the nominated ideal anatomical location to apply DBS were compared to the contacts selected for chronic DBS at 6 months. Then, machine learning algorithms (Logistic regression (LR), Support Vector Machine (SVM), Random forest (RF)) incorporating normalized ERNA, normalized beta oscillations and anatomical data were applied to explore whether combining factors could improve the probability of predicting the clinician-chosen contact. The simple-ranking method and machine learning method were validated using 10-fold nested cross-validation (CV), repeated 10 times. The probability that the model predicted the clinician-chosen contact (predictive value) was calculated as the mean performance of the nested CV folds (Vabalas *et al.*, 2019). Differences between models were evaluated using the Friedman rank sum test and Nemenyi test for multiple comparisons. The machine learning algorithms were built using Scikit-Learn 0.23.2 (Pedregosa *et al.*, 2011) on Python 3.8.5 (Millman and Aivazis, 2011).

All other data processing and statistical analysis were performed using Minitab 18 and R Project 3.4.3 (R core team, Vienna, Austria).

3 Lesser-known aspects of deep brain stimulation for Parkinson's disease: Programming sessions, hardware surgeries, residential care admissions and deaths

San San Xu, FRACP[1,2,3], Charles B. Malpas, MPsych, PhD[4,5], Kristian J. Bulluss, FRACS, PhD [1,6], Hugh J. McDermott, PhD[1,2], Tomas Kalincik, MD, PhD[4,7], Wesley Thevathasan, FRACP, DPhil[1,3,4,7]

[1]Bionics Institute, East Melbourne, Victoria, Australia.

[2]Department of Medical Bionics, The University of Melbourne, East Melbourne, Victoria, Australia.

[3]Department of Neurology, Austin Hospital, Heidelberg, Victoria, Australia.

[4]CORe, Department of Medicine, The University of Melbourne, Parkville, Victoria, Australia.

[5]Melbourne School of Psychological Sciences, University of Melbourne, Parkville, Victoria, Australia.

[6]MS Centre, Department of Neurology, The Royal Melbourne Hospital, Parkville, Victoria, Australia.

[7]Department of Neurosurgery, St Vincent's Hospital Melbourne, Fitzroy, and Department of Neurosurgery, Austin Hospital, Heidelberg, Victoria, Australia.

[8]Department of Medicine, The University of Melbourne, Parkville, Victoria, Australia.

Abstract word count: 300

Manuscript word count: 3994

Number of figures: 2

Number of tables: 3

Key words: deep brain stimulation; Parkinson's disease; programming; complications; outcomes

Abbreviation: DBS = deep brain stimulation, STN = subthalamic nucleus, GPi = Globus pallidus interna, PD = Parkinson's disease, MBS = Medicare Benefits Scheme, PBS = Pharmaceutical Benefits Scheme, BDM = register of Births, Deaths and Marriages, IPG = implantable pulse generator, SMD = standardised mean differences, IQR = interquartile range, SD = standard deviation, HR = hazard ratios, CI = confidence interval, SMR = standardised mortality ratio, ET = essential tremor

3.1 Abstract

Objective: The long-term treatment burden, duration of community living, and survival of patients with Parkinson's disease (PD) after deep brain stimulation (DBS) implantation is unclear. This study aims to determine the frequency of programming, repeat hardware surgeries (of the intracranial electrode, implantable pulse generator (IPG) and extension-cable), and the timings of residential care and death in patients with PD treated with DBS.

Methods: In this cross-sectional, population-based study, individual-level data was collected from the Australian government covering a 15-year period (2002-2016) on 1849 patients with PD followed from DBS implantation.

Results: The mean DBS implantation age was 62.6 years and mean follow-up 5.0 years. Mean annual programming rates were 6.9 in the first year and 2.8 in subsequent years. 51.4% of patients required repeat hardware surgery. 11.3% of patients had repeat intracranial electrode surgery (including an overall 1.1% of patients who were completely explanted). 47.6% of patients had repeat IPG/extension-cable surgery including for presumed battery depletion. 6.2% of patients had early repeat IPG/extension-cable surgery (within one year of any previous such surgery). 30-day post-operative mortality was 0.3% after initial DBS implantation and 0.6% after any repeat hardware surgery. 25.3% of patients were admitted into residential care and 17.4% died. The median interval to residential care and death was 10.2 and 11.4 years, respectively. Age over 65 years was associated with fewer repeat hardware surgeries for presumed complications (any repeat surgery of electrodes, extension-cables and early IPG surgery) and greater rates of residential care admission and death.

Conclusions: Data from a large cohort of patients with PD treated with DBS found that the median lifespan after surgery is ten years. Repeat hardware surgery, including of the intracranial electrodes, is common. These findings support development of technologies to reduce therapy burden such as enhanced surgical navigation, hardware miniaturisation and improved battery efficiency.

3.2 Manuscript

Introduction

Deep brain stimulation (DBS) targeting the subthalamic nucleus (STN) or globus pallidus interna (GPi) in Parkinson's disease (PD) can substantially improve quality of life in selected patients. Over 150,000 people with PD are estimated to have received this therapy worldwide (Hariz, 2017). The motor and nonmotor impact of DBS in PD is well described, for up to 15-years post implantation (Fasano *et al.*, 2010; Castrioto *et al.*, 2011; Zibetti *et al.*, 2011; Odekerken *et al.*, 2016; Limousin and Foltynie, 2019). However, relatively unexplored is the long-term burden imposed by the therapy itself (such as programming and repeat hardware surgeries) and moreover, the duration that these patients remain living in the community and survive. Yet these lesser-known aspects of DBS for PD are crucial to understand for clinical decision-making, health care resourcing and therapy development.

Thus here, in a cross-sectional study using individual-level data from the Australian government (registering medical services, medication dispensing and death), we assessed all 1849 patients identified as having PD and implanted with DBS using private health insurance over a 15-year period. Referenced to the time of initial DBS implantation, we analysed the occurrence of sessions to program stimulation, repeat hardware surgeries, and admissions to residential care and death.

Methods

Cohort selection

Data from de-identified individual patients were requested from three linked national databases held by the Australian Government; the Medicare Benefits Schedule (MBS), the Pharmaceutical Benefits Scheme (PBS) and the register of Births, Deaths and Marriages (BDM). Ethics approval and patient consent were not required as this information is available on request by the general public. The MBS and PBS are national-government funded healthcare schemes in Australia which subsidise outpatient medical services (such as DBS programming) and medications (such as levodopa) for all Australians and inpatient services for those who

utilise private health insurance. Our data do not capture inpatient services (e.g. DBS surgeries) for Australians without private health insurance (around 40%) (ABS, 2017), which is provided by state-government funded public hospitals. However, the majority of DBS systems are implanted in private facilities in Australia (MSAC, 2006).

The MBS codes medical services as 'item numbers' which include various types of consultations and eight specific DBS services (Table 3.1). The PBS documents the dispensing of medications. The exact timing of PBS and MBS data is liable to clerical error (as these systems are designed to register billable events) so we conservatively assumed that these occurred within a 30-day window of the date documented. In contrast, the BDM registry records the specific date of death according to certificates completed by medical practitioners (Births Deaths and Marriages Victoria, 2019).

Data were requested for all patients with any DBS related item number in a 15-year period from 1st January 2002, when DBS was first funded by the Australian Government, until the nominated endpoint of 31st December 2016. DBS is funded in Australia for the treatment of PD, essential tremor and dystonia and the indication is not coded. In order to identify patients with PD, we selected those who were prescribed levodopa for at least 12 months (Charles *et al.*, 2002; Okun, 2012). The neurosurgical target is also not coded. Common clinical practice in Australia suggests that the majority of patients were implanted in the STN (and less often in the GPi) for motor fluctuations, with some patients implanted in the thalamic region for tremor (Poortvliet *et al.*, 2015). The follow-up duration was calculated from the date of DBS implantation to the study endpoint of 31st December 2016 or date of death (whichever occurred first).

Analysis of DBS events

Specific MBS item numbers fund DBS related surgical procedures and intraoperative target localisation by the neurologist (Table 3.1). The first occurrence of electrode implantation (40850 or 40851) was considered the date of initial DBS implantation. DBS surgery in Australia during the study period was performed by a limited number of surgical teams (< 20) (Poortvliet *et al.*, 2015). The widely practised DBS implantation method for PD in Australia is to use MRI planning, framed stereotaxy and intraoperative navigation assisted by a neurologist with single-track microelectrode recordings and clinical assessments on awake patients (Machado *et al.*, 2006; Montgomery Jr, 2012).

After surgery, the MBS funds the neurologist to program DBS (40862), recorded once for unilateral or twice for bilateral adjustments. We considered one or more DBS programming item numbers on the same day as a single programming session.

The indication for repeat hardware surgeries was not coded. A specific item number funds the revision or removal of brain electrodes (40854) and placement, removal, or replacement of the extension-cable (40858). Combining item numbers yielded a basic classification of repeat hardware surgeries including identifying the occurrence of whole system explantation (Supplementary table 3.1).

Specific item numbers segregate IPG placement (40852) from IPG removal or replacement (40856). We classified the first occurrence of IPG placement occurring within six months of the electrode implantation (to account for staged procedures) as the initial, un-complicated subcutaneous system placement. Otherwise, IPG and/or extension-cable item numbers were grouped as occurring within one year ('early') or after one year ('late') relative to any previous such surgery (including initial IPG implantation). The 'early repeat surgery' group will capture procedures for complications such as infection, erosion, malposition, electrical malfunction and discomfort (Lyons *et al.*, 2004; Patel *et al.*, 2015). Within this group, we identified instances where there was removal, then replacement of both the IPG and extension-cable two weeks to six months later, and classified these as 'presumed surgery for infection/erosion' (Pepper *et al.*, 2013; Bjerknes *et al.*, 2014; Hardaway *et al.*, 2017; Helmers *et al.*, 2018). The 'late repeat surgery' group will capture procedures for complications and uncomplicated battery depletion (Oh *et al.*, 2002; Patel *et al.*, 2015; Helmers *et al.*, 2018). Within that group, isolated IPG procedures were considered due to 'presumed battery depletion' (Goodman *et al.*, 2006; Ondo *et al.*, 2007; Halpern *et al.*, 2011) . In further analyses, we sought relationships between surgical complications and various factors such as patient age, residential care admission and death. We considered that the following repeat surgeries were due to a 'presumed complication'; early repeat surgery of the IPG/extension-cable and any repeat surgery of the intracranial electrodes or extension-cable. However, as the indications for surgery were not specifically coded, we sought to identify complications and battery depletions based on assumptions such as the predominant use of dual channel rather than single channel IPGs (e.g. Kinetra rather than Soletra, Medtronic Inc. Dublin).

Analysis of residential care admissions and death

A medical assessment by a family physician is standard practice for patients entering residential care (Reed, 2015). Such visits are funded by specific residential care MBS item numbers (e.g. 5265, 5028), the first of which was considered to represent the timing of admission into residential care. Date of death is recorded in the BDM database.

Statistical analysis

Data processing and statistical analysis was conducted using R Project version 3.4.3 (R Development Core Team, 2017). Normality was tested using the Shapiro-Wilk test. To compare the study and excluded cohorts, we calculated the standardized mean differences (SMD) across the variables of interest, setting the threshold for mean difference at > 0.1. Descriptive statistics employed mean and standard deviation (SD) or median and 1st to 3rd interquartile range (IQR). Categorical variables were assessed as a percentage of the total cohort of 1849 patients, unless stated otherwise. The proportion of patients needing repeat surgeries after DBS implantation and the median times to IPG change, residential facility placement and death were evaluated using the Kaplan-Meier method. Sociodemographic and clinical determinants (age at surgery, gender, residential care admissions) of surgical complication rates, community living, and survival were analysed in a univariate logistic regression model and multivariable Cox proportional hazards regression model. An Andersen-Gill model for recurrent events was used to analyse the association between the number of IPG changes and the risk of early IPG complication and adjusted for gender and age at the time of IPG surgery. Hazard ratios (HR) are shown with a 95% confidence interval (CI). The number of deaths in this cohort was compared to the expected number of deaths based on mortality rates in Australia from 2002-2016. A standardised mortality ratio (SMR) adjusted for gender and age, was calculated using the Poisson regression. The model was built using the popEpi package (Miettinen *et al.*, 2016) on R Project version 3.4.3 (R Development Core Team, 2017).

Results

Cohort selection and demographic details

3095 patients registered DBS related item numbers in the MBS database between 1st January 2002 to 31st December 2016, of which 2348 (75.9%) had been dispensed levodopa for over a

year and thus considered to have PD (Figure 3.1). The 747 excluded DBS patients (who were not dispensed levodopa for over 12 months) likely represent those implanted for essential tremor and dystonia (the other funded indications in Australia).

499 of the 2348 PD DBS patients (21.3%) were excluded as their date of initial DBS implantation was unknown and comprised two groups: (1) 452 had no documented DBS implantation. 42 recorded their first DBS related item number in 2002, suggesting that DBS had been implanted before the study period. The remaining 410 patients may have been implanted in the state-government funded public hospitals. These patients could represent almost all PD patients implanted with DBS in that system, with subsequent outpatient encounters such as DBS programming being funded by MBS and captured in our dataset. (2) 47 patients had DBS implantation documented over 30 days after their first DBS item number. This may simply reflect instances of clerical error outside the tolerance of this study (30 days) or represent patients implanted in a state-government funded public hospital who had DBS re-implanted or co-implanted using private health insurance.

Thus, the final study cohort comprised 1849 PD patients with a documented date of initial DBS implantation during the study period. The mean age at initial DBS implantation was 62.6 (SD 8.9) years and 64.9% (1200/1849) were male. Their demographic details including gender distribution and age at residential care admission and death did not differ from the excluded group of 499 PD-DBS (Table 3.2, SMD < 0.06 across all comparators). However, the excluded PD-DBS group had a higher rate of residential care admission (SMD = 0.2) and death (SMD = 0.2) during the study period.

Initial DBS implantation

The annual rate that the cohort was implanted with DBS grew over the initial ten years of the study period then plateaued (Figure 3.2A). The mean postoperative follow-up was 5.0 (SD 3.2) years. The vast majority of patients had simultaneous bilateral implantation (95.9%, 1773/1849) and intra-operative target localisation by a neurologist (91.5%, 1692/1849) at the time of DBS surgery.

Programming

In the first year after surgery, there was an average of 6.9 (SD 5.0) programming sessions, which decreased to 2.8 (SD 2.3) annually in subsequent years (Supplementary table 3.2).

Repeat hardware surgery

51.2% of patients (946/1849) had repeat hardware surgery (1718 procedures) during follow up after initial DBS implantation (Table 3.3). 10.5% of patients (194/1849) had repeat hardware surgery (252 procedures) within one year of initial DBS implantation (Supplementary table 3.3).

Surgery of the intracranial electrodes

11.3% of patients (209/1849) had repeat surgery (301 procedures) involving the intracranial electrodes (Table 3.3). This included an overall 1.1% of patients (21/1849) with a whole system explant, of whom 16/21 were reimplanted during the study period. The proportion of surviving patients with at least one repeat surgery of an intracranial electrode at five years was 12.2% and at ten years was 15.1% (Supplementary figure 3.1). Intracranial electrode surgery accounted for 17.5% (301/1718) of repeat hardware surgeries.

Surgery of the IPG and/or extension-cable

47.6% of patients (880/1849) had repeat surgery (1417 procedures) of the IPG and/or extension-cable (Table 3). 1043 procedures involved only the IPG, 339 procedures involved the IPG and extension-cable and 35 procedures involved only the extension-cable.

Early (< one year) repeat surgery of the IPG and/or extension-cable

6.2% of patients (114/1849) had early repeat surgery of the IPG/extension-cable. The proportion of surviving patients who had early repeat surgery of the IPG and/or extension-cable at five years was 5.7% and at ten years was 10.7%. 3.8% of patients (70/1849) had early repeat surgery of both the IPG and extension-cables. This included an overall 2.8% of patients (52/1849) who had removal, then replacement two weeks to six months later, of both the IPG and extension-cable (presumed surgery for infection/erosion). 2.2% of patients (40/1849) had early repeat surgery of the IPG alone. 1.0% of patients (18/1849) had early repeat surgery of the extension-cable alone.

Late (> one year) repeat surgery of the IPG and/or extension-cable

45.0% of patients (832/1849) had late repeat surgery of the IPG/extension-cable. The proportion of surviving patients who had late repeat surgery at five years was 63.5% and at ten years was 99.1%. 35.1% of patients (649/1849) had late repeat surgery of the IPG alone (presumed replacement for uncomplicated battery depletion). 12.1% of patients (224/1849) had late repeat surgery of both the IPG and extension-cables. 0.8% of patients (14/1849) had late repeat surgery of the extension-cable alone.

Predictive factors

A greater number of preceding IPG changes was associated with a higher rate of early repeat surgery of the IPG/extension-cable (HR 3.7, 95% CI 3.0-4.6, p <0.001). Early repeat surgery of the IPG/extension-cable was not associated with patient gender (male HR 1.1, 95% CI 0.8 – 1.7, p = 0.5) or age at the time of the procedure (HR 1.0, 95% CI 0.9-1.0, p = 0.10).

15.8% of patients (292/1849) had repeat hardware surgery for a presumed complication (i.e. early repeat surgery of the IPG/extension-cable and any repeat surgery of the intracranial electrodes or extension-cable). The proportion of surviving patients who had repeat hardware surgery for a presumed complication at five years was 16.4% and at ten years was 24.3%.

Univariate analysis revealed an association between DBS implantation age over 65, residential care facility admission and repeat hardware surgery for a presumed complication. On multivariable analysis, DBS implantation age over 65 was associated with a lower rate of repeat hardware surgery for a presumed complication (HR 0.7, 95% CI 0.5-0.9, p = 0.003) and residential care admission was associated with a higher rate of repeat hardware surgery for a presumed complication (HR 1.5, 95% CI 1.2-1.9, p = 0.002).

Residential care admission

The mean age at entry into residential care was 69.9 (SD 6.9) years, which did not differ between genders (male = 69.8 SD 6.9, female = 70.2 SD 7.0, p = 0.5). 2.8% of patients (51/1849) had initial DBS implantation whilst in residential care. 25.3% (467/1849) were admitted into residential care after DBS implantation during the study period. The median time from DBS implantation to residential care admission was 10.2 years (IQR = 5.2-14.0) (Figure 3.2B).

Predictive factors

DBS implantation age over 65 was associated with a higher rate of residential care admissions (HR 3.6, 95% CI 3.0-4.4, p <0.001). Gender (male; HR 0.8, 95% CI 0.7-1.0, p = 0.09) and repeat hardware surgery for a presumed complication (HR 0.9, 95% CI 0.8-1.2, p = 0.6) were not associated factors.

Death

17.4% of patients (321/1849) died during the study period. The mean age at death was 72.9 (SD 7.0) years with no difference between genders (male = 72.9 SD 6.8, female = 72.9 SD 7.6, p = 0.9). The median time from initial DBS implantation to death was 11.4 years (IQR = 7.9-15.0) (Figure 3.2C). Of patients who died, 68.8% (221/321) were in residential care. The median time from residential care admission to death was 4.2 years (IQR = 2.1-8.6) (Figure 3.2D).

The overall standardised mortality ratio was 2.3 (95% CI 2.0-2.6, p = 0.004) compared to the general Australian population, adjusted for gender and age (male SMR = 2.2, 95% CI 1.8-2.5, female SMR = 2.5, 95% CI 1.9-3.2).

Perioperative deaths

0.6% of patients (11/1849) died within 30 days of any DBS surgery. The risk of peri-operative death after initial DBS implantation was 0.3% (5/1849) and after any repeat hardware surgery was 0.6% (6/946). The death rate per procedure was as follows; 0.3% (5/1849) after initial DBS implantation, 0.5% (1/209) after repeat surgery of the intracranial electrodes, 1.0% (1/100) after early repeat surgery of the IPG/extension-cable and 0.5% (4/832) after late repeat surgery of the IPG/extension-cable (Supplementary table 3.4).

Predictive factors

Univariate analysis revealed an association between DBS implantation age over 65, admission into residential care, repeat hardware surgery for a presumed complication and survival. On multivariable analysis, DBS implantation age over 65 (HR 2.5, 95% CI 2.0-3.2, p<0.001) and admission into residential care (HR 2.8, 95% CI 2.2-3.6, p<0.001) were associated with reduced survival.

Discussion

We used linked government databases, containing data on individual patients, to determine the treatment burden, and the timing of residential care and death, in patients with PD implanted with DBS. We identified 1849 patients with PD implanted with DBS within a 15-year period in Australia funded by private health insurance. The average age at initial implantation was 62.6 years old. Average annual programming rates declined from 6.9 in the first year to 2.8 in subsequent years. Surgery for presumed complications were common, affecting 16.4% of surviving patients five years after DBS surgery and 24.3% of surviving patients ten years after DBS surgery. Residential care admission occurred at a median of 10.2 years, and death after a median of 11.4 years, after initial DBS implantation. In patients with DBS implanted after age 65 years, repeat surgery for presumed complications were less frequent and transition to residential care and death were more common.

We acknowledge limitations in this study. First, the cohort reflects clinical practice in Australia, and may not be generalisable to all health services. Second, we identified patients with PD based on being prescribed levodopa for over 12 months (Gibb and Lees, 1988a; Bronstein *et al.*, 2011). An indeterminant but likely small number of patients with essential tremor or dystonia (the other funded indications) may have received long term levodopa and thus been included. Third, the surgical target was not coded. Therefore, our cohort will comprise a heterogeneity of targets, indications, and underlying PD phenotypes. Although the STN is the preferred DBS target for PD motor fluctuations in Australia, many patients will have been implanted in the GPi (Poortvliet *et al.*, 2015). Moreover, some patients will have been implanted in the thalamus for tremor predominant PD, which may carry a different prognosis (Marras *et al.*, 2002; Rajput *et al.*, 2009; Selikhova *et al.*, 2009). Fourth, our identification of 'presumed' complications and uncomplicated battery depletions was based on assumptions which may have led to the over-estimation or under-estimation of the true rate of these events. Fifth, we assessed only DBS implantations funded by private health insurance, raising a socioeconomic bias. However, such insurance is held by around 60% of Australians (ABS, 2017) and funds a large proportion of DBS surgeries in Australia (MSAC, 2006). We identified a cohort of 499 PD patients which likely included those implanted without private insurance. This group did not differ in age at residential care admission or death compared with the study group. Patients in the study cohort may have moved overseas or relinquished their private health insurance after DBS implantation, with subsequent DBS procedures missed by our data. However, the rate of patients over 50 relinquishing private health insurance in

Australia was low in the study period (APRA, 2019). Finally, we did not have an available control group of matched PD patients who did not receive DBS.

Programming

Our study is the first to systematically explore DBS programming rates. Programming was most frequent in the first postoperative year (mean 6.9 sessions), as expected to tailor settings and account for stun effect and medication washout (Mestre *et al.*, 2016). Thereafter, programming rates stabilized at three sessions annually. Such rates of programming could be considered modest, given that more programming is reported to improve outcomes in PD (Okun *et al.*, 2005; Moro *et al.*, 2006). Importantly, these results precede directional devices, which have greater programming complexity (Schüpbach *et al.*, 2017).

Repeat hardware surgeries

A reliable estimate of hardware surgeries after DBS implantation has been limited by the absence of standardised classification and reporting (Videnovic and Metman, 2008). Surgery to replace or revise DBS hardware has primarily been assessed in studies from high-volume, academic single centres as retrospective database reviews (Joint *et al.*, 2002; Oh *et al.*, 2002; Blomstedt and Hariz, 2005; Voges *et al.*, 2006; Videnovic and Metman, 2008; Falowski *et al.*, 2015). Such studies could underestimate complication rates. We found that 15.8% of patients had repeat surgery for a presumed complication, a similar rate to previous reports (Umemura *et al.*, 2003; Doshi, 2011; Jitkritsadakul *et al.*, 2017). Prior studies suggest that repeat surgery of intracranial electrodes is needed in 5% to 13% of patients (Oh *et al.*, 2002; Lyons *et al.*, 2004; Voges *et al.*, 2006; Falowski *et al.*, 2015; Patel *et al.*, 2015). An intriguing population level study by Rolston and colleagues analysed over 28,000 DBS related procedures from two large North American databases and suggested that intracranial electrode surgery accounted for 15% and 34% of procedures (Rolston *et al.*, 2016). In our cohort, intracranial electrode surgery accounted for 17.5% of all repeat hardware surgeries. However, our study also contained individual-level data capable of assessing the rates per patient. Here, we found that 11.3% of the 1849 patients had repeat surgery involving the intracranial electrodes. 1.1% of patients had a whole system explant, supporting published literature of similar rates of intracranial infection (Bjerknes *et al.*, 2014; Tolleson *et al.*, 2014; Fernández-Pajarín *et al.*, 2017). Previous reported rates of IPG infections vary greatly, ranging from 1% - 15% (Oh *et al.*, 2002; Lyons *et al.*, 2004; Voges *et al.*, 2006; Sillay *et al.*, 2008; Videnovic and Metman,

2008; Gorgulho *et al.*, 2009; Follett *et al.*, 2010; Vergani *et al.*, 2010; Fenoy and Simpson Jr, 2012; Bjerknes *et al.*, 2014). We estimated that 2.8% of patients had early repeat surgery of the IPG/extension-cable for presumed infection/erosion. However, the true infection/erosion rate may be greater, as our analysis would miss patients treated outside of our assumptions (e.g. infections not treated with device explantation, devices reimplanted within two weeks of explantation or devices not reimplanted within six months of explantation).

An important consideration is that only complications resulting in surgery were recorded. Complications may have been tolerated without intervention. Advanced age was associated with a lower rate of repeat hardware surgery for a presumed complication, corroborating findings from Rolston et al (Rolston *et al.*, 2016). Furthermore, a study of an older veterans database in the United States found significantly lower electrode removal rates (8.7%) and electrode revision rates (6.5%) (Stroupe *et al.*, 2019). This may reflect a reluctance to re-operate on older patients, rather than indicating lower rates of complications in the elderly.

We found that repeat hardware surgeries conferred significant risk. In keeping with previous reports, the peri-operative mortality after DBS implantation was 0.3%[34, 36, 54]. Interestingly, 30-day mortality was greater (0.6%) with repeat hardware surgery (including an IPG change). This may relate to the increasing frailty of patients over time (Shinall *et al.*, 2020). Importantly, a greater number of preceding IPG procedures was also associated with an increased risk of early repeat surgery of the IPG/extension-cable (Pepper *et al.*, 2013; Thrane *et al.*, 2014; Fytagoridis *et al.*, 2016).

Our findings demonstrate that patients remain in the community and survive for over ten years after DBS implantation, during which time repeat hardware surgeries are common. These additional surgeries are risky, costly and impose therapy burden on patients and health services (Dang *et al.*, 2019; Deng *et al.*, 2020). Our findings support the development of technologies to reduce repeat hardware surgery, such as improved surgical navigation to decrease electrode misplacement, and strategies to minimise hardware complications and IPG depletion. Automated methods to identify the relevant anatomical and functional locations to guide lead implantation (Telkes *et al.*, 2016; Dembek *et al.*, 2019; Horn, 2019) and assist clinician programming (Fernández-García *et al.*, 2017; Tinkhauser *et al.*, 2018; Telkes *et al.*, 2020) are under development. Directional leads can offer partial compensation for suboptimal lead location, though are associated with increasing programming complexity (Schüpbach *et al.*, 2017). Methods exploring the miniaturization, cranialization and antibiotic impregnation of

IPG devices could significantly reduce repeat IPG procedures (Krauss *et al.*, 2020). Development of closed loop DBS systems could substantially improve programming burden and lengthen battery life (Little *et al.*, 2013; Priori *et al.*, 2013; Meidahl *et al.*, 2017).

DBS long-term outcomes

The median survival after DBS implantation was 11.4 years. Previously, reported survival rates after DBS have varied greatly, with ten year survival ranging from 50-70% (Castrioto *et al.*, 2011; Lilleeng *et al.*, 2014; Ngoga *et al.*, 2014; Rocha *et al.*, 2014; Bang Henriksen *et al.*, 2016; Hitti *et al.*, 2019). Disparities in survival may be attributed to differences in follow-up duration, single-centre biases and analysis of discrete patient subgroups (Castrioto *et al.*, 2011; Zibetti *et al.*, 2011; Lilleeng *et al.*, 2014; Ngoga *et al.*, 2014; Rocha *et al.*, 2014; Bang Henriksen *et al.*, 2016; Weaver *et al.*, 2017; Contarino *et al.*, 2018). For example, the United States veterans' database assessed an older cohort (average implantation age of 69 years) and reported a median survival from surgery of only seven years (Weaver *et al.*, 2017).

Our finding of a standardised mortality ratio of 2.3 is similar to that reported in other PD patients (Schrag *et al.*, 1998; Hely *et al.*, 2008), including those who have had DBS (Schüpbach *et al.*, 2007; Cubo *et al.*, 2018). Furthermore, we found an average duration from residential care until death of four years, which is similar to all patients with PD (Hely *et al.*, 1999; Kempster *et al.*, 2010). A body of evidence suggests that DBS could possibly improve disease progression and/or survival in PD (Wallace *et al.*, 2007; Harnack *et al.*, 2008; Spieles-Engemann *et al.*, 2010). Three clinical studies have attempted to address this issue, comparing PD patients treated with DBS to various control groups (historical population based (Lilleeng *et al.*, 2014), propensity-score matched (Weaver *et al.*, 2017) or patients with PD who declined DBS (Ngoga *et al.*, 2014)). Two of these studies suggested a potential modest benefit from DBS (Ngoga *et al.*, 2014; Weaver *et al.*, 2017). Importantly, our study did not have a control group, so we were unable to specifically address this issue.

Conclusion

Data from a large cohort of patients with PD who underwent DBS found that the median lifespan after surgery is over ten years. Repeat surgery, including that of the intracranial electrodes, is common and increases risk for further surgery and mortality. These findings

support the development of technologies to reduce therapy burden such as enhanced surgical navigation, hardware miniaturisation and improved battery efficiency.

Authors' contributions

SS.X was involved with the conception, organisation and execution of the research project, the design and execution of the statistical analysis and the writing and review of the manuscript. C.B.M was involved in the execution of the research project and the design and execution of the statistical analysis and the review and critique of the manuscript. K.J.B was involved in the conception, organisation and execution of the research project and the review and critique of the manuscript. H.J.M was involved in the conception and organisation of the research project and the review and critique of the manuscript. T.K was involved in the organisation and execution of the research project and design and execution of the statistical analysis and the review and critique of the manuscript. W.T was involved in the conception, organisation, and execution of the research project and in the writing, review and critique of the manuscript.

Funding

This work was supported by the Colonial Foundation, St Vincent's Hospital Research Endowment Fund, and the National Health and Medical Research Council (project grant #1103238). The Bionics Institute acknowledges the support it receives from the Victorian Government through its operational infrastructure program. SS.X is supported by the National Health and Medical Research Council. T.K is supported by the National Health and Medical Research Council and the Faculty of Medicine, Dentistry and Health Sciences, University of Melbourne. W.T is supported by Lions International and the National Health and Medical Research Council.

Competing interests

W.T., K.J.B., H.J.M. are founders and hold shares and /or options in DBS Technologies Pty Ltd which plans to commercialise the use of neuronal signals to improve DBS. W.T., K.J.B., H.J.M. are named inventors on related patents, which are assigned to DBS Technologies. SS.X holds options in DBS Technologies Pty Ltd. W.T. has received honoraria from Medtronic and Boston Scientific. All other authors report no competing interests.

3.3 References

ABS.Stat datasets. [cited 9th February 2021]; Available from: http://stat.data.abs.gov.au/

ABS. Health Service Usage and Health Related Actions, Australia, 2014-15 Australian Bureau of Statistics; 2017.

APRA. Private health insurance statistical trends. Australian Prudential Regulation Authority 2019(September 2019).

Bang Henriksen M, Johnsen EL, Sunde N, Vase A, Gjelstrup MC, Ostergaard K. Surviving 10 years with deep brain stimulation for Parkinson's disease--a follow-up of 79 patients. Eur J Neurol 2016; 23(1): 53-61.

Births Deaths and Marriages Victoria. Legal requirements for doctors. 2019 14/06/2019 [cited 2019 16/07/2019]; Available from: https://www.bdm.vic.gov.au/service-partnersmedical-practitioners/legal-requirements-for-doctors

Bjerknes S, Skogseid IM, Sæhle T, Dietrichs E, Toft M. Surgical site infections after deep brain stimulation surgery: frequency, characteristics and management in a 10-year period. PloS one 2014; 9(8): e105288-e.

Blomstedt P, Hariz M. Hardware-related complications of deep brain stimulation: a ten year experience. Acta neurochirurgica 2005; 147(10): 1061-4.

Bronstein JM, Tagliati M, Alterman RL, Lozano AM, Volkmann J, Stefani A, *et al.* Deep brain stimulation for Parkinson disease: an expert consensus and review of key issues. Archives of neurology 2011; 68(2): 165-.

Castrioto A, Lozano AM, Poon Y-Y, Lang AE, Fallis M, Moro E. Ten-year outcome of subthalamic stimulation in Parkinson disease: a blinded evaluation. Archives of neurology 2011; 68(12): 1550-6.

Charles P, Van Blercom N, Krack P, Lee S, Xie J, Besson G, *et al.* Predictors of effective bilateral subthalamic nucleus stimulation for PD. Neurology 2002; 59(6): 932-4.

Contarino MF, Marinus J, van Hilten JJ. Does deep brain stimulation of the subthalamic nucleus prolong survival in Parkinson's Disease? Movement Disorders 2018; 33(6): 947-9.

Cubo E, Rajalingam R, Fasano A, Munhoz RP, Lang A, Calvo S, *et al.* A 21-year retrospective study of the Toronto Western Hospital deep brain stimulation cohort. Movement Disorders 2018; 33(5): 850-2.

Dang TTH, Rowell D, Connelly LB. Cost-Effectiveness of Deep Brain Stimulation With Movement Disorders: A Systematic Review. Movement Disorders Clinical Practice 2019; 6(5): 348-58.

Dembek TA, Roediger J, Horn A, Reker P, Oehrn C, Dafsari HS, *et al.* Probabilistic Sweetspots Predict Motor Outcome for DBS in Parkinson's Disease. Annals of neurology 2019.

Deng H, Yue JK, Wang DD. Trends in safety and cost of deep brain stimulation for treatment of movement disorders in the United States: 2002–2014. British Journal of Neurosurgery 2020: 1-8.

Doshi PK. Long-term surgical and hardware-related complications of deep brain stimulation. Stereotactic and functional neurosurgery 2011; 89(2): 89-95.

Falowski SM, Ooi YC, Bakay RA. Long-Term Evaluation of Changes in Operative Technique and Hardware-Related Complications With Deep Brain Stimulation. Neuromodulation 2015; 18(8): 670-7.

Fasano A, Romito LM, Daniele A, Piano C, Zinno M, Bentivoglio AR, *et al.* Motor and cognitive outcome in patients with Parkinson's disease 8 years after subthalamic implants. Brain : a journal of neurology 2010; 133(9): 2664-76.

Fenoy AJ, Simpson Jr RK. Management of device-related wound complications in deep brain stimulation surgery. Journal of neurosurgery 2012; 116(6): 1324-32.

Fernández-García C, Foffani G, Dileone M, Catalán-Alonso M, González-Hidalgo M, Barcía J, *et al.* Directional local field potential recordings for symptom-specific optimization of deep brain stimulation. Movement disorders: official journal of the Movement Disorder Society 2017; 32(4): 626.

Fernández-Pajarín G, Sesar A, Ares B, Relova J, Arán E, Gelabert-González M, *et al.* Delayed complications of deep brain stimulation: 16-year experience in 249 patients. Acta neurochirurgica 2017; 159(9): 1713-9.

Follett KA, Weaver FM, Stern M, Hur K, Harris CL, Luo P, *et al.* Pallidal versus subthalamic deep-brain stimulation for Parkinson's disease. New England Journal of Medicine 2010; 362(22): 2077-91.

Fytagoridis A, Heard T, Samuelsson J, Zsigmond P, Jiltsova E, Skyrman S, *et al.* Surgical replacement of implantable pulse generators in deep brain stimulation: adverse events and risk factors in a multicenter cohort. Stereotactic and functional neurosurgery 2016; 94(4): 235-9.

Gibb W, Lees A. The relevance of the Lewy body to the pathogenesis of idiopathic Parkinson's disease. Journal of Neurology, Neurosurgery & Psychiatry 1988; 51(6): 745-52.

Goodman R, Kim B, McClelland S, Senatus P, Winfield L, Pullman S, *et al.* Operative techniques and morbidity with subthalamic nucleus deep brain stimulation in 100 consecutive patients with advanced Parkinson’s disease. Journal of Neurology, Neurosurgery & Psychiatry 2006; 77(1): 12-7.

Gorgulho A, Juillard C, Uslan DZ, Tajik K, Aurasteh P, Behnke E, *et al.* Infection following deep brain stimulator implantation performed in the conventional versus magnetic resonance imaging–equipped operating room. Journal of neurosurgery 2009; 110(2): 239-46.

Halpern CH, McGill KR, Baltuch GH, Jaggi JL. Longevity analysis of currently available deep brain stimulation devices. Stereotactic and functional neurosurgery 2011; 89(1): 1-5.

Hardaway FA, Raslan AM, Burchiel KJ. Deep Brain Stimulation-Related Infections: Analysis of Rates, Timing, and Seasonality. Neurosurgery 2017; 83(3): 540-7.

Hariz M. My 25 Stimulating Years with DBS in Parkinson's Disease. Journal of Parkinson's disease 2017; 7(s1): S33-S41.

Harnack D, Meissner W, Jira JA, Winter C, Morgenstern R, Kupsch A. Placebo-controlled chronic high-frequency stimulation of the subthalamic nucleus preserves dopaminergic nigral neurons in a rat model of progressive Parkinsonism. Experimental neurology 2008; 210(1): 257-60.

Helmers A-K, Lübbing I, Birkenfeld F, Witt K, Synowitz M, Mehdorn HM, *et al.* Complications of impulse generator exchange surgery for deep brain stimulation: a single-center, retrospective study. World neurosurgery 2018; 113: e108-e12.

Hely MA, Morris JG, Traficante R, Reid WG, O'Sullivan DJ, Williamson PM. The Sydney multicentre study of Parkinson's disease: progression and mortality at 10 years. Journal of Neurology, Neurosurgery & Psychiatry 1999; 67(3): 300-7.

Hely MA, Reid WG, Adena MA, Halliday GM, Morris JG. The Sydney multicenter study of Parkinson's disease: the inevitability of dementia at 20 years. Movement disorders 2008; 23(6): 837-44.

Hitti FL, Ramayya AG, McShane BJ, Yang AI, Vaughan KA, Baltuch GH. Long-term outcomes following deep brain stimulation for Parkinson's disease. Journal of neurosurgery 2019; 132(1): 205-10.

Horn A. The impact of modern-day neuroimaging on the field of deep brain stimulation. Current opinion in neurology 2019; 32(4): 511-20.

Jitkritsadakul O, Bhidayasiri R, Kalia SK, Hodaie M, Lozano AM, Fasano A. Systematic review of hardware-related complications of Deep Brain Stimulation: Do new indications pose an increased risk? Brain Stimulation 2017; 10(5): 967-76.

Joint C, Nandi D, Parkin S, Gregory R, Aziz T. Hardware-related problems of deep brain stimulation. Movement Disorders 2002; 17(S3).

Kempster PA, O'sullivan SS, Holton JL, Revesz T, Lees AJ. Relationships between age and late progression of Parkinson's disease: a clinico-pathological study. Brain : a journal of neurology 2010; 133(6): 1755-62.

Krauss JK, Lipsman N, Aziz T, Boutet A, Brown P, Chang JW, *et al.* Technology of deep brain stimulation: current status and future directions. Nature Reviews Neurology 2020: 1-13.

Lilleeng B, Brønnick K, Toft M, Dietrichs E, Larsen J. Progression and survival in Parkinson's disease with subthalamic nucleus stimulation. Acta Neurologica Scandinavica 2014; 130(5): 292-8.

Limousin P, Foltynie T. Long-term outcomes of deep brain stimulation in Parkinson disease. Nat Rev Neurol 2019; 15(4): 234-42.

Little S, Pogosyan A, Neal S, Zavala B, Zrinzo L, Hariz M, *et al.* Adaptive deep brain stimulation in advanced Parkinson disease. Annals of neurology 2013; 74(3): 449-57.

Lyons KE, Wilkinson SB, Overman J, Pahwa R. Surgical and hardware complications of subthalamic stimulation A series of 160 procedures. Neurology 2004; 63(4): 612-6.

Machado A, Rezai AR, Kopell BH, Gross RE, Sharan AD, Benabid AL. Deep brain stimulation for Parkinson's disease: surgical technique and perioperative management. Movement disorders: official journal of the Movement Disorder Society 2006; 21(S14): S247-S58.

Marras C, Rochon P, Lang AE. Predicting motor decline and disability in Parkinson disease: a systematic review. Archives of neurology 2002; 59(11): 1724-8.

Meidahl AC, Tinkhauser G, Herz DM, Cagnan H, Debarros J, Brown P. Adaptive Deep Brain Stimulation for Movement Disorders: The Long Road to Clinical Therapy. Movement Disorders 2017; 32(6): 810-9.

Mestre TA, Lang AE, Okun MS. Factors influencing the outcome of deep brain stimulation: Placebo, nocebo, lessebo, and lesion effects. Movement Disorders 2016; 31(3): 290-8.

Miettinen J, Rantanen M, Seppa K. Package 'popEpi'. Google Scholar; 2016.

Montgomery Jr EB. Microelectrode targeting of the subthalamic nucleus for deep brain stimulation surgery. Movement Disorders 2012; 27(11): 1387-91.

Moro E, Poon Y-YW, Lozano AM, Saint-Cyr JA, Lang AE. Subthalamic nucleus stimulation: improvements in outcome with reprogramming. Archives of neurology 2006; 63(9): 1266-72.

MSAC. Deep brain stimulation for symptoms of Parkinson's disease: Medical Services Advisory Committee, Commonwealth of Australia; 2006.

Ngoga D, Mitchell R, Kausar J, Hodson J, Harries A, Pall H. Deep brain stimulation improves survival in severe Parkinson's disease. Journal of Neurology, Neurosurgery & Psychiatry 2014; 85(1): 17-22.

Odekerken VJ, Boel JA, Schmand BA, de Haan RJ, Figee M, van den Munckhof P, *et al*. GPi vs STN deep brain stimulation for Parkinson disease Three-year follow-up. Neurology 2016; 86(8): 755-61.

Oh MY, Abosch A, Kim SH, Lang AE, Lozano AM. Long-term hardware-related complications of deep brain stimulation. Neurosurgery 2002; 50(6): 1268-76.

Okun MS. Deep-brain stimulation for Parkinson's disease. New England Journal of Medicine 2012; 367(16): 1529-38.

Okun MS, Tagliati M, Pourfar M, et al. Management of referred deep brain stimulation failures: A retrospective analysis from 2 movement disorders centers. Archives of Neurology 2005; 62(8): 1250-5.

Ondo WG, Meilak C, Vuong KD. Predictors of battery life for the Activa® Soletra 7426 Neurostimulator. Parkinsonism & related disorders 2007; 13(4): 240-2.

Patel DM, Walker HC, Brooks R, Omar N, Ditty B, Guthrie BL. Adverse Events Associated With Deep Brain Stimulation for Movement DisordersAnalysis of 510 Consecutive Cases. Operative Neurosurgery 2015; 11(1): 190-9.

Pepper J, Zrinzo L, Mirza B, Foltynie T, Limousin P, Hariz M. The risk of hardware infection in deep brain stimulation surgery is greater at impulse generator replacement than at the primary procedure. Stereotactic and functional neurosurgery 2013; 91(1): 56-65.

Poortvliet P, Silburn PA, Coyne T, Chenery H. Deep brain stimulation for Parkinson disease in Australia: current scientific and clinical status. Internal medicine journal 2015; 45(2): 134-9.

Priori A, Foffani G, Rossi L, Marceglia S. Adaptive deep brain stimulation (aDBS) controlled by local field potential oscillations. Experimental neurology 2013; 245: 77-86.

R Development Core Team. R: A language and environment for statistical computing. . Vienna, Austria: R Foundation for Statistical Computing; 2017.

Rajput A, Voll A, Rajput M, Robinson C, Rajput A. Course in Parkinson disease subtypes: a 39-year clinicopathologic study. Neurology 2009; 73(3): 206-12.

Reed R. Models of general practitioner services in residential aged care facilities. Australian Family Physician 2015; 44: 176-9.

Rocha S, Monteiro A, Linhares P, Chamadoira C, Basto MA, Reis C, *et al.* Long-term mortality analysis in Parkinson's disease treated with deep brain stimulation. Parkinson's Disease 2014; 2014.

Rolston JD, Englot DJ, Starr PA, Larson PS. An unexpectedly high rate of revisions and removals in deep brain stimulation surgery: Analysis of multiple databases. Parkinsonism Relat Disord 2016; 33: 72-7.

Schrag A, Ben-Shlomo Y, Brown R, David Marsden C, Quinn N. Young-onset Parkinson's disease revisited—clinical features, natural history, and mortality. Movement disorders: official journal of the Movement Disorder Society 1998; 13(6): 885-94.

Schüpbach M, Chabardes S, Matthies C, Pollo C, Steigerwald F, Timmermann L, *et al.* Directional leads for deep brain stimulation: Opportunities and challenges. Movement Disorders 2017; 32(10): 1371-5.

Schüpbach MWM, Welter ML, Bonnet AM, Elbaz A, Grossardt BR, Mesnage V, *et al.* Mortality in patients with Parkinson's disease treated by stimulation of the subthalamic nucleus. Movement Disorders 2007; 22(2): 257-61.

Selikhova M, Williams D, Kempster P, Holton J, Revesz T, Lees A. A clinico-pathological study of subtypes in Parkinson's disease. Brain : a journal of neurology 2009; 132(11): 2947-57.

Shinall MC, Jr, Arya S, Youk A, Varley P, Shah R, Massarweh NN, *et al.* Association of Preoperative Patient Frailty and Operative Stress With Postoperative Mortality. JAMA Surgery 2020; 155(1): e194620-e.

Sillay KA, Larson PS, Starr PA. Deep brain stimulator hardware-related infections: incidence and management in a large series. Neurosurgery 2008; 62(2): 360-7.

Spieles-Engemann A, Behbehani M, Collier T, Wohlgenant S, Steece-Collier K, Paumier K, *et al.* Stimulation of the rat subthalamic nucleus is neuroprotective following significant nigral dopamine neuron loss. Neurobiology of disease 2010; 39(1): 105-15.

Stroupe KT, Smith B, Weaver FM, Gonzalez B, Huo Z, Cao L, *et al.* Healthcare Utilization and Costs for Patients With Parkinson's Disease After Deep Brain Stimulation. Movement Disorders Clinical Practice 2019; 6(5): 369-78.

Telkes I, Jimenez-Shahed J, Viswanathan A, Abosch A, Ince NF. Prediction of STN-DBS electrode implantation track in Parkinson's disease by using local field potentials. Frontiers in neuroscience 2016; 10: 198.

Telkes I, Sabourin S, Durphy J, Adam O, Sukul V, Raviv N, *et al.* Functional Use of Directional Local Field Potentials in the Subthalamic Nucleus Deep Brain Stimulation. Frontiers in human neuroscience 2020; 14: 145.

Thrane JF, Sunde NA, Bergholt B, Rosendal F. Increasing infection rate in multiple implanted pulse generator changes in movement disorder patients treated with deep brain stimulation. Stereotactic and functional neurosurgery 2014; 92(6): 360-4.

Tinkhauser G, Pogosyan A, Debove I, Nowacki A, Shah SA, Seidel K, *et al.* Directional local field potentials: A tool to optimize deep brain stimulation. Movement Disorders 2018; 33(1): 159-64.

Tolleson C, Stroh J, Ehrenfeld J, Neimat J, Konrad P, Phibbs F. The factors involved in deep brain stimulation infection: a large case series. Stereotactic and functional neurosurgery 2014; 92(4): 227-33.

Umemura A, Jaggi J, Hurtig H, Siderowf A, Colcher A, Stern M, *et al.* Deep brain stimulation for movement disorders: morbidity and mortality in 109 patients. Journal of neurosurgery 2003; 98(4): 779-84.

Vergani F, Landi A, Pirillo D, Cilia R, Antonini A, Sganzerla EP. Surgical, medical, and hardware adverse events in a series of 141 patients undergoing subthalamic deep brain stimulation for Parkinson disease. World Neurosurgery 2010; 73(4): 338-44.

Videnovic A, Metman LV. Deep brain stimulation for Parkinson's disease: Prevalence of adverse events and need for standardized reporting. Movement Disorders 2008; 23(3): 343-9.

Voges J, Waerzeggers Y, Maarouf M, Lehrke R, Koulousakis A, Lenartz D, *et al.* Deep-brain stimulation: long-term analysis of complications caused by hardware and surgery—experiences from a single centre. Journal of Neurology, Neurosurgery & Psychiatry 2006; 77(7): 868-72.

Wallace BA, Ashkan K, Heise CE, Foote KD, Torres N, Mitrofanis J, *et al.* Survival of midbrain dopaminergic cells after lesion or deep brain stimulation of the subthalamic nucleus in MPTP-treated monkeys. Brain : a journal of neurology 2007; 130(8): 2129-45.

Weaver FM, Stroupe KT, Smith B, Gonzalez B, Huo Z, Cao L, *et al.* Survival in patients with Parkinson's disease after deep brain stimulation or medical management. Movement Disorders 2017; 32(12): 1756-63.

Zibetti M, Merola A, Rizzi L, Ricchi V, Angrisano S, Azzaro C, *et al.* Beyond nine years of continuous subthalamic nucleus deep brain stimulation in Parkinson's disease. Movement Disorders 2011; 26(13): 2327-34.

3.4 Figures

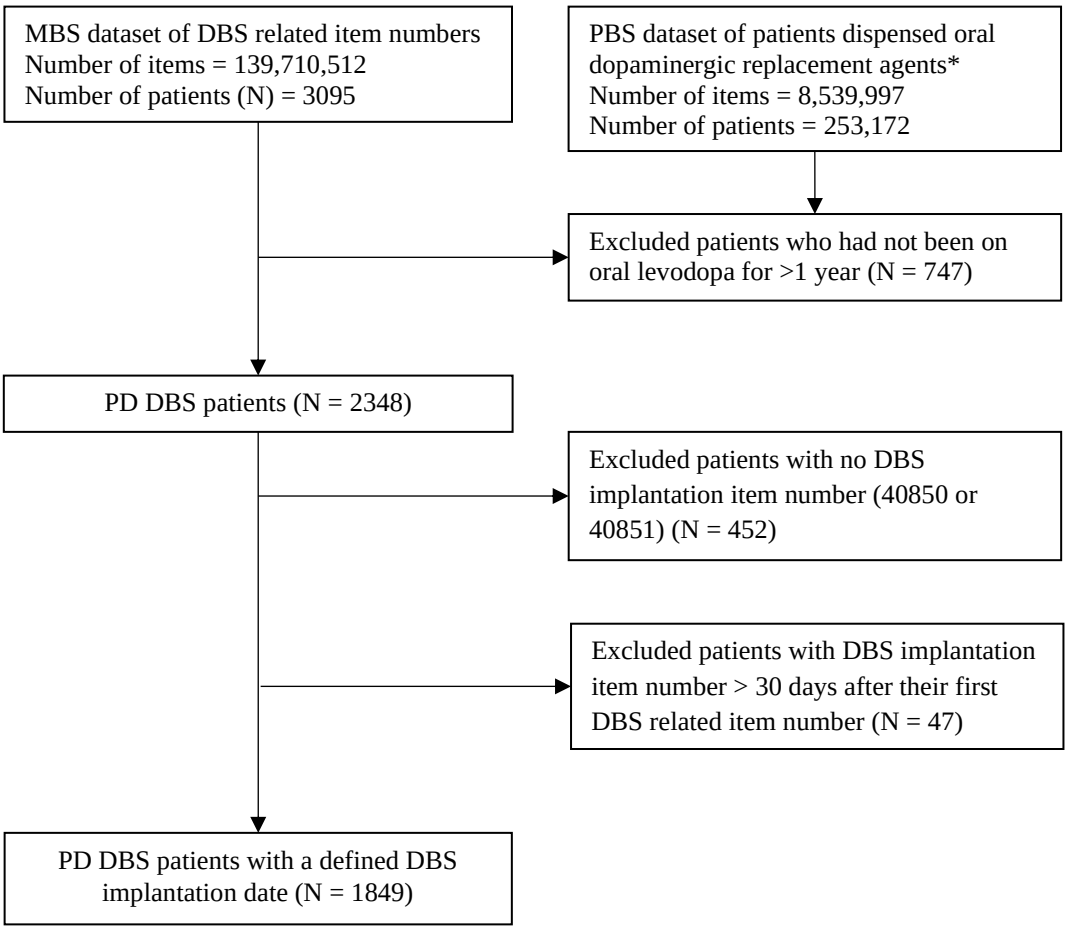

Figure 3.1: Derivation of Parkinson's disease DBS cohort

PD = Parkinson's disease

*PBS dataset included levodopa preparations, pramipexole, rasagiline and rotigotine

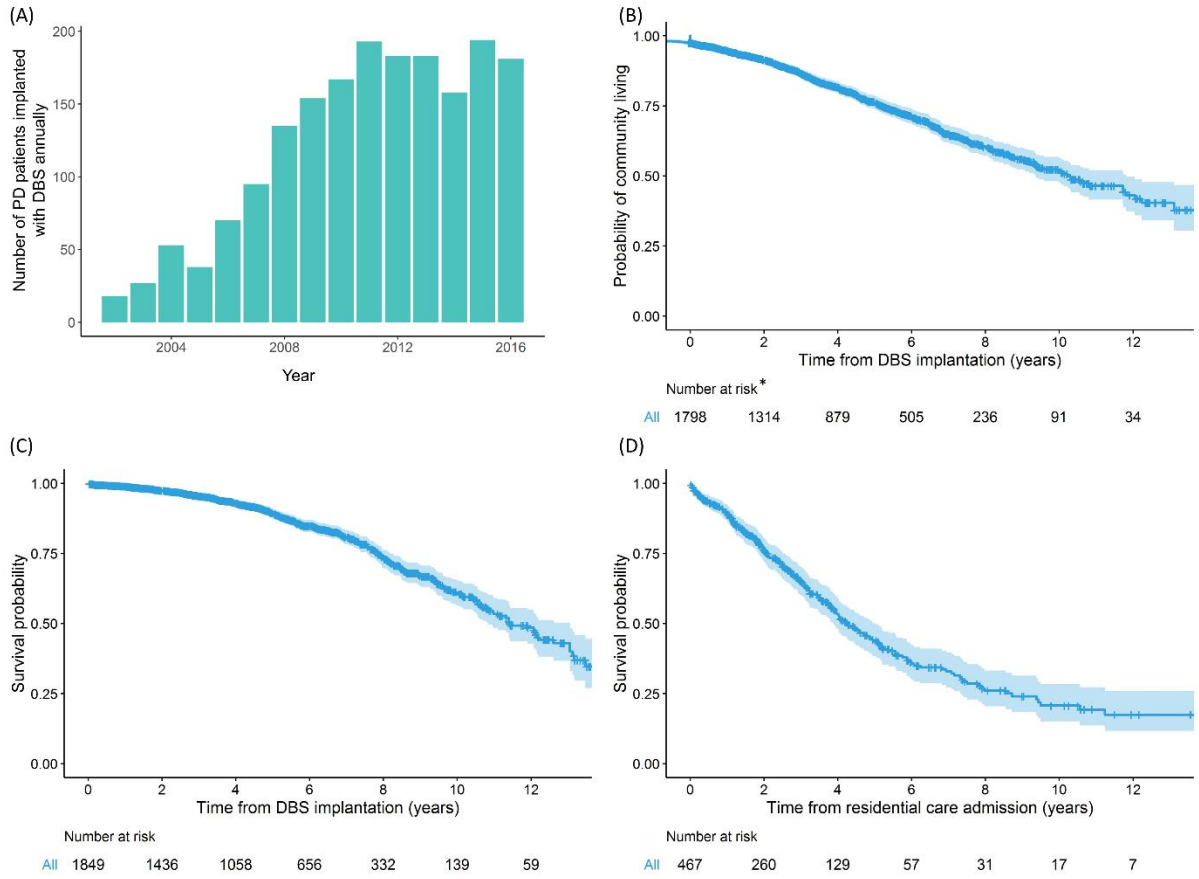

Figure 3.2: The number of patients with Parkinson's disease implanted with deep brain stimulation funded by private health insurance annually in Australia between 2002-2016 (A). The duration of community living (B) and survival (C) after DBS implantation and the duration of survival after admission into residential care (D).

*51 patients had deep brain stimulation implantation whilst in residential care.

3.5 Tables

Table 3.1: Medicare Benefits Schedule item numbers associated with deep brain stimulation

Item number	Interpretation of item number
40850	Unilateral DBS procedure for the treatment of PD, ET, or dystonia
40851	Bilateral DBS procedure for the treatment of PD, ET, or dystonia
40852	Subcutaneous placement of DBS IPG for the treatment of PD, ET, or dystonia
40854	Unilateral revision or removal of brain electrode for the treatment of PD, ET, or dystonia
40856	Unilateral removal or replacement of IPG for the treatment of PD, ET, or dystonia
40858	Unilateral placement, removal, or replacement of extension cable for the treatment of PD, ET, or dystonia
40860	Unilateral target localisation incorporating anatomical and physiological techniques, including intra-operative clinical evaluation by a neurologist, for the insertion of brain electrode for the treatment of PD, ET, or dystonia
40862	Unilateral programming of DBS for treatment of PD, ET, or dystonia

DBS = deep brain stimulation, PD = Parkinson's disease, ET = essential tremor, IPG = implantable pulse generator

Table 3.2: Characteristics at baseline of patients with Parkinson's disease included in the deep brain stimulation cohort and excluded cohort

	Study cohort (N = 1849)	**Excluded cohort (N = 499)**	**SMD**
Gender (Male (%))	1200 (64.9%)	314 (62.9%)	0.04
Medications during study period*			
Pramipexole	1325 (71.7%)	323 (64.7%)	0.1
Rotigotine	434 (23.5%)	90 (18.0%)	0.1
Rasagiline	756 (40.9%)	185 (37.1%)	0.08
Age at first recorded DBS item number (years)	62.6 SD 8.9	62.0 SD 11.2	0.06
Follow-up period (years)	5.0 SD 3.2	5.2 SD 3.8	0.01
Residential care	467 (25.3%)	174 (34.9%)	0.2
Age at residential care admission	69.9 SD 6.9	69.5 SD 8.8	0.05
Deaths	321 (17.4%)	125 (25.1%)	0.2
Age at death	72.9 SD 7.0	72.6 SD 8.3	0.04

DBS = deep brain stimulation, SMD = standardised mean difference

Data presented as mean and standard deviation (SD)

*All patients were prescribed levodopa for a minimum of 12 months during the study period

Table 3.3: Repeat hardware surgery after DBS implantation

	Procedure number	**Number of patients (%)**	**Years from DBS (Median and IQR)**
Repeat hardware surgeries	1718	946 (51.2)	
Intracranial procedures			
All intracranial procedures	301	209 (11.3)	
Electrode replacement	182	164 (8.9)	12 (1 - 37)
Target localisation during repeat surgery	111		
Bilateral electrode replacement	90	85 (4.6)	8 (0.5 - 36)
Unilateral electrode replacement	92	85 (4.6)	16 (6 - 40)
Electrode revision	97	76 (4.1)	14 (2 - 43)
Target localisation during revision surgery	4		
Electrode explant	22	21 (1.1)	24 (9 - 48)
Electrode reimplantation	18	16 (0.9)	
Subcutaneous procedures			
All subcutaneous procedures	1417	880 (47.6)	
Early IPG procedures	130	100 (5.4)	7 (3 - 43)
IPG and extension-cable	88	70 (3.8)	
IPG only	42	40 (2.2)	
Possible infection	64	52 (2.8)	
Late IPG procedures	1252	832 (45.0)	54 (41 - 77)
IPG and extension-cable	251	224 (12.1)	
IPG only	1001	649 (35.1)	
Extension-cable	35	32 (1.7)	11 (1 - 30)

PD = Parkinson’s disease, IPG = implantable pulse generator, IQR = interquartile range

3.6 Supplementary Material

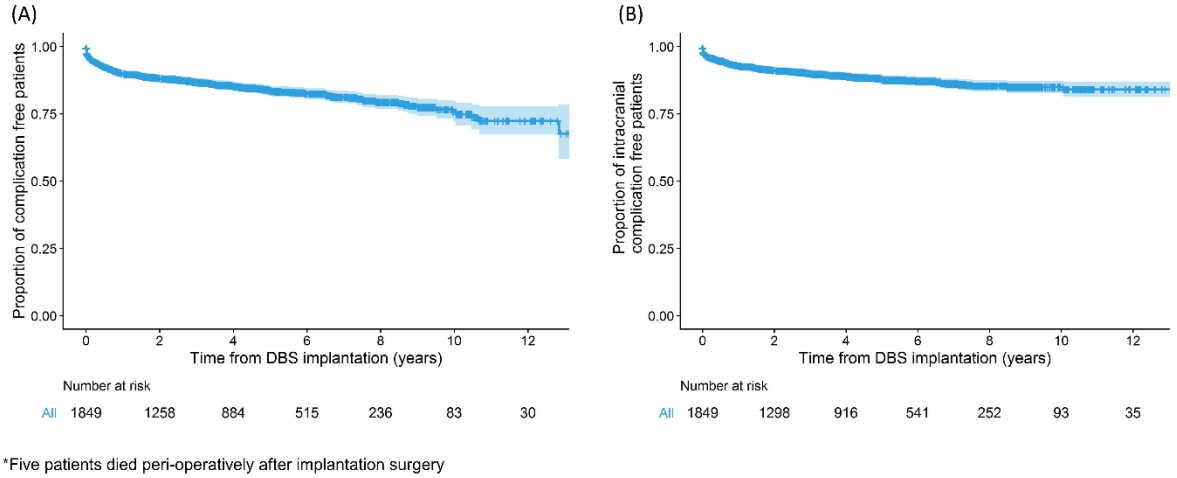

Supplementary figure 3.1: Time to hardware complication requiring surgery.

(A) Time to any hardware complication requiring surgery. (B) Time to intracranial hardware complication requiring surgery

Supplementary table 3.1: Interpretation of same day item numbers for repeat hardware surgery after deep brain stimulation implantation surgery.

Intracranial surgeries	
Electrode replacement surgery	
Unilateral	*Bilateral*
40850	40851
40850 + 40852	40851 + 40852
40850 + 40854	40851 + 40854
40850 + 40856	40851 + 40856
40850 + 40858	40851+ 40858
40850 + 40852 + 40856	40851 + 40852 + 40858
40850 + 40852 + 40858	40851 + 40854 + 40858
40850 + 40854 + 40856	40851 + 40856 + 40858
40850 + 40854 + 40858	40851 + 40852 + 40854 + 40858
40850 + 40852 + 40854 + 40858	40851 + 40852 + 40856 + 40858
40850 + 40852 + 40856 + 40858	40851 + 40854 + 40856 + 40858
40850 + 40854 + 40856 + 40858	40851 + 40852 + 40854 + 40856 + 40858
Electrode removal or revision procedure	
40854	
40854 + 40856	
40854 + 40858	
40852 + 40854 + 40858	
40854 + 40856 + 40858	
Whole system explant*	
40854 + 40856 + 40858	
Subcutaneous surgeries	
IPG procedure (without extension-cable)	
40852	
40856	
40852 + 40856	
IPG with extension-cable procedure	
40852 + 40858	
40856 + 40858	
40852 + 40856 + 40858	
Extension-cable procedure	
40858	

IPG = implantable pulse generator

* An electrode procedure was deemed to be a whole system explant if no further programming sessions were recorded after this combination of item numbers

Supplementary table 3.2: Number of programming sessions after deep brain stimulation surgery

Years from DBS	Programming session number	Patient number
1	6.9 SD 5.0	1831*
2	3.0 SD 2.6	1338
3	2.7 SD 2.0	1106
4	2.8 SD 2.2	950
5	2.8 SD 2.6	769
6	2.6 SD 2.3	571
7	2.4 SD 1.7	414
8	2.6 SD 2.1	293
9	2.7 SD 1.9	186
10	2.2 SD 1.5	129
11	3.2 SD 3.4	77
12	2.7 SD 2.2	42
13	2.0 SD 1.2	30
14	3.7 SD 4.2	11
15	3.0	1

DBS = deep brain stimulation

Programming session number is presented as mean and standard deviation (SD)

*Eighteen patients had no DBS programming sessions recorded, including five patients who died within 30 days of DBS implantation.

Supplementary table 3.3: Repeat hardware surgeries within one year of DBS implantation

	Procedure number	**Number of patients (%) (N = 1849)**
Repeat surgeries	252	194 (10.5)
Intracranial procedures		
All intracranial procedures	148	130 (7.0)
Electrode replacement	93	91 (4.9)
Bilateral electrode replacement	53	53 (2.9)
Unilateral electrode replacement	40	40 (2.2)
Electrode revision	46	43 (2.3)
Electrode explant	9	9 (0.5)
Electrode reimplantation	6	6 (0.3)
Subcutaneous procedures		
All subcutaneous procedures	103	83 (4.5)
IPG and extension-cable	65	53 (2.9)
IPG only	20	19 (1.0)
Extension-cable	18	18 (1.0)

Supplementary table 3.4: Patient characteristics and related surgeries in cohort who died within 30 days of a procedure

Patient	Implant age	Gender	Year of DBS implant	Year of final procedure	Preceding surgery	Days from procedure
1	72	M	2009	2009	DBS implant	0
2	74	M	2010	2010	DBS implant	27
3	74	F	2011	2011	DBS implant	0
4	67	M	2014	2014	DBS implant	7
5	69	F	2016	2016	DBS implant	1
6	59	M	2006	2012	Bilateral electrode replacement surgery	18
7	62	M	2013	2014	Early IPG and extension-cable surgery	14
8	73	M	2004	2009	Late IPG surgery (battery change)	0
9	73	M	2005	2013	Late IPG surgery (battery change)	21
10	85	M	2010	2014	Late IPG surgery (battery change)	0
11	63	M	2011	2016	Late IPG surgery (battery change)	0

DBS = deep brain stimulation, IPG = implantable pulse generator

4 Towards guided and automated programming of subthalamic area stimulation in Parkinson's disease

San San Xu, FRACP[1,2,3], Nicholas C. Sinclair, BEng (Hons)/BSci[1,2], Kristian J. Bulluss, FRACS, PhD[1,4,6], Thushara Perera, PhD[1,2], Wee-Lih Lee, PhD[1,2], Hugh J. McDermott, PhD[1,2], Wesley Thevathasan, FRACP, DPhil[1,3,5]

[1]Bionics Institute, East Melbourne, Victoria, Australia.

[2]Medical Bionics Department, The University of Melbourne, East Melbourne, Victoria, Australia.

[3]Department of Neurology, Austin Hospital, Heidelberg, Victoria, Australia.

[4]Department of Neurosurgery, St Vincent's Hospital Melbourne, Fitzroy, and Department of Neurosurgery, Austin Hospital, Heidelberg, Victoria, Australia.

[5]Department of Medicine, The University of Melbourne, Parkville, Victoria, Australia.

[6]Department of Surgery, The University of Melbourne, Parkville, Victoria, Australia.

Abstract word count: 300

Manuscript word count: 3946

Number of figures: 4

Number of tables: 2

Keywords: deep brain stimulation; Parkinson's disease; subthalamic nucleus; evoked potentials; local field potentials

Abbreviations: STN = subthalamic nucleus, DBS = deep brain stimulation, PD = Parkinson's disease, LFP = local field potentials, HFO = high frequency oscillations, ERNA = evoked resonant neural activity, UPDRS = Unified Parkinson's Disease Rating Scale, ANOVA = analysis of variance, MEM = mixed-effects model, LED = levodopa equivalent dose, MF = motor fluctuations, mA = milliamps, μs = microseconds.

4.1 Abstract

Background and objectives: Selecting the ideal contact to apply subthalamic nucleus (STN) deep brain stimulation (DBS) in Parkinson's disease (PD) can be an arduous process, with outcomes highly dependent on clinician expertise. This study assesses whether intraoperatively recorded neuronal signals, and anatomical location of contacts, can assist programming.

Material and Methods: In 28 hemispheres (14 patients) implanted with STN-DBS for PD, the four contacts on each lead were ranked according to proximity to a nominated ideal anatomical location and power of the following neuronal signals: evoked resonant neural activity (ERNA), beta oscillations, and high frequency oscillations (HFO). We assessed how these rankings predicted, on each lead; i) the motor benefit from DBS applied through each contact, ii) the 'ideal' contact to apply DBS.

Results: The ranking of contacts according to each factor predicted motor benefit from STN-DBS, as follows; ERNA (r^2 = 0.50, AIC 1039.9), beta (r^2 = 0.50, AIC 1041.6), HFO (r^2 = 0.44, AIC 1057.2) and anatomy (r^2 = 0.49, AIC 1048.0). Combining ERNA, beta and HFO ranking data yielded the strongest predictive model (r^2 = 0.61, AIC 1021.5). The 'ideal' contact (yielding maximal benefit) was ranked first according to each factor in the following proportion of hemispheres; ERNA 18/28, beta 17/28, anatomy 16/28, HFO 7/28. Across hemispheres, the maximal available DBS benefit did not differ from that yielded by contacts chosen by clinicians for chronic therapy, or contacts ranked first according to ERNA.

Conclusions: ERNA, beta oscillations and anatomy similarly predicted how motor benefit from STN-DBS varied across contacts on each lead. This could assist programming by providing a probability ranking of contacts akin to a 'monopolar survey'. However, these factors identified the 'ideal' contact in only a proportion of hemispheres. More advanced signal processing and anatomical techniques may be needed for full automation of contact selection.

4.2 Manuscript

Introduction

In patients with Parkinson's disease (PD) implanted with subthalamic nucleus (STN) deep brain stimulation (DBS), the most critical step in programming is to select the ideal contact on each lead to apply stimulation (Volkmann *et al.*, 2006). Currently, this is largely achieved by trial and error, often through a 'monopolar survey', where DBS is delivered through each contact to provide a ranking according to efficacy and therapeutic window (Volkmann *et al.*, 2006). Such approaches are time consuming, and rely heavily upon clinician expertise (Picillo *et al.*, 2016). Moreover, clinical assessments during programming can be confounded by patient fatigue, stun effect and the variable latencies of different therapeutic effects of DBS (Temperli *et al.*, 2003; Mestre *et al.*, 2016). Unsurprisingly, many patients gain suboptimal benefit due to inappropriate contact choice (Okun *et al.*, 2005; Moro *et al.*, 2006). One potential solution is to use objective data, such as anatomical mapping of contacts on postoperative imaging (Horn and Kühn, 2015; Petersen *et al.*, 2018) and neuronal signals recorded from DBS electrodes during surgery, to guide (and ultimately automate) contact selection. Candidate neuronal signals include beta oscillations (Ince *et al.*, 2010; Fernández-García *et al.*, 2017; Tinkhauser *et al.*, 2018; Telkes *et al.*, 2020), high frequency oscillations (HFO) (Özkurt *et al.*, 2011) and the recently described evoked resonant neural activity (ERNA) (Sinclair *et al.*, 2018; Ramirez-Zamora *et al.*, 2020). However, the utility of these data, alone or in combination, to aid contact choice for STN-DBS has not been extensively explored.

Thus here, in 28 hemispheres in 14 patients with PD implanted with STN-DBS, we assessed how well anatomy, and the aforementioned neuronal signals can predict, on each lead; i) the motor benefit from STN-DBS applied through each contact and ii) the 'ideal' contact (yielding maximal motor benefit) to apply DBS. We hypothesized that contact ranking according to all the assessed factors would predict DBS benefit and that a combination of factors would improve this prediction. We hypothesized that the assessed factors would correctly predict the ideal contact in a proportion of hemispheres.

Material and methods

Participants, surgery, and signal recordings

We assessed 14 patients (28 hemispheres) with PD implanted with STN-DBS between February 2016 and February 2018. Fifteen patients were initially recruited but one withdrew before clinical assessment. Written informed consent was obtained from all participants. Intraoperative assessments and clinical data have previously been reported in ten patients (Sinclair *et al.*, 2018). The study was approved by the St Vincent's Public (HREC-D 071/14), St Vincent's Private (R0236-15), and Austin (SSA/15/Austin/266) Human Research Ethics Committees. Patient's characteristics are summarised in Table 4.1. The mean improvement in Unified Parkinson's Disease Rating Scale (UPDRS) part III on-DBS/off-medications compared to off-DBS/off-medications at follow-up was 53.3% SD 16.5.

Quadripolar electrodes (Medtronic, model 3387) were implanted bilaterally targeting the STN during awake neurosurgery as previously described (Sinclair *et al.*, 2018). The substantia nigra pars reticulata was the target for the deepest contact, with the middle two contacts targeting the STN and the superior contact targeting the zona incerta. Electrode extension leads were externalised intra-operatively through the scalp and connected to a highly configurable, custom neurostimulator with the ability to deliver tailored stimulation (Slater *et al.*, 2015). Neuronal signals were measured with the patient at rest immediately after lead implantation. Neuronal activity was recorded at each contact in a monopolar configuration and re-referenced to an average of the four unstimulated contacts in the contralateral hemisphere for common mode noise suppression. Local field potentials (LFPs) were recorded during an off-stimulation period of 15 seconds using a biosignal amplifier (g.USBamp, g.tec medical engineering GmbH, Schiedlberg, Austria) with a 38.4 kHz sampling rate, prior to ERNA assessment. To detect ERNA, burst stimulation was applied to each electrode for ten seconds, comprising ten symmetric 60 µs biphasic pulses in each second, delivered at 3.375 mA and 130 Hz. Recordings were not obtained from one ventral contact (in the substantia nigra pars reticulata) due to a technical fault. After the recording period, the electrode extension leads were connected to the subcutaneous pulse generator under general anaesthesia.

Signal processing

Signals were processed and analysed using MATLAB R2017a (Mathworks, Massachusetts, USA). ERNA recordings were zero-phase forward-reverse filtered using a 2nd-order

Butterworth high-pass filter (f_c = 2 Hz) and a 2nd-order Butterworth band-stop filter (f_c = 49-51 Hz) and further processed using a 21-point centered moving-average filter. Evoked potentials following the last pulse of each burst of stimulation were then extracted and detrended to remove baseline offsets. ERNA was recorded in all hemispheres. ERNA power was calculated by squaring the average of the root mean square amplitude from 4 to 20 milliseconds measured at the contact of interest immediately after burst stimulation was applied to each of the other three contacts of the lead.

LFP power was measured over arbitrarily defined frequency bands and detectable in all hemispheres. Peaks in beta and HFO bands were visually identifiable in only a proportion of hemispheres (beta 19/28, HFO 3/28). Beta power was calculated over the 13-30 Hz frequency band (van Wijk *et al.,* 2017). For beta recordings, Blackman-Harris windowed epochs of 1 second were processed using short-time Fourier transformation. HFO power was calculated over the 200-400 Hz frequency band (van Wijk *et al.*, 2017). For HFO recordings, sharp spikes, likely from power line interference, were removed using 2nd-order Butterworth notch filters with cutoff frequencies set to +/- 0.5 Hz of the spike frequency based on visual inspection. Given the large frequency band occupied by HFOs, epochs of 1 second were processed using Thomson's multi-taper spectral estimates (20 tapers) to better deliver a smoothed spectrum estimate (Sinclair *et al.*, 2019b).

Routine DBS programming

Post-operatively, DBS programming was performed by two experienced DBS neurologists (W.T., SS.X) from a high-volume DBS service (>50 de-novo implantations annually). Clinicians were blinded to the neuronal signal recordings. Electrodes were localised by manually fusing the pre-operative MRI and post-operative CT on a planning station (StealthStation™ S7, Medtronic, Dublin, Ireland). The resultant images were available for visual inspection to assist programming.

Contact anatomical localisation

Each patient's pre-operative brain MRI was co-registered with the postoperative CT (BRAINSFit, 3D Slicer) and contacts were visually identified from the related artefact. Contacts were ranked in order of proximity to a nominated ideal anatomical location (Supplementary figure 4.1). This ideal location was determined using a local landmark

targeting method and, if needed, adjusted after direct visual inspection according to the following method. First, on the native scan of each patient, the adjacent red nucleus was identified and referenced as follows; along the anterior border ('Bejjani line'), 2mm inferior to the superior border and 3mm from the lateral border (Bejjani *et al.*, 2000). This method is reported to closely approximate the clinically effective stimulation site and to accommodate for interpatient STN variability (Andrade-Souza *et al.*, 2005). Euclidean distance from each contact to this location was calculated using a dedicated script on MATLAB R2017a, yielding an initial ranking of contacts. Second, each contact was visualised by an expert clinician (SS.X.) and rankings adjusted if necessary (30/111 contacts), taking into account factors such as centrality of each contact within the STN and width of the STN at that location (ideally $\geq$ 2mm) (Tripoliti *et al.*, 2008; Hershey *et al.*, 2010).

DBS benefit on movement

Motor benefit was assessed three to eighteen months after STN-DBS surgery (range: 92 - 586 days; mean: 306 days) to minimise stun effect and to capture a span of timepoints. The primary motor outcome was the sum of the hemibody motor subscores (part III, items 20-26) of the UPDRS, recorded by the same movement disorders specialist (SS.X.). The motor score in all patients was initially recorded 'off medication' and 'off stimulation' following overnight withdrawal of dopaminergic medication and a 45-minute DBS wash-out period. Monopolar stimulation was then applied to each contact in both hemispheres simultaneously in a counterbalanced order and motor outcomes assessed after a wash-in period of 15 minutes (Temperli *et al.*, 2003). Stimulation parameters (amplitude, pulse width and frequency) were as employed for chronic therapy and then amplitude adjusted if necessary, as follows; reduced by 10% if chronic electrode configuration was bipolar, and reduced by 25%, 50% or 75% if side effects emerged. Amplitude adjustments due to side effects were accounted for in the statistical model. If the clinician selected electrode configuration was bipolar or discordant across hemispheres (e.g. top contact in left and bottom contact in right hemisphere), the chronic stimulation settings were included as a separate condition in the counterbalanced design. The cathode chosen by the clinician for chronic therapy at the time of the experiments, in monopolar or bipolar configuration, was classified as the clinician selected contact. Both the movement disorders specialist (SS.X.) and patient were blinded to the electrode configuration during the 'on stimulation' conditions.

Statistical analysis

To evaluate how well the 'monopolar survey' could be predicted, a mixed-effects model (MEM) (McCulloch and Neuhaus, 2005) evaluated the correlation between the ranking of contacts in each hemisphere according to the predictive factors and the percentage motor benefit in the contralateral hemibody with DBS applied to each contact. Percentage motor benefit was calculated according to the following equation:

$$UDPRS\ DBS\ benefit\ (\%) = \frac{Off\ DBS\ UPDRS - On\ DBS\ UPDRS}{Off\ DBS\ UPDRS} \times 100$$

In the MEM, patients, and hemispheres (nested into patients), were explored as random effects. Hemisphere was not a significant random effect in the model and removed from the final analysis. The order of conditions and tolerated stimulation level at each contact (25%, 50%, 75% or 100% of chronic amplitude) were assessed as fixed effects. Only stimulation level correlated with UPDRS DBS benefit ($r^2 = 0.39$, AIC 1063.6, $p < 0.001$) and thus retained in the model as a fixed effect. The rankings of contacts according to ERNA power, beta power, HFO power and anatomical location were assigned as fixed effects to build the final MEM.

Spearman's rank-order correlation was used to evaluate associations between neuronal signals. A repeated-measures analysis of variance (ANOVA) model compared the DBS benefit in each hemisphere at; the first ranked contact according to the factors of interest, the clinician selected contact, and the maximal available DBS benefit. ANOVA was also used to determine; 1) the variation in UPDRS DBS benefit across the four contacts in each hemisphere, 2) the variation in neuronal signal power across the four contacts in each hemisphere, and 3) the variation in neuronal signal power across the four contacts ranked according to proximity to the nominated ideal anatomical location to apply DBS.

The ANOVA model was built using Minitab 18 (Minitab Inc., Pennsylvania, USA) and multiple comparisons corrected using the Tukey method. The MEM was built using the lme4 package (Bates *et al.*, 2007) on R Project 4.0.3 (R core team, Vienna, Austria). The MEMs were compared using ANOVA with Bonferroni-holm method employed for post-hoc analysis. Corrected p-values are shown in all figures. Results were deemed significant if $p < 0.05$.

Data statement

Anonymized data can be made available at the request of qualified investigators for the purpose of replicating procedures and results, subject to an embargo of 24 months from the date of article publication.

Results

Characterisation of neuronal signals and stimulation levels

Neuronal signals in the STN region and their relative anatomical location

ERNA, beta and HFO power varied across the four contacts in each hemisphere ranked according to signal power (repeated measures ANOVA, ERNA $F_{3, 94} = 23.4$, $p<0.001$; beta $F_{3, 94} = 22.0$, $p<0.001$; HFO $F_{3, 94} = 53.1$, $p<0.001$, Figure 4.1). Across all contacts, there was a correlation between ERNA power and beta power ($r_s = 0.57$, $p <0.001$), ERNA power and HFO power ($r_s = 0.74$, $p <0.001$) and beta power and HFO power ($r_s = 0.58$, $p <0.001$).

ERNA, beta, and HFO power varied across the four contacts ranked according to proximity to the nominated ideal anatomical location (repeated measures ANOVA, ERNA $F_{3, 94} = 11.4$, $p<0.001$; beta $F_{3, 94} = 4.9$, $p = 0.003$; HFO $F_{3, 94} = 19.3$, $p <0.001$). ERNA, beta, and HFO power were greatest at contacts ranked as closer to the nominated ideal anatomical location (Figure 4.2A-C).

Adjustment of DBS amplitudes due to side effects

Stimulation amplitude was reduced (from chronic therapy) due to side effects (for example, visual change, nausea, capsular side effects) in 29 out of 111 contacts; to 75% in 17 contacts, 50% in 11 contacts, and 25% in one contact. No amplitude reductions were required at contacts selected by the clinician for chronic therapy. Reductions occurred more often in contacts located further from the nominated ideal anatomical target (10 times in the two best-ranked contacts and 19 times in the two worst-ranked contacts.). However, stimulation amplitudes were sometimes reduced at contacts ranked first according to anatomy (five hemispheres), ERNA (two hemispheres), beta (three hemispheres), and HFO (five hemispheres).

Predicting the 'monopolar survey' ranking of contacts according to motor benefit

UPDRS DBS benefit varied across the four contacts in each hemisphere ranked according to efficacy (repeated measures ANOVA, $F_{3, 94} = 137.6$, $p<0.001$, Figure 4.2D).

Individual predictive factors

UPDRS DBS benefit correlated with the ranking of contacts according to ERNA power ($r^2 = 0.50$, AIC 1039.9, $p <0.001$), beta power ($r^2 = 0.50$, AIC 1041.6, $p <0.001$), HFO power ($r^2 = 0.44$, 1057.2, $p <0.001$) and proximity to the ideal anatomical location ($r^2 = 0.49$, AIC 1048.0, $p <0.001$) (Figure 4.3A-D).

Combinations of the predictive factors

The best two-factor predictive model for UPDRS DBS benefit incorporated ERNA power and HFO power rankings ($r^2 = 0.57$, AIC 1028.0, Table 4.2). This model was more predictive than the models of either factor alone (ERNA power; $r^2 = 0.50$, AIC 1039.9, $p < 0.001$ and HFO power; $r^2 = 0.44$, 1057.2, $p <0.001$).

The best three-factor predictive model for UPDRS DBS benefit incorporated ERNA power, HFO power and beta power rankings ($r^2 = 0.61$, AIC 1021.5). This model was more predictive than the two-factor predictive model of ERNA power and HFO power rankings ($p = 0.006$). The inclusion of anatomy ranking into the three-factor model (ERNA power, HFO power and beta power) did not yield a more predictive model ($r^2 = 0.63$, AIC 1022.1, $p = 0.15$).

Predicting the ideal contact to apply STN-DBS

Across hemispheres, UPDRS DBS benefit varied between contacts grouped into the following categories; contacts yielding the maximal available benefit, contacts clinically selected for chronic DBS, and contacts ranked first according to each predictive factor (repeated measures ANOVA, $F_{5, 149} = 11.9$, $p<0.001$, Figure 4.3E).

Within hemispheres, there was a significant difference between the UPDRS DBS benefit at the first ranked contact and the remaining three contacts on each lead according to ERNA power, but not beta power, HFO power or anatomical location (Figure 4.3A-D, Bonferroni-holm multiple comparisons).

Contacts yielding the maximal UPDRS DBS benefit

The maximal UPDRS DBS benefit in each hemisphere (mean benefit 62.2% SEM 3.9) did not differ from the UPDRS DBS benefit arising from contacts clinically selected for chronic therapy (mean benefit 60.7% SEM 4.0, Tukey method $p = 1.0$) or contacts ranked first according to ERNA (mean benefit 49.4% SEM 5.5, Tukey method $p = 0.1$). The maximal UPDRS DBS benefit in each hemisphere was greater than the UPDRS DBS benefit arising from contacts ranked first according to anatomy (mean benefit 45.0% SEM 5.3, Tukey method $p = 0.02$), beta oscillations (mean benefit 43.4% SEM 5.9, Tukey method $p = 0.006$) and HFOs (mean benefit 27.7% SEM 5.8, Tukey method $p < 0.001$).

However, the UPDRS DBS benefit from contacts ranked first according to ERNA power was not significantly different from contacts ranked first according to beta power, or anatomical location. The UPDRS DBS benefit from contacts ranked first according to ERNA, beta oscillations and anatomy was greater than contacts ranked first according to HFOs (Tukey method ERNA and HFO $p = 0.001$, beta and HFO $p = 0.03$, anatomy and HFO $p = 0.01$).

Contacts ranked first according to each predictive factor were the same as those yielding the maximal UPDRS DBS benefit in the following proportion of hemispheres; ERNA 18/28, beta oscillations 17/28, anatomy 16/28, HFO 7/28 (Figure 4.4A).

Contacts clinically selected for chronic DBS

The clinically selected contacts for chronic therapy yielded the maximal UPDRS DBS benefit in 25/28 hemispheres. This contact (cathode for monopolar or bipolar DBS) usually corresponded to the contacts ranked first according to ERNA power (20/28 hemispheres) and anatomy (19/28 hemispheres), and less often to contacts ranked first according to beta power (14/28 hemispheres) and HFO power (10/28 hemispheres) (Figure 4.4B).

Discussion

Here, in patients with PD implanted with STN-DBS, we assessed how well anatomy and neuronal signals (beta oscillations, HFO and ERNA) predicted, on each lead; i) the ‘monopolar survey’ degree of motor benefit from STN-DBS applied through each contact, and ii) the ideal contact to apply DBS. ERNA, beta oscillations, and anatomy were all similarly predictive of UPDRS DBS benefit. The strongest predictive model resulted from combining ERNA, beta

and HFO rankings data. The 'ideal contact' on each lead was ranked first according to ERNA, beta oscillations, and anatomy in a similar proportion of hemispheres (18/28, 17/28 and 16/28, respectively) and less often according to HFOs (7/28). Contacts ranked first according to ERNA (but not the other factors) yielded significantly greater UPDRS DBS benefit than the remaining three contacts on each lead.

Several limitations of this study need to be acknowledged. We evaluated how the assessed factors could predict the efficacy of STN-DBS across contacts on each lead. Randomised controlled trials usually determine such efficacy according to quality of life and disability (Deuschl *et al.*, 2006; Williams *et al.*, 2010; Odekerken *et al.*, 2013). Conversely, our single-session experimental study could only assess acute motor effects of DBS and was thus prone to confounds such as stimulation carry-over effects and patient fatigue (Temperli *et al.*, 2003; Mazzoni *et al.*, 2007). However, order effects were non-significant in our statistical analyses. Moreover, the long-term clinical relevance of our results is supported by the high concordance between the clinician-chosen DBS contact and the contact identified as ideal during the study. Our sample size may have been insufficient to detect significant differences across all comparisons – but was powered to discriminate clinically relevant outcomes at an individual level, consistent with previous studies of a similar nature (Ince *et al.*, 2010; Tinkhauser *et al.*, 2018; Telkes *et al.*, 2020). We employed DBS parameters that were used for chronic therapy, with clinician programming guided by the clinical response to DBS over time and the anatomical location of electrodes. This may have favoured outcomes from the contacts clinically chosen for chronic DBS and the 'ideal contact' according to anatomy, with stimulation levels being excessive or insufficient at other locations. Excessive DBS can degrade motor performance, but the clinical impact of this is considered modest (Chen *et al.*, 2006a). In contacts further from the neural target, increasing DBS can produce greater motor benefit (Kuncel and Grill, 2004), though a saturation of benefit can be observed (Moro *et al.*, 2002). The duration of experiments was limited by patient tolerance. Thus, we applied DBS bilaterally, and performed a comprehensive motor evaluation on each hemibody. Our results could therefore be confounded by ipsilateral effects of DBS, but these confer only around a 20% motor benefit in PD (Nakamura *et al.*, 2007; Tabbal *et al.*, 2008).

Here, we provide evidence that contact selection, a crucial aspect of programming STN-DBS in PD, could be guided using objective data. All the assessed factors could (variably) predict the degree of motor benefit afforded by DBS applied through the contacts on each lead - akin to the results of a 'monopolar survey'. Such information, perhaps presented as probability

rankings, could help narrow programming choices. This could reduce the time costs and error rates associated with DBS programming, especially if developed for newer devices with greater programming complexity such as directional electrodes and simultaneous delivery through multiple independent current sources (Timmermann *et al.*, 2015; Fernández-García *et al.*, 2017; Schüpbach *et al.*, 2017; Tinkhauser *et al.*, 2018; Telkes *et al.*, 2020). Supporting long term relevance, neuronal signals recorded during electrode implantation predicted clinical outcomes many months after surgery. However, the most important aspect of contact selection is to identify the single best contact to apply chronic DBS. The ideal contact on each lead was almost always ranked as first or second according to ERNA, beta oscillations and anatomy. However, these factors ranked the ideal contact as first in only around two thirds of hemispheres or less.

Combining information from the assessed factors did improve prediction of the ideal contact to apply STN-DBS at a group level. This raises the possibility that each factor may only account for a proportion of the information required to determine the ideal stimulation location. Alternatively, there may be better methods of capturing and analysing neuronal signal and anatomical data for this purpose. For example, in this study, a potential confound could be the 3mm spacing between the midpoint of adjacent contacts. The ideal DBS location may be situated between these contacts. Greater spatial resolution, afforded by leads with smaller between-contact spacing and/or directional arrays, could improve the predictive performance of all the factors assessed.

ERNA has many attributes suggesting it could be an ideal neuronal biomarker to tailor STN-DBS. For example, unlike spontaneously occurring LFPs, ERNA occurs with a predictable latency after DBS pulses and is of a much larger amplitude. ERNA has a complex waveform with many measurable features such as amplitude, frequency, and decay function. In this study, for the purpose of localising DBS in the STN region, we elected to assess the root mean square amplitude of ERNA over a specific time window (4-20 milliseconds) and evoking stimulus (after a 3.375mA DBS pulse). However, it is possible that other ERNA variables may better suit this purpose, which will be the focus of future work.

Unlike such evoked activity, there is already a large body of work exploring the relationship of spontaneous LFPs recorded from the STN, especially beta oscillations, and motor deficits of PD (Kühn *et al.*, 2006; Hammond *et al.*, 2007; Ray *et al.*, 2008; Kühn *et al.*, 2009). For example, the utility of beta power to guide STN-DBS programming on directional leads has been specifically assessed, with similar findings to this study (the ideal contact was correctly

identified in 63% of leads) (Tinkhauser *et al.*, 2018). However, metrics of beta oscillations other than power may be more predictive of the ideal STN-DBS location, such as spectral divisions (Priori *et al.*, 2004; van Wijk *et al.*, 2016; Meidahl *et al.*, 2019; Tinkhauser *et al.*, 2019), beta burst duration (Tinkhauser *et al.*, 2017b) and the spatial distribution of oscillations (Zaidel *et al.*, 2010; van Wijk *et al.*, 2017; Lu *et al.*, 2020).

Compared to beta band activity, the relationship between HFOs and PD motor function remains poorly understood (López-Azcárate *et al.*, 2010; Wang *et al.*, 2014; van Wijk *et al.*, 2016). Intriguingly, we found that the contacts ranked second according to HFO power produced the greatest UPDRS DBS benefit. One explanation is that HFOs recorded in the STN could play a prokinetic role, being enhanced with voluntary movement and dopaminergic medication (Foffani *et al.*, 2003; López-Azcárate *et al.*, 2010). Indeed, a negative correlation between HFO power and akinesia and rigidity is reported in some studies (López-Azcárate *et al.*, 2010; Wang *et al.*, 2014). However, simply assessing HFO power may not accurately represent the complexity of activity over the broad 200-400 Hz band. For example, shifts in spectral divisions of HFO occur after levodopa administration and correlate with motor scores (Özkurt *et al.*, 2011). Phase amplitude coupling of HFOs with beta oscillations has been measured at clinically effective contacts (Yang *et al.*, 2014) and is attenuated by dopamine administration and DBS (López-Azcárate *et al.*, 2010; Özkurt *et al.*, 2011; van Wijk *et al.*, 2016).

Clinician aids have already been developed using the anatomical mapping of contacts to assist DBS programming (Horn and Kühn, 2015; Petersen *et al.*, 2018; Dembek *et al.*, 2019). Importantly, our study highlights that, like the other assessed factors, structural anatomy imperfectly identified the ideal STN-DBS contact. Interestingly, the addition of anatomical information to neuronal signal rankings did not improve the predictive model of the 'monopolar survey'. As ERNA (Sinclair *et al.*, 2018), beta oscillations (Kühn *et al.*, 2005; Telkes *et al.*, 2016; Horn *et al.*, 2017b; Tamir *et al.*, 2020) and HFO (Wang *et al.*, 2014; van Wijk *et al.*, 2017) all tended to localise to the dorsal STN, perhaps this rendered structural anatomy redundant in identifying this location. However, when considered alone, anatomy was similarly predictive of the ideal contact to apply STN-DBS as ERNA and beta oscillations. Advanced imaging techniques such as tractography and modelling volumes of tissue activated could improve the performance of anatomy for this specific function. Moreover, such methods could complement the functional information provided by neuronal signals, for example by identifying the location of pathways relevant to side effects (Vanegas-Arroyave *et al.*, 2016; Akram *et al.*, 2017; Mahlknecht *et al.*, 2017).

The insights revealed by this study are important to understand, given the established use of anatomy to localise STN-DBS and the emerging availability of LFPs recorded via commercial intra-operative recording systems (Marmor *et al.*, 2017; Ozturk *et al.*, 2020) and implantable pulse generators capable of monitoring bioelectric signals (Young, 2020). Our results also highlight the potential utility of ERNA, a novel neuronal signal with attributes that have barely been explored. We found that a simple metric of ERNA performed as well as anatomy and beta oscillations in predicting the ideal contact to apply STN-DBS.

.

Authors' contributions

Dr San San Xu, Mr Nicholas C. Sinclair, Dr Kristian J. Bulluss, Professor Hugh J. McDermott and Associate Professor Wesley Thevathasan were involved in the conception and design of the study. Dr San San Xu, Dr Kristian J. Bulluss and Associate Professor Wesley Thevathasan recruited patient for the study. Dr San San Xu, Mr Nicholas C. Sinclair, Dr Thushara Perera and Dr Wee-Lih Lee were involved in data acquisition. Dr San San Xu analysed the data, including statistical analysis. Dr San San Xu and Associate Professor Wesley Thevathasan interpreted the data. Dr San San Xu prepared the manuscript draft with important intellectual input from Associate Professor Wesley Thevathasan. All authors were involved in the review and critique of the manuscript and approved the final manuscript.

Funding

The work was funded by the National Health and Medical Research Council, Colonial Foundation, St Vincent's Hospital Research and Lions International. The Bionics Institute acknowledges the support it receives from the Victorian Government through its Operational Infrastructure Support Program.

Competing Interests

Mr Nicholas C. Sinclair, Dr Kristian J. Bulluss, Professor Hugh J. McDermott and Associate Professor Wesley Thevathasan are founders and hold options in DBS Technologies Pty Ltd which plans to commercialize the use of neuronal signals to improve DBS. They are named inventors on related patents, which are assigned to DBS Technologies Pty Ltd. Dr Kristian J. Bulluss, Professor Hugh J. McDermott and Associate Professor Wesley Thevathasan hold shares in DBS Technologies Pty Ltd. Dr San San Xu holds options in DBS Technologies Pty Ltd. Dr Thushara Perera holds options in DBS Technologies Pty Ltd and is a named inventor on related patents, which are assigned to DBS Technologies. Associate Professor Wesley Thevathasan has received honoraria from Medtronic and Boston Scientific. Dr Wee-Lih Lee reports no conflicts of interest.

4.3 References

Akram H, Sotiropoulos SN, Jbabdi S, Georgiev D, Mahlknecht P, Hyam J, *et al.* Subthalamic deep brain stimulation sweet spots and hyperdirect cortical connectivity in Parkinson's disease. Neuroimage 2017; 158: 332-45.

Andrade-Souza YM, Schwalb JM, Hamani C, Eltahawy H, Hoque T, Saint-Cyr J, *et al.* Comparison of three methods of targeting the subthalamic nucleus for chronic stimulation in Parkinson's disease. Neurosurgery 2005; 56(2 Suppl): 360-8; discussion -8.

Bates D, Sarkar D, Bates MD, Matrix L. The lme4 package. R package version 2007; 2(1): 74.

Bejjani B-P, Dormont D, Pidoux B, Yelnik J, Damier P, Arnulf I, *et al.* Bilateral subthalamic stimulation for Parkinson's disease by using three-dimensional stereotactic magnetic resonance imaging and electrophysiological guidance. Journal of neurosurgery 2000; 92(4): 615-25.

Chen CC, Brucke C, Kempf F, Kupsch A, Lu CS, Lee ST, *et al.* Deep brain stimulation of the subthalamic nucleus: a two-edged sword. Curr Biol 2006; 16(22): R952-3.

Dembek TA, Roediger J, Horn A, Reker P, Oehrn C, Dafsari HS, *et al.* Probabilistic Sweetspots Predict Motor Outcome for DBS in Parkinson's Disease. Annals of neurology 2019.

Deuschl G, Schade-Brittinger C, Krack P, Volkmann J, Schäfer H, Bötzel K, *et al.* A Randomized Trial of Deep-Brain Stimulation for Parkinson's Disease. New England Journal of Medicine 2006; 355(9): 896-908.

Fernández-García C, Foffani G, Dileone M, Catalán-Alonso M, González-Hidalgo M, Barcía J, *et al.* Directional local field potential recordings for symptom-specific optimization of deep brain stimulation. Movement disorders: official journal of the Movement Disorder Society 2017; 32(4): 626.

Foffani G, Priori A, Egidi M, Rampini P, Tamma F, Caputo E, *et al.* 300-Hz subthalamic oscillations in Parkinson’s disease. Brain : a journal of neurology 2003; 126(10): 2153-63.

Hammond C, Bergman H, Brown P. Pathological synchronization in Parkinson's disease: networks, models and treatments. Trends in neurosciences 2007; 30(7): 357-64.

Hershey T, Campbell MC, Videen TO, Lugar HM, Weaver PM, Hartlein J, *et al.* Mapping Go–No-Go performance within the subthalamic nucleus region. Brain : a journal of neurology 2010; 133(12): 3625-34.

Horn A, Kühn AA. Lead-DBS: a toolbox for deep brain stimulation electrode localizations and visualizations. Neuroimage 2015; 107: 127-35.

Horn A, Neumann WJ, Degen K, Schneider GH, Kühn AA. Toward an electrophysiological “sweet spot” for deep brain stimulation in the subthalamic nucleus. Human brain mapping 2017; 38(7): 3377-90.

Ince NF, Gupte A, Wichmann T, Ashe J, Henry T, Bebler M, *et al.* Selection of optimal programming contacts based on local field potential recordings from subthalamic nucleus in patients with Parkinson's disease. Neurosurgery 2010; 67(2): 390-7.

Kühn AA, Kupsch A, Schneider GH, Brown P. Reduction in subthalamic 8–35 Hz oscillatory activity correlates with clinical improvement in Parkinson's disease. European Journal of Neuroscience 2006; 23(7): 1956-60.

Kühn AA, Trottenberg T, Kivi A, Kupsch A, Schneider G-H, Brown P. The relationship between local field potential and neuronal discharge in the subthalamic nucleus of patients with Parkinson's disease. Experimental neurology 2005; 194(1): 212-20.

Kühn AA, Tsui A, Aziz T, Ray N, Brücke C, Kupsch A, *et al.* Pathological synchronisation in the subthalamic nucleus of patients with Parkinson's disease relates to both bradykinesia and rigidity. Experimental neurology 2009; 215(2): 380-7.

Kuncel AM, Grill WM. Selection of stimulus parameters for deep brain stimulation. Clinical neurophysiology 2004; 115(11): 2431-41.

López-Azcárate J, Tainta M, Rodríguez-Oroz MC, Valencia M, González R, Guridi J, *et al.* Coupling between beta and high-frequency activity in the human subthalamic nucleus may be a pathophysiological mechanism in Parkinson's disease. Journal of Neuroscience 2010; 30(19): 6667-77.

Lu CW, Chou KL, Patil PG. Correspondence of optimal stimulation and beta power varies regionally in STN DBS for Parkinson disease. Parkinsonism & Related Disorders 2020; 78: 124-8.

Mahlknecht P, Akram H, Georgiev D, Tripoliti E, Candelario J, Zacharia A, *et al.* Pyramidal tract activation due to subthalamic deep brain stimulation in Parkinson's disease. Movement Disorders 2017; 32(8): 1174-82.

Marmor O, Valsky D, Joshua M, Bick AS, Arkadir D, Tamir I, *et al.* Local vs. volume conductance activity of field potentials in the human subthalamic nucleus. Journal of Neurophysiology 2017; 117(6): 2140-51.

Mazzoni P, Hristova A, Krakauer JW. Why don't we move faster? Parkinson's disease, movement vigor, and implicit motivation. Journal of neuroscience 2007; 27(27): 7105-16.

McCulloch CE, Neuhaus JM. Generalized linear mixed models. Encyclopedia of biostatistics 2005; 4.

Meidahl AC, Moll CK, van Wijk BC, Gulberti A, Tinkhauser G, Westphal M, *et al.* Synchronised spiking activity underlies phase amplitude coupling in the subthalamic nucleus of Parkinson's disease patients. Neurobiology of disease 2019; 127: 101-13.

Mestre TA, Lang AE, Okun MS. Factors influencing the outcome of deep brain stimulation: Placebo, nocebo, lessebo, and lesion effects. Movement Disorders 2016; 31(3): 290-8.

Moro E, Esselink R, Xie J, Hommel M, Benabid A, Pollak P. The impact on Parkinson’s disease of electrical parameter settings in STN stimulation. Neurology 2002; 59(5): 706-13.

Moro E, Poon Y-YW, Lozano AM, Saint-Cyr JA, Lang AE. Subthalamic nucleus stimulation: improvements in outcome with reprogramming. Archives of neurology 2006; 63(9): 1266-72.

Nakamura K, Christine CW, Starr PA, Marks Jr WJ. Effects of unilateral subthalamic and pallidal deep brain stimulation on fine motor functions in Parkinson's disease. Movement disorders 2007; 22(5): 619-26.

Odekerken VJ, van Laar T, Staal MJ, Mosch A, Hoffmann CF, Nijssen PC, *et al.* Subthalamic nucleus versus globus pallidus bilateral deep brain stimulation for advanced Parkinson's disease (NSTAPS study): a randomised controlled trial. The Lancet Neurology 2013; 12(1): 37-44.

Okun MS, Tagliati M, Pourfar M, et al. Management of referred deep brain stimulation failures: A retrospective analysis from 2 movement disorders centers. Archives of Neurology 2005; 62(8): 1250-5.

Özkurt TE, Butz M, Homburger M, Elben S, Vesper J, Wojtecki L, *et al.* High frequency oscillations in the subthalamic nucleus: a neurophysiological marker of the motor state in Parkinson's disease. Experimental neurology 2011; 229(2): 324-31.

Ozturk M, Kaku H, Jimenez-Shahed J, Viswanathan A, Sheth SA, Kumar S, *et al.* Subthalamic Single Cell and Oscillatory Neural Dynamics of a Dyskinetic Medicated Patient With Parkinson's Disease. Frontiers in Neuroscience 2020; 14(391).

Petersen MV, Husch A, Parsons CE, Lund TE, Sunde N, Østergaard K. Using automated electrode localization to guide stimulation management in DBS. Annals of Clinical and Translational Neurology 2018; 5(7): 888-94.

Picillo M, Lozano AM, Kou N, Munhoz RP, Fasano A. Programming deep brain stimulation for Parkinson's disease: the Toronto western hospital algorithms. Brain stimulation 2016; 9(3): 425-37.

Priori A, Foffani G, Pesenti A, Tamma F, Bianchi A, Pellegrini M, *et al.* Rhythm-specific pharmacological modulation of subthalamic activity in Parkinson's disease. Experimental neurology 2004; 189(2): 369-79.

Ramirez-Zamora A, Giordano J, Gunduz A, Alcantara J, Cagle JN, Cernera S, *et al.* Proceedings of the Seventh Annual Deep Brain Stimulation Think Tank: Advances in Neurophysiology, Adaptive DBS, Virtual Reality, Neuroethics and Technology. Frontiers in Human Neuroscience 2020; 14: 54.

Ray NJ, Jenkinson N, Wang S, Holland P, Brittain JS, Joint C, *et al.* Local field potential beta activity in the subthalamic nucleus of patients with Parkinson's disease is associated with improvements in bradykinesia after dopamine and deep brain stimulation. Experimental Neurology 2008; 213(1): 108-13.

Schüpbach M, Chabardes S, Matthies C, Pollo C, Steigerwald F, Timmermann L, *et al.* Directional leads for deep brain stimulation: Opportunities and challenges. Movement Disorders 2017; 32(10): 1371-5.

Sinclair NC, McDermott HJ, Bulluss KJ, Fallon JB, Perera T, Xu SS, *et al.* Subthalamic nucleus deep brain stimulation evokes resonant neural activity. Annals of neurology 2018; 83(5).

Sinclair NC, McDermott HJ, Fallon JB, Perera T, Brown P, Bulluss KJ, *et al.* Deep brain stimulation for Parkinson's disease modulates high-frequency evoked and spontaneous neural activity. Neurobiology of Disease 2019: 104522.

Slater KD, Sinclair NC, Nelson TS, Blamey PJ, Mcdermott HJ. neuroBi: a highly configurable neurostimulator for a retinal prosthesis and other applications. IEEE journal of translational engineering in health and medicine 2015; 3: 1-11.

Tabbal SD, Ushe M, Mink JW, Revilla FJ, Wernle AR, Hong M, *et al.* Unilateral subthalamic nucleus stimulation has a measurable ipsilateral effect on rigidity and bradykinesia in Parkinson disease. Experimental neurology 2008; 211(1): 234-42.

Tamir I, Wang D, Chen W, Ostrem JL, Starr PA, de Hemptinne C. Eight cylindrical contact lead recordings in the subthalamic region localize beta oscillations source to the dorsal STN. Neurobiology of Disease 2020; 146: 105090.

Telkes I, Jimenez-Shahed J, Viswanathan A, Abosch A, Ince NF. Prediction of STN-DBS electrode implantation track in Parkinson's disease by using local field potentials. Frontiers in neuroscience 2016; 10: 198.

Telkes I, Sabourin S, Durphy J, Adam O, Sukul V, Raviv N, *et al.* Functional Use of Directional Local Field Potentials in the Subthalamic Nucleus Deep Brain Stimulation. Frontiers in human neuroscience 2020; 14: 145.

Temperli P, Ghika J, Villemure JG, Burkhard PR, Bogousslavsky J, Vingerhoets FJ. How do parkinsonian signs return after discontinuation of subthalamic DBS? Neurology 2003; 60(1): 78-81.

Timmermann L, Jain R, Chen L, Maarouf M, Barbe MT, Allert N, *et al.* Multiple-source current steering in subthalamic nucleus deep brain stimulation for Parkinson's disease (the VANTAGE study): a non-randomised, prospective, multicentre, open-label study. The Lancet Neurology 2015; 14(7): 693-701.

Tinkhauser G, Pogosyan A, Debove I, Nowacki A, Shah SA, Seidel K, *et al.* Directional local field potentials: A tool to optimize deep brain stimulation. Movement Disorders 2018; 33(1): 159-64.

Tinkhauser G, Pogosyan A, Tan H, Herz DM, Kühn AA, Brown P. Beta burst dynamics in Parkinson’s disease OFF and ON dopaminergic medication. Brain : a journal of neurology 2017; 140(11): 2968-81.

Tinkhauser G, Shah AS, Fischer P, Peterman K, Debove I, Nygyuen K, *et al.* Electrophysiological differences between Upper and Lower Limb movements in the human subthalamic nucleus. Clinical Neurophysiology 2019.

Tomlinson CL, Stowe R, Patel S, Rick C, Gray R, Clarke CE. Systematic review of levodopa dose equivalency reporting in Parkinson's disease. Mov Disord 2010; 25(15): 2649-53.

Tripoliti E, Zrinzo L, Martinez-Torres I, Tisch S, Frost E, Borrell E, *et al.* Effects of contact location and voltage amplitude on speech and movement in bilateral subthalamic nucleus deep brain stimulation. Movement Disorders 2008; 23(16): 2377-83.

van Wijk BC, Beudel M, Jha A, Oswal A, Foltynie T, Hariz MI, *et al.* Subthalamic nucleus phase–amplitude coupling correlates with motor impairment in Parkinson’s disease. Clinical Neurophysiology 2016; 127(4): 2010-9.

van Wijk BCM, Pogosyan A, Hariz MI, Akram H, Foltynie T, Limousin P, *et al.* Localization of beta and high-frequency oscillations within the subthalamic nucleus region. NeuroImage Clinical 2017; 16: 175-83.

Vanegas-Arroyave N, Lauro PM, Huang L, Hallett M, Horovitz SG, Zaghloul KA, *et al.* Tractography patterns of subthalamic nucleus deep brain stimulation. Brain : a journal of neurology 2016; 139(4): 1200-10.

Volkmann J, Moro E, Pahwa R. Basic algorithms for the programming of deep brain stimulation in Parkinson's disease. Movement Disorders 2006; 21(S14).

Wang J, Hirschmann J, Elben S, Hartmann CJ, Vesper J, Wojtecki L, *et al.* High-frequency oscillations in Parkinson's disease: Spatial distribution and clinical relevance. Movement Disorders 2014; 29(10): 1265-72.

Williams A, Gill S, Varma T, Jenkinson C, Quinn N, Mitchell R, *et al.* Deep brain stimulation plus best medical therapy versus best medical therapy alone for advanced Parkinson's disease (PD SURG trial): a randomised, open-label trial. The Lancet Neurology 2010; 9(6): 581-91.

Yang AI, Vanegas N, Lungu C, Zaghloul KA. Beta-coupled high-frequency activity and beta-locked neuronal spiking in the subthalamic nucleus of Parkinson's disease. Journal of Neuroscience 2014; 34(38): 12816-27.

Young DT. Medtronic Receives CE Mark Approval for the Percept™ PC Neurostimulator DBS System with BrainSense™ Technology. Dublin: Medtronic; 2020.

Zaidel A, Spivak A, Grieb B, Bergman H, Israel Z. Subthalamic span of β oscillations predicts deep brain stimulation efficacy for patients with Parkinson's disease. Brain : a journal of neurology 2010; 133(7): 2007-21.

4.4 Figures

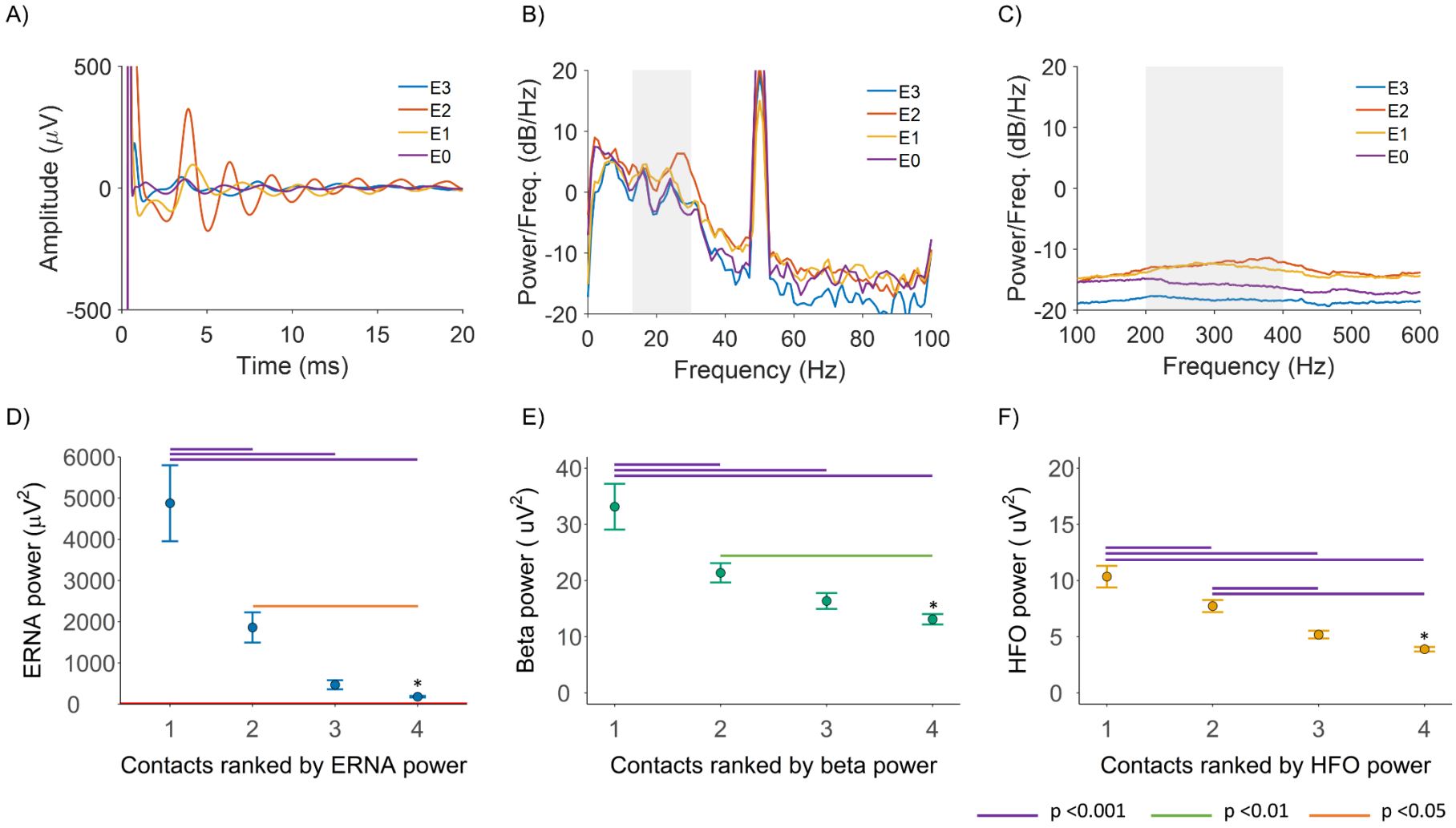
A)
B)
C)
D)
E)
F)
Amplitude (μV)
Time (ms)
Power/Freq. (dB/Hz)
Frequency (Hz)
E3
E2
E1
E0
ERNA power (μV²)
Contacts ranked by ERNA power
Beta power (uV²)
Contacts ranked by beta power
HFO power (uV²)
Contacts ranked by HFO power
p <0.001
p <0.01
p <0.05

Figure 4.1: The ERNA amplitude (A) and power spectral density of beta (B) and HFO (C) recorded at each of the four contacts in the right hemisphere of participant 1. E0 = most ventral contact in the substantia nigra pars reticulata; E1 = ventral STN contact; E2 = dorsal STN contact; E3 = most dorsal contact in the zona incerta. ERNA power (D), beta power (E) and HFO power (F) at contacts ranked according to the neuronal signal power. Red horizontal line in (D) above the x-axis represents the power range for beta oscillations and HFO.

*At rankings 1-3, n = 28 hemispheres. At ranking 4, n = 27 hemispheres, as recordings were not obtained in one ventral contact due to a technical fault. Bars represent standard error of means.

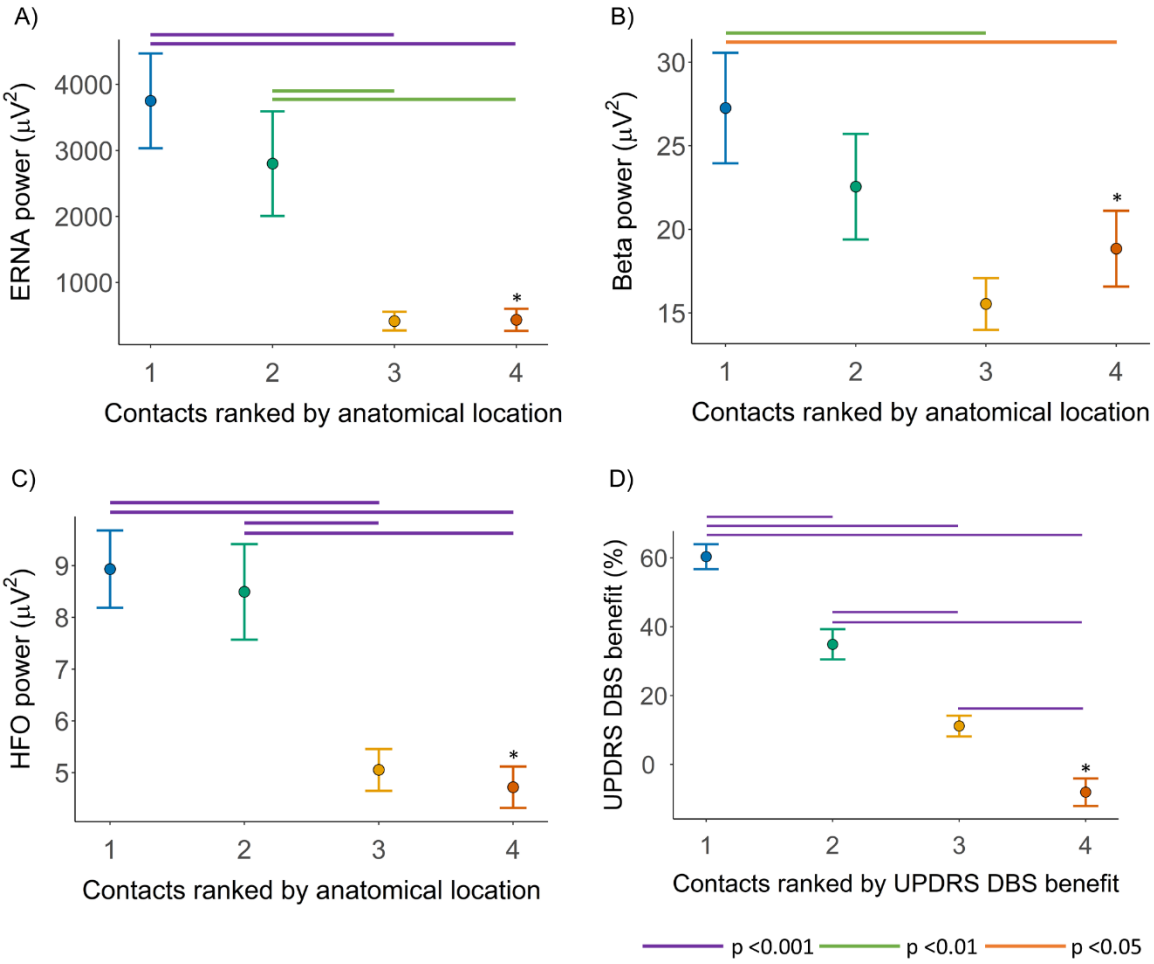

Figure 4.2: ERNA power (A), beta power (B) and HFO power (C) at contacts ranked according to proximity to the nominated ideal anatomical location for DBS in the STN region. (D) Hemibody UPDRS DBS benefit at contacts ranked according to the degree of motor benefit with DBS.

*At rankings 1-3, n = 28 hemispheres. At ranking 4, n = 27 hemispheres, as recordings were not obtained in one ventral contact due to a technical fault. Bars represent standard error of means.

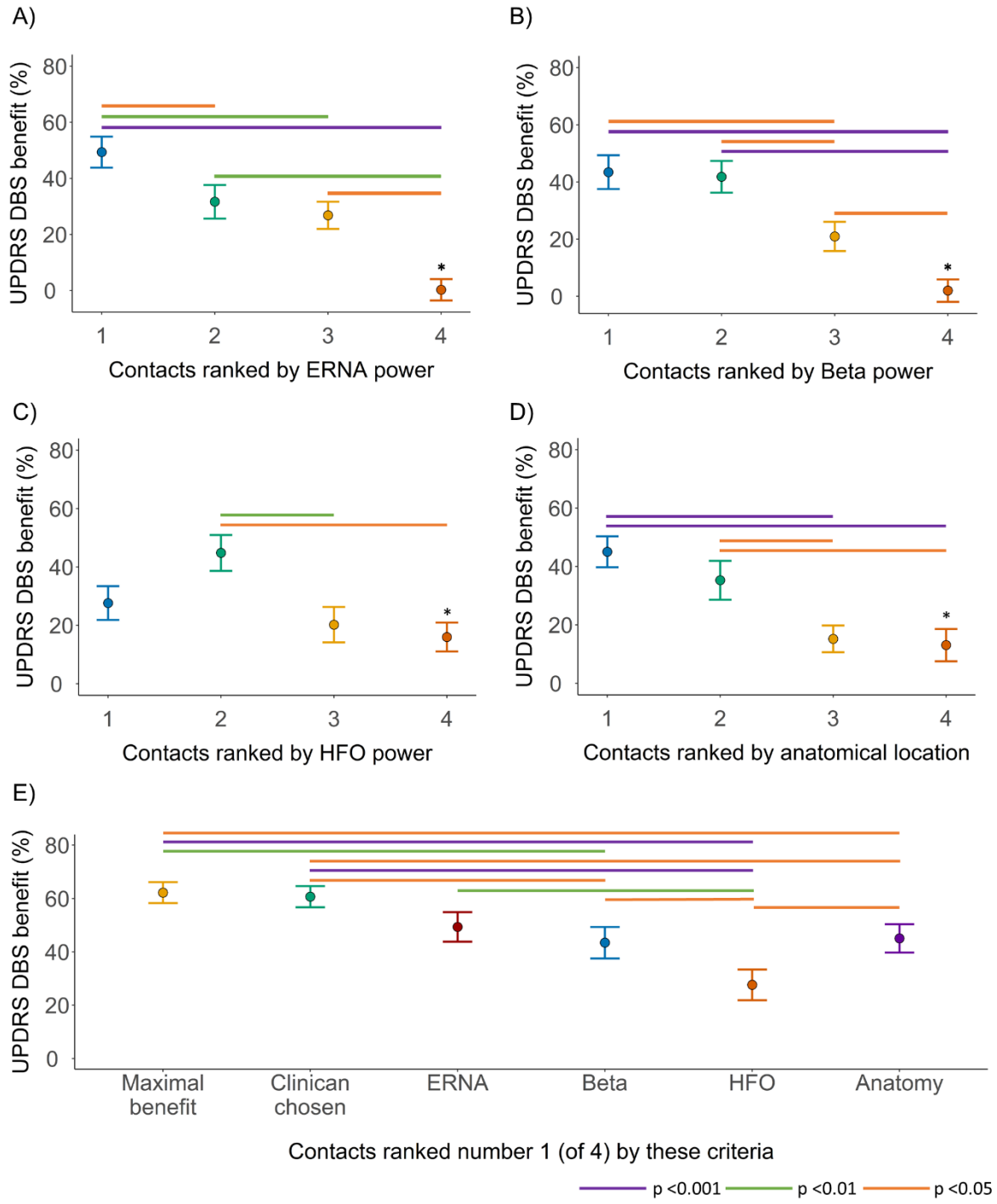

Figure 4.3: Hemibody UPDRS DBS benefit at contacts ranked according to ERNA power (A), beta power (B), HFO power (C), and proximity to the nominated ideal anatomical location (D). Hemibody UPDRS DBS benefit at the contact yielding maximal benefit, at the contact chosen

by the clinician for chronic DBS and at the contact ranked first according to ERNA power, beta power, HFO power and proximity to the nominated ideal anatomical location (E).

In A) to D), raw means (dots) and standard errors (bars) are presented in the figures, while statistical analyses employed fitted means adjusted for fixed and random effects. *At rankings 1-3, n = 28 hemispheres. At ranking 4, n = 27 hemispheres, as recordings were not obtained in one ventral contact due to a technical fault.

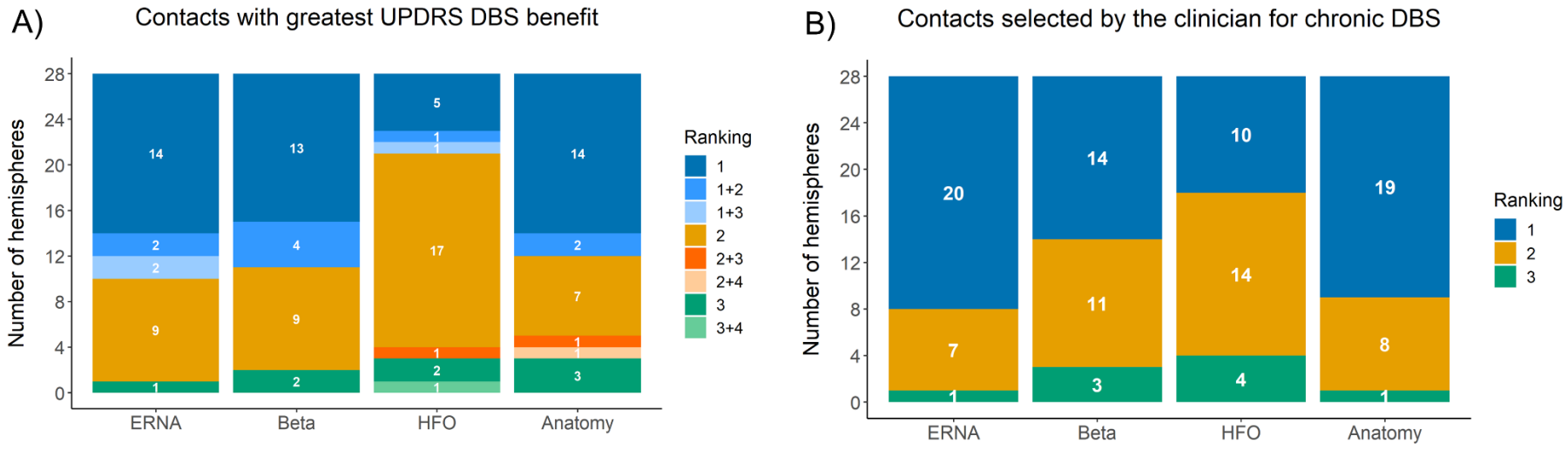

Figure 4.4: (A) The relationship between contacts yielding greatest motor benefit (UPDRS) with DBS and the ranking of those contacts according to the various factors. In four hemispheres, the UPDRS DBS benefit was the same in two different contacts and both contact rankings are represented. (B) The relationship between contacts selected by the clinician for chronic DBS and the ranking of those contacts according to the various factors.

4.5 Tables

Table 4.1: Characteristics of the 14 study patients including clinical features at the time of initial DBS surgery and chronic DBS parameters recorded at the time of experiments.

Patient	Age (years)	Gender	Disease duration (years)	Indication for DBS	Pre-op LED (mg)	Post-op LED (mg)	Hemisphere	Contacts	Current (mA)	Pulse width (µsec)	Frequency (Hertz)	Post-op improvement in UPDRS part III on/off DBS (%)*
1	64	M	8	MF	1250	50	Left	1-/2+	4.2	60	130	59.0
							Right	2-/C+	3.5	60	130	
2	74	F	8	MF	1200	250	Left	2-/1+	4.2	60	130	41.7
							Right	2-/C+	4.2	60	130	
3	62	M	8	MF	1200	250	Left	2-/C+	4.2	60	180	46.2
							Right	2-/C+	4.2	60	180	
4	66	F	10	MF	1250	175	Left	2-/C+	3.5	60	130	61.0
							Right	2-/C+	2.3	60	130	
5	55	M	10	MF	1100	250	Left	2-/C+	2.6	60	130	23.1
							Right	2-/C+	2.7	60	130	
6	56	F	8	MF	600	12.5	Left	2-/C+	3.7	90	180	43.2
							Right	2-/C+	3.5	60	180	
7	63	M	10	MF	1600	350	Left	1-/C+	3.7	90	130	67.4
							Right	2-/C+	4.3	60	130	

8	67	M	8	Tremor MF	800	250	Left	2-/C+	2.7	60	180	25.8
							Right	2-/C+	4.5	90	180	
9	63	F	8	Tremor MF	325	0	Left	2-/C+	2.1	60	180	47.2
							Right	2-/C+	5.1	90	180	
10	54	M	7	MF	100	0	Left	2-/C+	1.8	60	130	59.3
							Right	2-/C+	1.8	60	130	
11	65	F	4	Tremor MF	1050	200	Left	2-/C+	4.5	60	180	85.7
							Right	2-/C+	3.7	60	180	
12	67	M	9	MF	1300	0	Left	2-/C+	4.4	60	180	67.3
							Right	2-/C+	2.7	60	180	
13	64	F	5	MF	575	0	Left	2-/C+	2.3	60	130	68.5
							Right	2-/C+	3.6	60	130	
14	54	M	5	MF	650	0	Left	2-/1+	3.0	60	130	52.8
							Right	2-/1+	2.4	60	130	

DBS = deep brain stimulation. LED = levodopa equivalent dose (Tomlinson *et al.*, 2010). MF = motor fluctuations. For contacts; – is cathode and + is anode and C = case. The four contacts on each lead are numbered from ventral to dorsal as follows; 0, 1, 2, 3. For DBS; mA = milliamps and μs = microseconds.

*The UDPRS was assessed at the time of follow-up which ranged between three and eighteen months after STN-DBS surgery. Patients were evaluated in the off-medication state.

Table 4.2: Results of mixed-effects models assessing the degree to which contacts ranked according to ERNA power, beta power, HFO power, and anatomical location correlated with UPDRS DBS benefit.

Ranked variables in model	Predictive models for UPDRS DBS benefit		
	Conditional r^2	AIC	p value
ERNA	0.50	1039.9	<0.001
Beta	0.50	1041.6	<0.001
HFO	0.44	1057.2	<0.001
Anatomy	0.49	1048.0	<0.001
ERNA and Beta	0.53	1037.1	<0.001
ERNA and HFO	0.57	1028.0	<0.001
ERNA and anatomy	0.51	1043.2	<0.001
Beta and HFO	0.52	1040.9	<0.001
Beta and anatomy	0.54	1037.8	<0.001
HFO and anatomy	0.54	1043.1	<0.001
ERNA, HFO, beta	0.61	1021.5	<0.001
ERNA, beta and anatomy	0.54	1039.7	<0.001
ERNA, HFO and anatomy	0.58	1030.6	<0.001
Beta, HFO and anatomy	0.60	1026.5	<0.001
ERNA, HFO, beta and anatomy	0.63	1022.1	<0.001

4.6 Supplementary Material

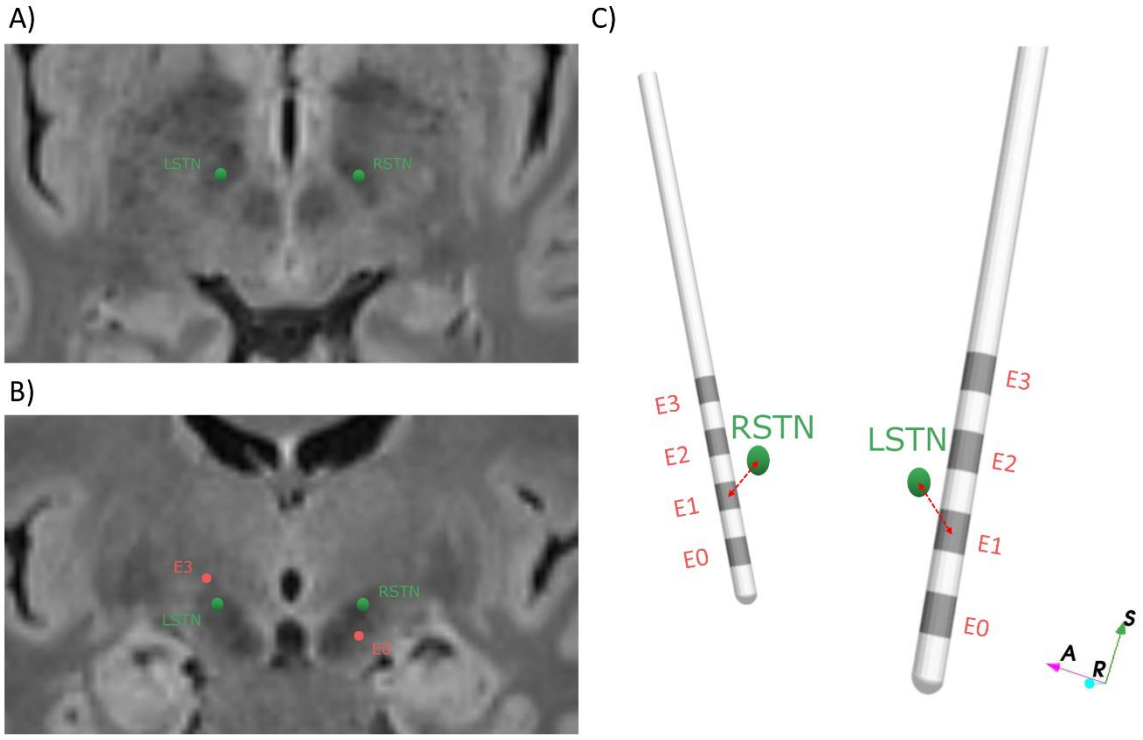

Supplementary figure 4.1: Representative images from a patient of the nominated ideal anatomical location (marked as a green dot) to apply DBS on a fluid-attenuated inversion recovery MRI scan, on axial views (A) and coronal views (B). In the same patient, a schematic diagram of the location of the quadripolar electrode array relative to the nominated ideal anatomical location to apply DBS (C). LSTN = left STN, RSTN = right STN, green dot = nominated ideal anatomical location, red dotted line = Euclidean distance from the E1 contact to the nominated ideal anatomical location, A = anterior, R = right, S = superior. The four contacts on each lead are numbered from ventral to dorsal as follows; E0, E1, E2, E3.

5 Can brain signals & anatomy refine contact choice for deep brain stimulation in Parkinson's disease?

San San Xu, FRACP[1,2,3], Wee-Lih Lee, PhD[1,2], Thushara Perera, PhD[1,2], Nicholas C. Sinclair, BEng (Hons)/BSci[1,2], Kristian J. Bulluss, FRACS, PhD[1,4,6], Hugh J. McDermott, PhD[1,2] , Wesley Thevathasan, FRACP, DPhil[1,3,5]

[1]Bionics Institute, East Melbourne, Australia.
[2]Medical Bionics Department, The University of Melbourne, East Melbourne, Australia.
[3]Department of Neurology, Austin Hospital, Heidelberg, Australia.
[4]Department of Neurosurgery, St Vincent's Hospital Melbourne, Fitzroy, and Department of Neurosurgery, Austin Hospital, Heidelberg, Australia.
[5]Department of Medicine, The University of Melbourne, Parkville, Australia.
[6]Department of Surgery, The University of Melbourne, Parkville, Australia.

Manuscript word count: 1700
Abstract word count: 150
Number of figures: 1
Number of tables: 1

Key words: deep brain stimulation; Parkinson's disease; subthalamic nucleus; evoked potentials; beta oscillations

Abbreviations: CV = cross-validation, DBS = deep brain stimulation, ERNA = evoked resonant neural activity, GPe = globus pallidus externa, GPi = globus pallidus interna, LR = logistic regression, MNI = Montreal Neurological Institute, here referring to a standard stereotactic space, PD = Parkinson's disease, RF = random forest, RN = red nucleus, SD = standard deviation, STN = subthalamic nucleus, SVM = support vector machine, SyN = symmetric image normalization method

5.1 Abstract

Background: Selecting the ideal contact to apply subthalamic nucleus deep brain stimulation (STN-DBS) in Parkinson's disease (PD) is time-consuming and reliant on clinical expertise.

Objectives: To assess whether neuronal signals and anatomy can predict the contacts selected by long-term, expert-clinician programming of STN-DBS.

Methods: We evaluated 75 hemispheres of 42 PD patients receiving chronic monopolar STN-DBS. At each contact, beta oscillations and evoked resonant neural activity (ERNA) were recorded intraoperatively, and anatomical location assessed. How these factors predicted the contacts clinically selected for chronic DBS at 6 months postoperatively was evaluated using a simple-ranking method and machine learning algorithms.

Results: The probability that these factors predicted the clinician-chosen contact was as follows: ERNA 81%, anatomy 72%, beta oscillations 52%. ERNA performed significantly better than anatomy and beta oscillations. Combining data did not improve model performance.

Conclusion: Neuronal signals and anatomy could be utilised in probability-based algorithms to assist STN-DBS programming.

5.2 Manuscript

Introduction

The efficacy of subthalamic nucleus (STN) deep brain stimulation (DBS) for patients with Parkinson's disease (PD) relies on delivering stimulation to the ideal location(Dembek *et al.*, 2019). After implantation, stimulation location is determined by the selection of contact(s) on each lead by clinicians (Okun *et al.*, 2005; Volkmann *et al.*, 2006). Identifying the ideal contact is an arduous, time-consuming, and ultimately heuristic process dependent on expertise(Okun *et al.*, 2005; Moro *et al.*, 2006; Volkmann *et al.*, 2006). A potential solution is to develop aids that use supplementary data including anatomy (Horn and Kühn, 2015; Petersen *et al.*, 2018) or neuronal signals recorded from DBS leads to guide, and eventually automate, contact selection. Beta oscillations (Ince *et al.*, 2010; Fernández-García *et al.*, 2017; Tinkhauser *et al.*, 2018; Telkes *et al.*, 2020) have been explored for this purpose, and more recently, the novel signal, evoked resonant neural activity (ERNA) (Horn and Kühn, 2015; Petersen *et al.*, 2018; Sinclair *et al.*, 2018; Ramirez-Zamora *et al.*, 2020). Thus here, in a cohort of 75 hemispheres in 42 patients with PD receiving monopolar STN-DBS, we assessed how anatomical information and neuronal signals could be used individually, or in combination, to predict the contacts chosen by expert-clinician programming at 6 months postoperatively.

Methods

Cohort selection

We accessed data of 100 hemispheres from 50 consecutive patients with PD implanted with STN-DBS quadripolar leads (Medtronic 3387) between 8 February 2016 and 21 March 2019. Only hemispheres receiving monopolar DBS were included as neuronal signals were recorded from each of the individual contacts independently, whereas the DBS field created by complex configurations (e.g. bipolar or double monopolar) may not be well represented by the location of a single contact (McIntyre *et al.*, 2004; Chaturvedi *et al.*, 2013). Thus, the final study cohort comprised 75 hemispheres of 42 patients receiving monopolar DBS at 6 months postoperatively.

Patients were implanted by a single DBS team in Melbourne, Australia, using surgical methods described previously (Sinclair *et al.*, 2018). Postoperatively, programming was performed by two experienced DBS neurologists (W.T., SS.X) from a high-volume DBS service (>50 de-novo implantations annually). Clinicians were blinded to the neuronal signal recordings. Clinicians did routinely evaluate electrode location by manually fusing the pre-operative MRI and post-operative CT on a planning station (StealthStation^{TM} S7, Medtronic, Dublin, Ireland). Visual inspection of the resulting images assisted programming. Monopolar configuration was selected initially, changing to bipolar or interleaved configuration if clinically indicated. Programming information at 6 months after surgery was accessed from DBS programmer reports. Dorsal interleaved configuration was programmed in five hemispheres to minimize dyskinesias (Ramirez-Zamora *et al.*, 2015). These cases were classified as monopolar, ignoring the dorsal contact. Neuronal signal and anatomical data have been previously reported in 13 patients (Xu *et al.*, 2020). The study was approved by the St Vincent's Public Human Research Ethics Committees (HREC/17/SVHM/81 and HREC-D 071/14).

Neuronal signal recording and analysis

Immediately after lead implantation, neuronal activity was recorded at each contact in a monopolar configuration and re-referenced to an average of the four unstimulated contacts in the contralateral hemisphere. Neuronal signal analysis was performed using MATLAB R2017a (Mathworks, Massachusetts, USA) (Sinclair *et al.*, 2019b).

ERNA was recorded by sequentially applying bursts, at a rate of one per second, of ten symmetric biphasic pulses per second at 3.375mA, 60μs and 130Hz to each contact (Sinclair *et al.*, 2018). ERNA was recorded from the stimulating contact after the last pulse of each burst. ERNA amplitude was measured by averaging the root mean square amplitude from 3.5 to 20 milliseconds after the onset of the last pulse of each burst and squared to calculate power (Sinclair *et al.*, 2018). For beta recordings, Blackman-Harris windowed epochs of 1 second were processed using a short-time Fourier transform (Sinclair *et al.*, 2019b). Beta power was estimated over the 13-30Hz frequency band. For machine learning analysis, neuronal signals were normalized by dividing signal power recorded at a given contact by the sum of the signal power across the four contacts in each hemisphere.

Contact anatomical mapping

The pre-operative 3 Tesla MRI was reoriented to align the anterior and posterior commissures using an automated utility (NITRC, acpcdetect, v2.0). In a similar manner to the Lead-DBS image analysis pipeline (Horn *et al.*, 2019), the reoriented MRI and post-operative CT scans were co-registered with BRAINSFit (Fedorov *et al.*, 2012) (v4.11) and normalized into the Montreal Neurological Institute (MNI) 152 2009b (Collins *et al.*, 1999; Fonov *et al.*, 2011) space using Advanced Normalization Tools SyN (Avants *et al.*, 2008). The DBS leads were localized on CT images using the PaCER toolbox (Husch *et al.*, 2018) and visually confirmed (Figure 5.1A). Resulting contact coordinates were transformed into MNI space. An ideal anatomical location to apply STN-DBS for PD was nominated according to MNI coordinates provided by Horn et al (Horn *et al.*, 2017a). The Euclidean distance between this location and each contact was calculated using a custom Python script. The DISTAL atlas (Ewert *et al.*, 2018) was used to segment the STN and surrounding structures for 3D visualization.

Statistical analysis

First, in a simple-ranking method, contacts were ranked within each hemisphere according to ERNA power, beta oscillations power and Euclidean distance from the ideal anatomical location to apply STN-DBS. These rankings were compared to the contacts selected for chronic DBS at 6 months. Second, machine learning algorithms (Logistic regression (LR), Support Vector Machine (SVM), Random forest (RF)) incorporating normalized ERNA, normalized beta oscillations and anatomical data were applied to explore whether combining factors could improve the probability of predicting the clinician-chosen contact (Supplementary material). The two methods were validated using 10-fold nested cross-validation (CV), repeated 10 times. The probability that the model predicted the clinician-chosen contact (predictive value) was calculated as the mean performance of the nested CV folds (Vabalas *et al.*, 2019). Differences between models were evaluated using the Friedman rank sum test and Nemenyi test for multiple comparisons. The machine learning algorithms were built using Scikit-Learn 0.23.2 (Pedregosa *et al.*, 2011) on Python 3.8.5 (Millman and Aivazis, 2011). All other data processing and statistical analysis was performed using R Project 4.0.3 (Millman and Aivazis, 2011).

Results

Patient characteristics are outlined in Supplementary Table 1. Notably, the mean dopaminergic medication reduction 6 months after surgery was 89.9% (SD 14.0).

ERNA ranked contacts versus clinically selected contacts

In 61/75 hemispheres, the contacts ranked first according to ERNA matched the clinician-chosen contacts (Figure 5.1B). In the simple-ranking model, the probability that the first-ranked ERNA contact was selected by the clinician was 81.3% (SD 14.9).

Beta oscillation ranked contacts versus clinically selected contacts

In 39/75 hemispheres, the contacts ranked first according to beta oscillations matched the clinician-chosen contacts (Figure 5.1B). In the simple-ranking model, the probability that the first-ranked beta oscillation contact was selected by the clinician was 51.9% (SD 19.5).

Anatomy ranked contacts versus clinically selected contacts

In 54/75 hemispheres, the contacts ranked first according to anatomy matched the clinician-chosen contacts (Figure 5.1B). In the simple-ranking model, the probability that the first-ranked contact according to anatomy was selected by the clinician was 72.1% (SD 17.1).

Evaluation of single-factor and multi-factor model performance

There was a significant difference between ERNA, beta oscillations and anatomy models built using the simple-ranking method (Friedman $\chi^2 = 82.0$, $p < 0.001$). ERNA was more predictive than beta oscillations and anatomy (Nemenyi test, beta $p<0.001$, anatomy $p = 0.004$). Anatomy was more predictive than beta oscillations (Nemenyi test, $p<0.001$) (Figure 5.1C).

The clinician-chosen contact was predicted by any one of the three factors in 71/75 hemispheres. The clinician-chosen contact was predicted by more than one factor in 56/75 hemispheres: all three factors 27/75, ERNA and anatomy 22/75, ERNA and beta oscillations 6/75, beta oscillations and anatomy 1/75.

Three classification algorithms (LR, SVM and RF) were explored to evaluate the model performance of all factors (Supplementary figure 5.4). The RF classifier produced the best

model performance and was selected for subsequent analysis (Table 5.1). The probability that ERNA data predicted the clinician-chosen contact was 81.3% and this did not change significantly with inclusion of anatomy and/or beta oscillation information (Friedman $\chi^2 = 6.4$, $p = 0.10$) (Figure 5.1C).

Discussion

In 75 hemispheres of 42 patients receiving monopolar STN-DBS for PD, we found that anatomy and neuronal signals could predict the contacts selected by expert-clinician programming 6 months postoperatively. The predictive value of each factor was as follows: ERNA 81%, anatomy 72%, beta oscillations 52%. ERNA was significantly more predictive than beta oscillations and anatomy. Compared with using ERNA data alone, the addition of beta oscillation and anatomical information did not improve model performance.

In this study, we elected to use a real-world outcome of the contacts selected by expert clinicians as the 'gold standard'. However, the DBS programming heuristic can be complex, time-consuming and errors are not uncommon (Okun *et al.*, 2005; Moro *et al.*, 2006). Nonetheless, the programming clinicians were experienced and operating in a high-volume centre. Moreover, patients achieved an 89.9% reduction in dopaminergic medication doses with DBS. An alternative approach to identify the ideal contact is to systematically assess the acute motor impact of DBS at every contact in experimental sessions. Interestingly, a previous such study found that beta oscillation power identified the best contact for rigidity benefit in 12/19 hemispheres implanted with directional leads, a similar result to this study (Tinkhauser *et al.*, 2018). However, such acute studies are liable to confounds such as incomplete washout and missing DBS effects that evolve over longer timescales (Temperli *et al.*, 2003).

The error prone nature of DBS programming highlights the need for supplementary data to guide contact choice. However, in this study, no factor alone predicted the clinician-chosen contact in all hemispheres. For example, 81% of contacts ranked first by ERNA were clinically selected. In the other 19%, it is unknown whether the contacts ranked first by ERNA would have achieved equivalent or better outcomes than those selected by the clinicians. Future refinements to signal processing or the use of more advanced imaging techniques (Vanegas-Arroyave *et al.*, 2016; Akram *et al.*, 2017; Mahlknecht *et al.*, 2017) could better predict the

ideal contact to apply DBS. For example, neuronal signals and structural imaging may not inform on aberrant fibre tracts that can cause side effects.

This work is timely, as programming complexity has increased with the introduction of directional leads and multiple independent current control (Timmermann *et al.*, 2015; Schüpbach *et al.*, 2017; Vitek *et al.*, 2020). Previous literature has explored the potential of beta oscillations in guiding programming in directional leads (Fernández-García *et al.*, 2017; Tinkhauser *et al.*, 2018; Telkes *et al.*, 2020). Here, beta oscillations were less predictive of the clinical contact in omnidirectional electrodes compared with ERNA and anatomy. Directional leads could enhance the spatial resolution of ERNA recordings, though whether this would improve prediction of the ideal DBS location remains unknown. Clinician aids that assist lead localisation and identify the ideal anatomical location to apply DBS have been developed to guide programming (Horn and Kühn, 2015; Horn *et al.*, 2017a; Petersen *et al.*, 2018; Dembek *et al.*, 2019; Horn *et al.*, 2019). However, such methods require time and expertise to retrieve and analyse imaging, and accounting for the orientation of segments on directional electrodes is especially challenging (Sitz *et al.*, 2017). Moreover, we found that ERNA was more predictive of the clinical contact choice compared with anatomy. With the commercial availability of intra-operative recording systems and implantable pulse generators capable of monitoring bioelectric signals (Marmor *et al.*, 2017; Ozturk *et al.*, 2020; Young, 2020), automated processing of ERNA could be readily offered to clinicians to assist programming decisions.

Authors' contributions

SS.X was involved with the conception, organisation and execution of the research project, the statistical analysis and the writing of the first draft of the manuscript. W.L was involved in the organisation and execution of the research project and the statistical analysis and review and critique of the manuscript. T.P was involved in the organisation and execution of the research project and review and critique of the manuscript. N.C.S was involved in the organisation of the research project and the review and critique of the manuscript. K.J.B was involved in the organisation and execution of the research project and the review and critique of the manuscript. H.J.M was involved in the organisation and execution of the research project and the review and critique of the manuscript. W.T was involved in the conception, organisation and execution of the research project and the review and critique of the manuscript.

Funding

This study was funded through the National Health and Medical Research Council (Development grant #1177815, post graduate scholarship #1133295 (SS.X)). W.T is also supported through Lions International. All authors affiliated with the Bionics Institute acknowledge the support it receives from the Victorian Government through its operational infrastructure program.

Competing interests

N.C.S, K.J.B, H.J.M and W.T are founders and hold shares and options in DBS Technologies Pty Ltd which plans to commercialize the use of neuronal signals to improve DBS. They are named inventors on related patents, which are assigned to DBS Technologies Pty Ltd. SS.X holds options in DBS Technologies Pty Ltd. T.P holds options in DBS Technologies Pty Ltd and is a named inventor on related patents, which are assigned to DBS Technologies Pty Ltd. W.T has received honoraria from Medtronic and Boston Scientific. W.L has no relevant financial disclosures.

5.3 References

Dembek TA, Roediger J, Horn A, Reker P, Oehrn C, Dafsari HS, *et al.* Probabilistic Sweetspots Predict Motor Outcome for DBS in Parkinson's Disease. Annals of neurology 2019.

Hamel W, Fietzek U, Morsnowski A, Schrader B, Herzog J, Weinert D, *et al.* Deep brain stimulation of the subthalamic nucleus in Parkinson's disease: evaluation of active electrode contacts. Journal of Neurology, Neurosurgery & Psychiatry 2003; 74(8): 1036-46.

Horn A, Kühn AA, Merkl A, Shih L, Alterman R, Fox M. Probabilistic conversion of neurosurgical DBS electrode coordinates into MNI space. Neuroimage 2017; 150: 395-404.

Ince NF, Gupte A, Wichmann T, Ashe J, Henry T, Bebler M, *et al.* Selection of optimal programming contacts based on local field potential recordings from subthalamic nucleus in patients with Parkinson's disease. Neurosurgery 2010; 67(2): 390-7.

Moro E, Poon Y-YW, Lozano AM, Saint-Cyr JA, Lang AE. Subthalamic nucleus stimulation: improvements in outcome with reprogramming. Archives of neurology 2006; 63(9): 1266-72.

Okun MS, Tagliati M, Pourfar M, et al. Management of referred deep brain stimulation failures: A retrospective analysis from 2 movement disorders centers. Archives of Neurology 2005; 62(8): 1250-5.

Ramirez-Zamora A, Giordano J, Gunduz A, Alcantara J, Cagle JN, Cernera S, *et al.* Proceedings of the Seventh Annual Deep Brain Stimulation Think Tank: Advances in Neurophysiology, Adaptive DBS, Virtual Reality, Neuroethics and Technology. Frontiers in Human Neuroscience 2020; 14: 54.

Ramirez-Zamora A, Kahn M, Campbell J, DeLaCruz P, Pilitsis JG. Interleaved programming of subthalamic deep brain stimulation to avoid adverse effects and preserve motor benefit in Parkinson's disease. Journal of neurology 2015; 262(3): 578-84.

Schüpbach M, Chabardes S, Matthies C, Pollo C, Steigerwald F, Timmermann L, *et al.* Directional leads for deep brain stimulation: Opportunities and challenges. Movement Disorders 2017; 32(10): 1371-5.

Sinclair NC, McDermott HJ, Bulluss KJ, Fallon JB, Perera T, Xu SS, *et al.* Subthalamic nucleus deep brain stimulation evokes resonant neural activity. Annals of neurology 2018; 83(5).

Sinclair NC, McDermott HJ, Fallon JB, Perera T, Brown P, Bulluss KJ, *et al.* Deep brain stimulation for Parkinson's disease modulates high-frequency evoked and spontaneous neural activity. Neurobiology of Disease 2019: 104522.

Tinkhauser G, Pogosyan A, Debove I, Nowacki A, Shah SA, Seidel K, *et al.* Directional local field potentials: A tool to optimize deep brain stimulation. Movement Disorders 2018; 33(1): 159-64.

Tomlinson CL, Stowe R, Patel S, Rick C, Gray R, Clarke CE. Systematic review of levodopa dose equivalency reporting in Parkinson's disease. Mov Disord 2010; 25(15): 2649-53.

Volkmann J, Moro E, Pahwa R. Basic algorithms for the programming of deep brain stimulation in Parkinson's disease. Movement Disorders 2006; 21(S14).

Walker HC, Huang H, Gonzalez CL, Bryant JE, Killen J, Cutter GR, *et al.* Short latency activation of cortex during clinically effective subthalamic deep brain stimulation for Parkinson's disease. Movement Disorders 2012; 27(7): 864-73.

5.4 Figures

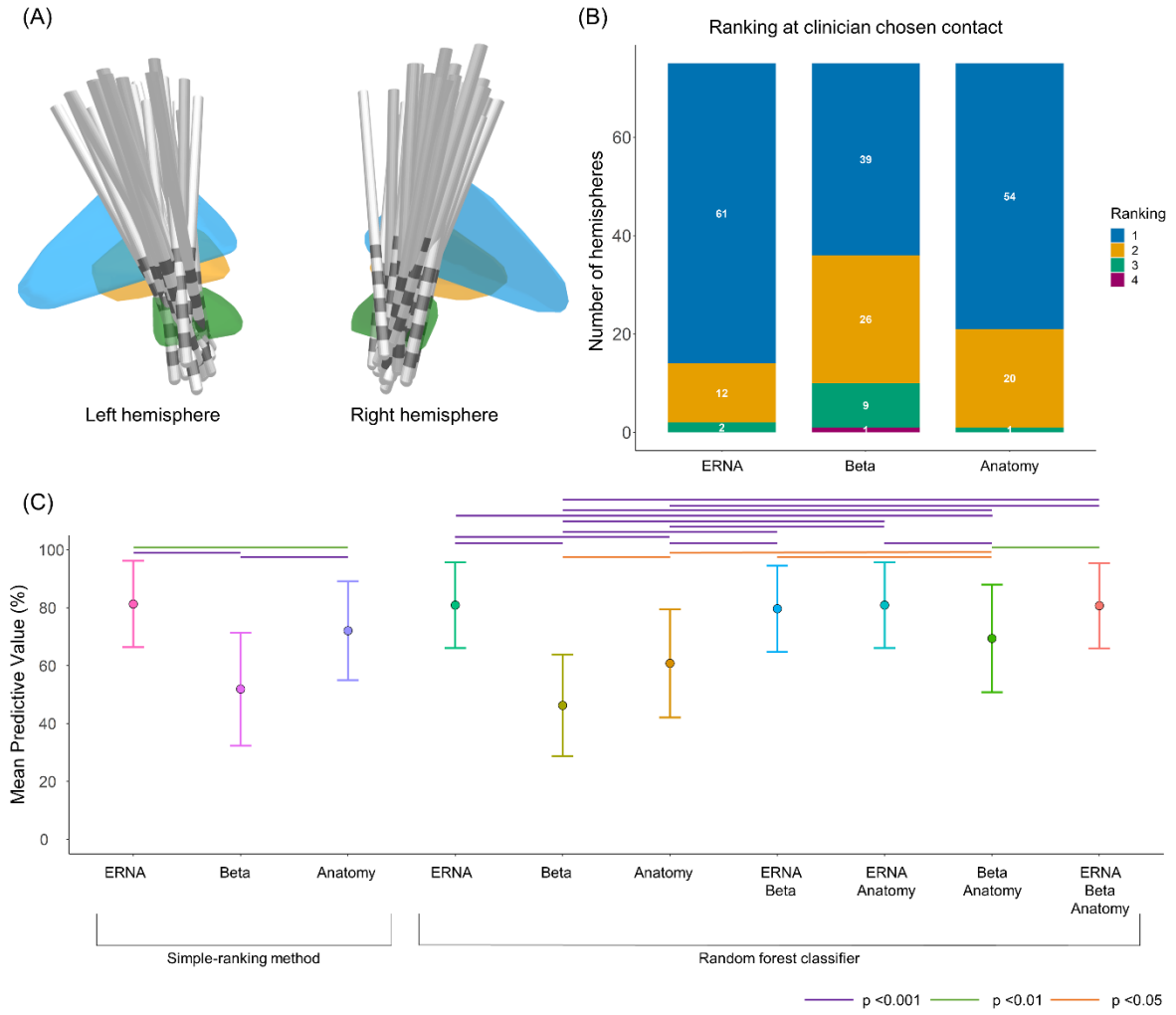

Figure 5.1: (A) Placement of DBS electrodes visualised in the MNI space. Blue = globus pallidus externa. Yellow = globus pallidus interna. Green = subthalamic nucleus. (B) The clinician-chosen contacts for chronic DBS and the corresponding ranking of those contacts according to ERNA power, beta oscillation power and anatomical location. (C) The mean predictive value of ERNA power, beta oscillation power and anatomical location using the simple-ranking method and random forest classifier.

Bars represent standard deviation. p values in figures are adjusted for multiple comparisons (Nemenyi test).

5.5 Tables

Table 5.1: The mean predictive value of the features of interest using different modelling techniques.

Analysis method	**Included factors**	**Mean predictive value (%)**	**SD**
Simple ranking method	ERNA	81.3	14.9
	Beta oscillations	51.9	19.5
	Anatomy	72.1	17.1
Logistic regression	Normalised ERNA, normalised beta oscillations, Anatomy	79.7	13.7
Support Vector Machine	Normalised ERNA, normalised beta oscillations, Anatomy	80.0	15.2
Random forest	Normalised ERNA, normalised beta oscillations, Anatomy	81.0	14.9
	Normalised ERNA	81.3	14.6
	Normalised beta oscillations	44.9	16.5
	Anatomy	60.7	18.7
	Normalised ERNA, normalised beta oscillations	80.1	15.7
	Normalised ERNA, Anatomy	81.4	14.7
	Normalised beta oscillations, Anatomy	69.8	18.0

Data is presented as mean and standard deviation (SD).

5.6 Supplementary material

Simple-ranking Method

A simple-ranking method was employed to determine the predictive value of each factor alone (ERNA power, beta oscillations power and Euclidean distance from the ideal anatomical location) in identifying the clinician-chosen contact (Supplementary figure 5.1). The method was validated using a 10-fold nested cross-validation (CV), repeated 10 times (Supplementary figure 5.3a and see model validation below).

Machine Learning Method

Three machine learning techniques – Logistic Regression (LR) (Dreiseitl and Ohno-Machado, 2002), Support Vector Machine (SVM) (Boser *et al.*, 1992) and Random Forest (RF) (Breiman, 2001) – were used to predict the probability of a contact being selected by the clinician for chronic DBS when using a combination of factors (Supplementary figure 5.2).

The performance of these learning algorithms was validated using a 10-fold nested CV, repeated 10 times (Supplementary figure 5.3a and see model validation below). The dataset was imbalanced due to the unequal class distribution between selected and non-selected electrodes (one selected, three unselected in each hemisphere). Thus, balanced class weight was applied during training to reduce bias in the classification model (Supplementary figure 5.3b). The hyperparameter selections used in our grid search are shown in Supplementary table 5.1, Supplementary table 5.2 and Supplementary table 5.3.

The RF classifier delivered the highest mean predictive value and was employed to evaluate all possible combinations of factors in a model (Supplementary figure 5.4).

Model Validation

The simple-ranking and machine learning models were validated using a 10-fold nested CV method, repeated 10 times. The dataset was separated into training and testing sets to ensure that data from the same patient was not used for both model development and model evaluation (Vabalas *et al.*, 2019) (Supplementary figure 5.3a).

Supplementary table 5.1: Logistic Regression

Hyperparameters	**Values**
Penalty	Elastic-net
Tolerance for stopping criteria	10^{-6}
Inverse of regularization strength, C	0, 10^0, 10^1, 10^3, 10^5
Ratio of L1 penalty	0, 0.25, 0.50, 0.75, 1.0
Max iteration number	3000

Supplementary table 5.2: Support Vector Machine

Hyperparameters	**Values**
Kernel	Radial basis function
Regularization strength, C	0, 10^0, 10^1, 10^3, 10^5
Tolerance for stopping criteria	10^{-6}

Supplementary table 5.3: Random Forest

Hyperparameters	**Values**
Number of decision trees	100
Maximum features per tree	Same as number of features
Quality of split criterion	Gini
Min samples per leaf	1, 5, 10, 20, 50
Max samples per tree (%)	50, 80, 100

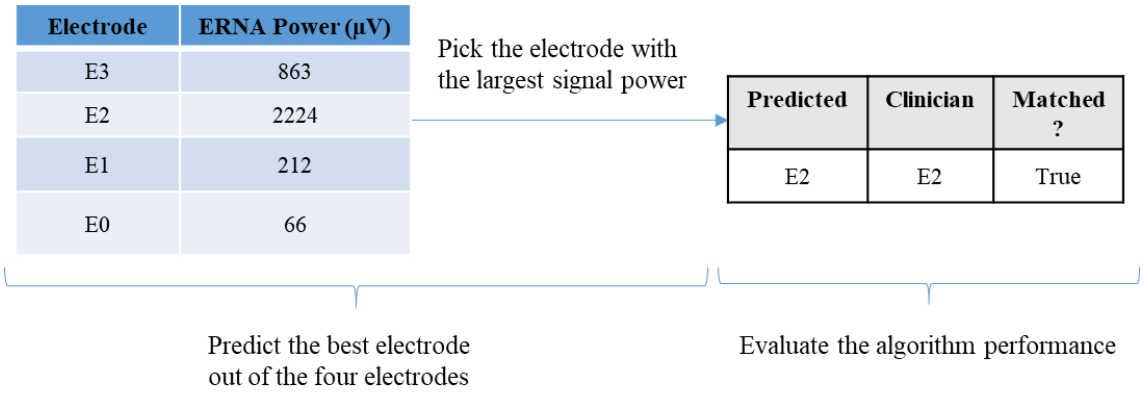

Supplementary figure 5.1: Simple-ranking method. Each contact on the DBS lead is ranked according to ERNA power, beta oscillations power or proximity to the ideal anatomical location. In this example, the contact measuring the largest ERNA power (E2) is predicted to be the best contact and coincides with the clinician-chosen chosen for chronic DBS. The simple-ranking method was then validated using a 10-fold nested cross-validation (CV) (Figure 3a), repeated 10 times.

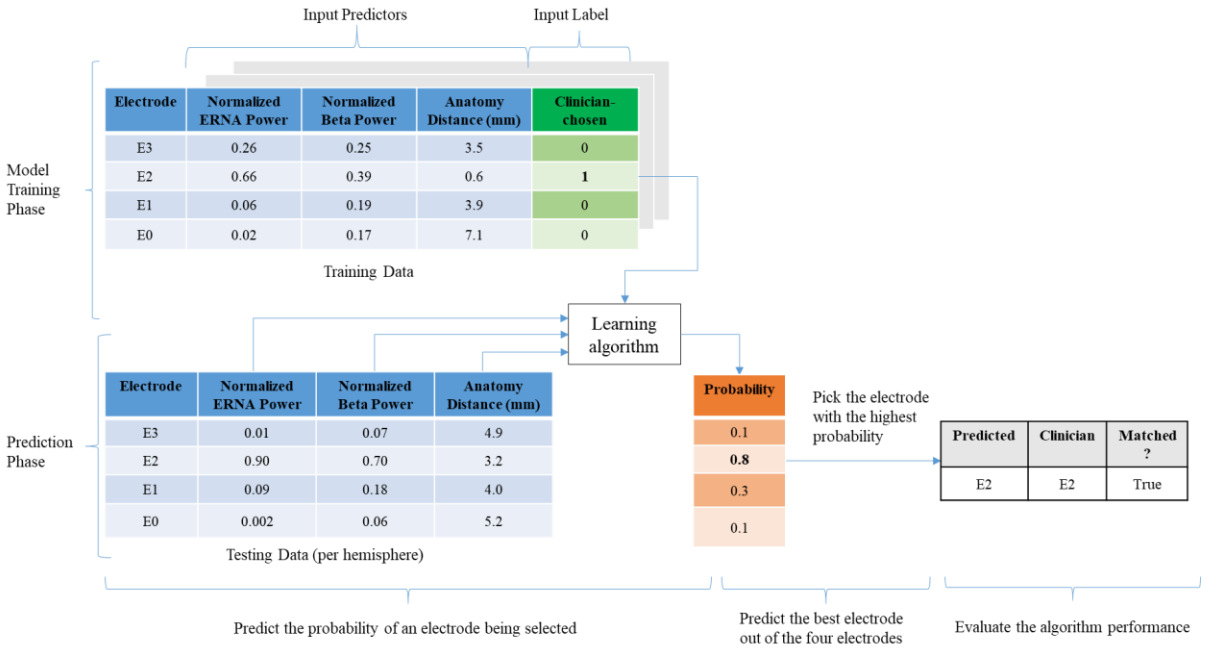

Supplementary figure 5.2: In the model training phase, a combination of factors is used to determine the optimal contact prediction through a learning algorithm. In the testing data, within each hemisphere, the probability that a given contact coincides with the clinician-chosen contact is calculated using the learning algorithm. Finally, the contact with the highest probability is compared to the clinician-chosen contact.

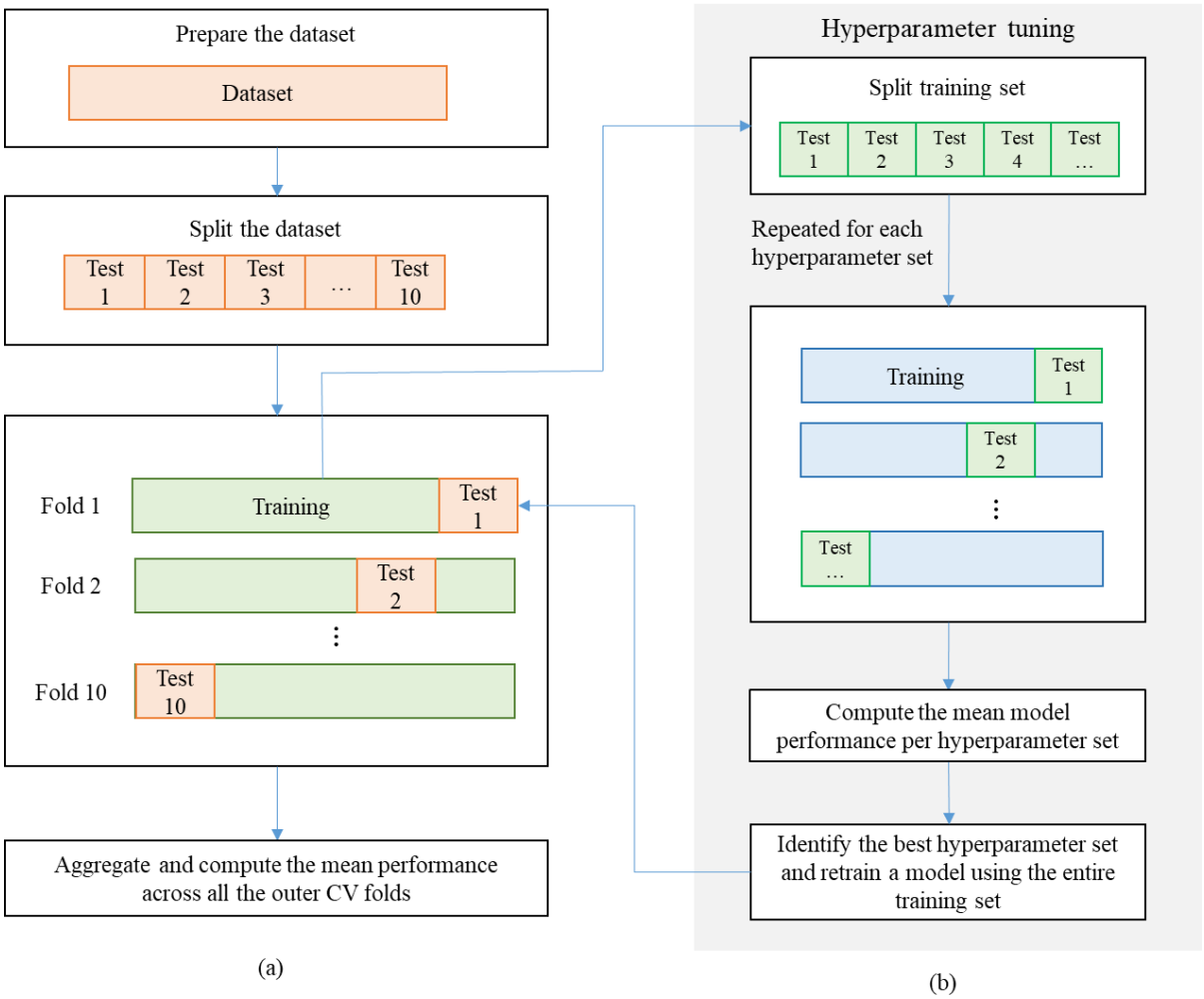

Supplementary figure 5.3: Nested cross-validation (CV) for algorithm training and testing. (a) illustrates the 10-fold nested outer CV used for evaluating the algorithm performance, which was repeated 10 ten times. (b) illustrates the inner CV used for hyperparameter tuning to find the optimal hyperparameters for each algorithm (Logistic Regression, Support Vector Machine and Random Forest). After identification of the optimal hyperparameter set, the algorithm was applied to the outer CV testing set to generate the predictive value of the model.

Note: Simple-ranking method does not require hyperparameter tuning.

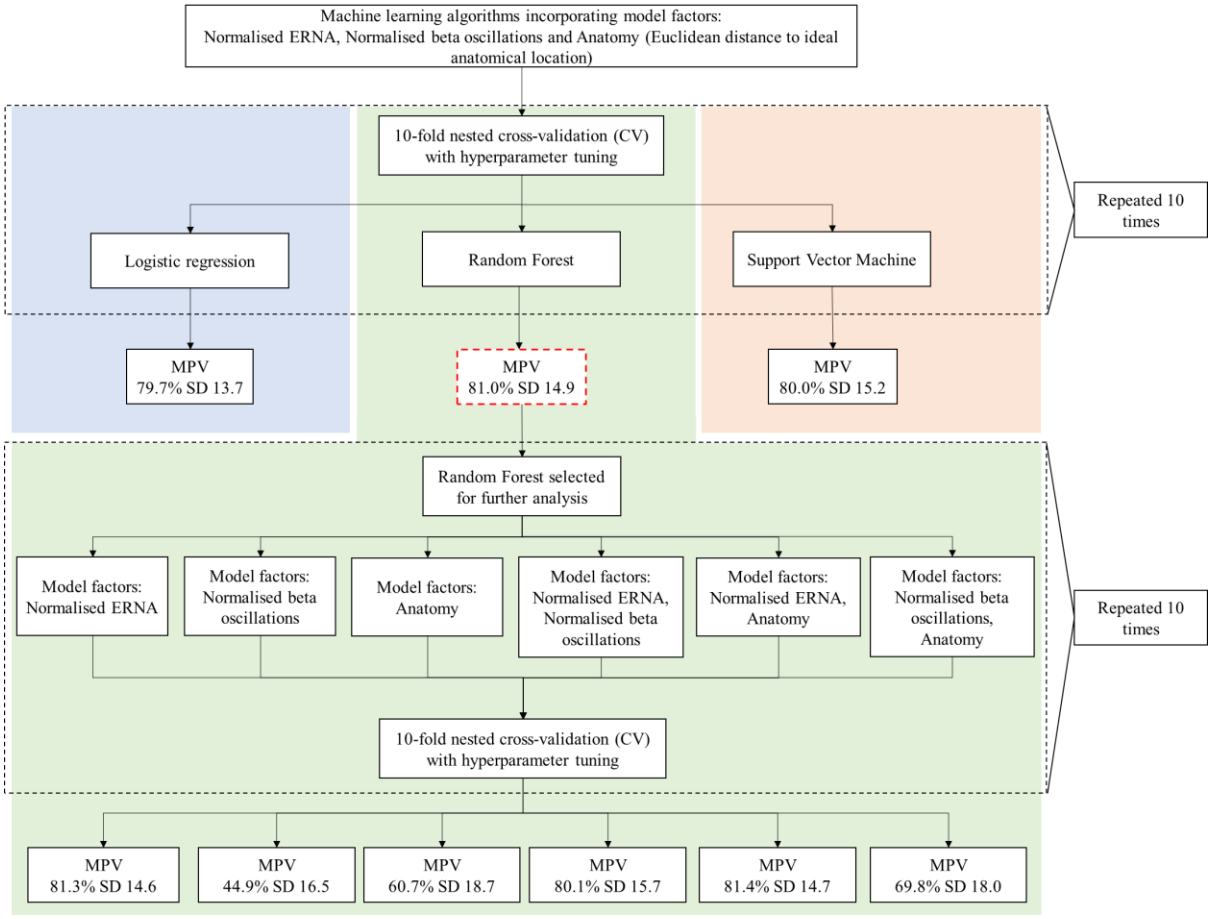

Supplementary figure 5.4: Machine learning algorithms. Three machine learning algorithms were evaluated to assess the mean predictive value of models employing a combination of factors. The Random Forest model produced the highest predictive value and was employed for further analysis of factor combinations. MPV = mean predictive value, SD = standard deviation

Appendix References

Boser BE, Guyon IM, Vapnik VN. A training algorithm for optimal margin classifiers. Proceedings of the fifth annual workshop on Computational learning theory. Pittsburgh, Pennsylvania, USA: Association for Computing Machinery; 1992. p. 144–52.

Breiman L. Random Forests. Machine Learning 2001; 45(1): 5-32.

Dreiseitl S, Ohno-Machado L. Logistic regression and artificial neural network classification models: a methodology review. Journal of biomedical informatics 2002; 35(5-6): 352-9.

Vabalas A, Gowen E, Poliakoff E, Casson AJ. Machine learning algorithm validation with a limited sample size. PloS one 2019; 14(11): e0224365.

6 Discussion and Conclusion

The first part of this thesis explores the current landscape of DBS in PD patients on a national level, identifying the burden of routine care, hardware complications and duration of therapy (Hypothesis 1). These results help inform on research priorities including improving surgical navigation, simplifying DBS programming, and prolonging battery life. The latter part of this thesis investigates a novel neurophysiological signal, ERNA, with the potential to address these shortcomings (Hypothesis 2), in particular pertaining to guidance for clinician programming and electrode implantation.

The limitations of each study are discussed in detail in the relevant chapters.

6.1 DBS database study (Chapter 3)

6.1.1 Key findings

A total of 1849 patients with PD in Australia were identified as having had DBS implantation surgery between 1st January 2002 and 31st December 2016 using linked national government databases. The number of patients with PD who underwent DBS increased substantially over the first ten years of the study period prior to plateauing. The average age at DBS implantation was 62.6 years old and 65% were male. The most common surgical procedure entailed bilateral intracranial lead implantation with attendance by a neurologist to assist in intra-operative target localisation. Programming requirements were highest in the first year after surgery, with a mean of 6.9 programming sessions, which decreased to 2.8 sessions annually thereafter. 51.2% of patients had repeat hardware surgery during follow up, with 10.5% of patients having repeat hardware surgery within the first year of DBS implantation surgery. 15.8% of repeat hardware surgery for a presumed complication and the proportion of surviving patients who had repeat hardware surgery for a complication at five years was 16.4% and at ten years was 24.3%. 11.3% of patients had hardware complication surgery involving the intracranial lead. The median time from DBS implantation to residential care admission was 10.2 years and median time to death, was 11.4 years. DBS implantation age

over 65 years was associated with less hardware complication surgeries and more residential care admissions and death during the study period. The overall standardised mortality ratio was 2.3 compared to the general Australian population, adjusted for gender and age.

6.1.2 Clinical implications

DBS programming

This is the first study to systematically evaluate DBS programming after implantation surgery. As expected, the programming frequency was greatest within the first year of DBS implantations, when regular adjustments are necessary to address stun effect and medication changes (Maltête *et al.*, 2008; Mestre *et al.*, 2016). Thereafter, programming rates were reasonably modest, and it is conceivable that a comprehensive exploration of parameters has not been undertaken in all patients. An estimated 40-60% of patients have been shown to achieve better motor outcomes with reprogramming performed by DBS clinicians (Okun *et al.*, 2005; Moro *et al.*, 2006). Crucially, the patients in this study had surgery prior to the advent of directional leads and stimulation delivery via multiple independent current control (Pollo *et al.*, 2014; Timmermann *et al.*, 2015). These new technologies have added complexity to the programming paradigm and are anticipated to increase the duration and frequency of programming sessions (Schüpbach *et al.*, 2017).

DBS hardware maintenance and complications

This is one of few studies reporting on DBS hardware maintenance and complications on a national level. Previous literature has largely focused on retrospective reviews in large, academic hospitals (Joint *et al.*, 2002; Oh *et al.*, 2002; Videnovic and Metman, 2008; Vergani *et al.*, 2010). These centres may have inherently lower complication rates due to greater experience and higher case volume or underreport complication rates due to publication bias (Videnovic and Metman, 2008; Sharma *et al.*, 2013; Hrabovsky *et al.*, 2017). Interestingly, a study of two North American databases, the Medicare database and NSQIP database, did report an intracranial electrode complication rate far higher than previously described, of 15% and 34% (Rolston *et al.*, 2016). However, this study lacked patient-specific data and instead, reported outcomes as a proportion of total procedures. Furthermore, the North American Medicare services are only available to PD patients over 65 years old and offered limited

information on the nature of the DBS procedures. The NSQIP database was more comprehensive, with a level of detail comparable to the Australian MBS system, though only 194 procedures were identified over a 9-year period. In contrast, our study of a comprehensive national database with individualised patient information revealed a lower, but significant electrode complication procedure rate of 11.3%.

An important consideration is that only complications that resulted in surgery were recorded. Some complications may not warrant intervention if they are tolerable or if the risks of intervention are high. To this end, advanced age was associated with a lower rate of hardware complication related procedures. Previous studies have also described a lower rate of complication surgeries in older patients (Rolston *et al.*, 2016; Stroupe *et al.*, 2019), probably reflecting the surgeon's reluctance to operate on this high risk cohort. Furthermore, we found that additional hardware procedures increase risks. The peri-operative mortality rate was lowest after the initial DBS implantation surgery (0.3%) and higher after any subsequent DBS related surgery (0.6%). The increasing frailty with disease progression and older age could contribute to the greater risk with successive procedures (Shinall *et al.*, 2020). Even routine hardware maintenance surgeries were not benign. With each successive IPG related procedure, including routine battery changes, the risk of having an IPG complication requiring surgery was almost four-fold higher, even after adjusting for age.

Community living and survival after DBS

The median time from DBS implantation to residential care admission was 10.2 years and older surgical age was associated with reduced duration of community living. This is the first cross-sectional study to evaluate the duration of community living in DBS patients with PD. In two single centre studies, with an average DBS implantation age of 60 years, the rate of residential care admission was vastly different at 42% (Bang Henriksen *et al.*, 2016) 10-years after surgery and 6% (Ngoga *et al.*, 2014) over 7-years after surgery. Interestingly, Ngoga and colleagues also reported on a control group of PD patients who were offered but declined DBS, with a far higher residential admission rate of 37% during the study period. The differences in follow-up duration may partially account for the reported discrepancies, but variations in DBS patient selection at single centres need to be considered.

The median time from DBS implantation to death was 11.4 years and older surgical age was associated with reduced duration of survival. Our finding of a standardised mortality ratio of

2.3 is similar to that reported in other PD patients (Schrag *et al.*, 1998; Hely *et al.*, 2008), including those who have had DBS (Schüpbach *et al.*, 2007; Cubo *et al.*, 2018). The mean duration from residential care admission to death was 4.2 years, paralleling results in the general PD population (Hely *et al.*, 1999; Hely *et al.*, 2005; Kempster *et al.*, 2010; Rizzone *et al.*, 2014). Unfortunately, the impact of DBS on life expectancy could not be evaluated due to the lack of a control group. Indeed, a major hindrance in DBS survival analysis is the absence of a quality control group (Contarino *et al.*, 2018). Even patients who have been offered but declined surgery may have intrinsic biases fundamental to their decision-making process. Survival after surgery has largely been reported in single-centre studies or discrete patient subgroups, with ten year survival rates ranging from 50 to 80% (Lilleeng et al., 2014; Ngoga et al., 2014; Rocha et al., 2014; Bang Henriksen et al., 2016; Cubo et al., 2018). Notably, in the United States veterans' database study, 620 veterans with DBS for PD had a median survival of only 7 years, though a significantly higher average implantation age of 69 years (Weaver *et al.*, 2017). A key advantage of our study is its generalisability, in that it encompasses PD patients with DBS across multiple centres in Australia captured by a national level government database.

6.1.3 Future direction

This study highlights several key issues in the management of DBS patients with PD. The duration of DBS therapy is over 10 years, during which time patients need routine device maintenance for programming and battery depletion. Many patients require additional procedures, including intracranial surgery and successive surgeries after DBS implantation increase complication rates and peri-operative mortality. These results encourage reflection on patient selection guidelines, including the age and stage of disease at which to implement DBS. Previous studies of DBS in a younger cohort of patients with early motor fluctuations (mean age 52 years old, mean duration of motor fluctuations 1.6 years) demonstrated that early intervention improved quality of life and reduced motor disability. On statistical modelling, early DBS was predicted to be more cost effective compared to standard medical therapy (Schuepbach *et al.*, 2013; Dams *et al.*, 2016). However, the long-term implications on the burden of care with early intervention and a longer duration of DBS therapy need to be considered.

Indeed, this study draws attention to the strain that DBS maintenance and complication management can place on patients, clinicians, and the healthcare system. Developing technologies to improve surgical navigation and minimise lead malposition, simplify programming and increase hardware durability and battery life are crucial. Aids that assist in post-operative electrode localisation, with the potential to guide clinician programming are under development, though have not been routinely incorporated into DBS workflows (Horn and Kühn, 2015; Petersen *et al.*, 2018). Newer devices with directional electrodes and multiple independent current sources can refine stimulation delivery, but have added even greater complexity to clinician programming (Timmermann *et al.*, 2015; Schüpbach *et al.*, 2017). Neurophysiological signals such as beta oscillations have been explored to guide surgical navigation, assist in DBS programming and act as a feedback signal in closed loop devices (Chen *et al.*, 2006b; Ince *et al.*, 2010; Little *et al.*, 2013; Priori *et al.*, 2013; Tinkhauser *et al.*, 2018). Commercial neurostimulators with beta measuring capabilities are now available (Quinn *et al.*, 2015; Neumann *et al.*, 2016b; Trager *et al.*, 2016; Alpha-Omega, 2020; Medtronic, 2020). However, recording challenges including low signal-to noise-ratio, cardioballistic artefact and small amplitude signals have limited widespread clinical use of these devices (Neumann *et al.*, 2019).

Finally, though Australia has a unique database that can inform on national DBS practices, accessing accurate and reliable data worldwide remains challenging (Videnovic and Metman, 2008). An international DBS database with standardised reporting procedures could be helpful in guiding clinical practice and future research directions.

6.2 ERNA studies (Chapters 4 and 5)

6.2.1 Key findings

The value of neuronal signals and the anatomical position of electrodes in predicting motor benefit and the clinician-chosen contact for chronic DBS was explored in a cohort of 50 consecutive patients implanted with STN DBS for PD. The acute motor benefit of DBS with stimulation applied to each contact on the quadripolar DBS lead was recorded in a subset of 14 patients (28 hemispheres).

ERNA power, beta power and contact anatomical location were all similarly predictive of acute motor benefit with DBS. The contact with the greatest ERNA power produced the best motor benefit in 64% of hemispheres. In the remaining hemispheres, the best acute motor benefit was almost always recorded at the contact measuring the second largest ERNA power (in 9/10 hemispheres). The best predictive model incorporated ERNA, HFO and beta information and the addition of anatomical information did not strengthen the model. Only the first-ranked contact according to ERNA produced a motor benefit with DBS that was significantly better than that measured at the three other contacts on the DBS lead. Furthermore, only first-ranked contacts according to ERNA power delivered an acute DBS benefit that did not differ significantly with the maximal available or the benefit afforded by the clinician-chosen contact.

ERNA power, and to a lesser extent, contact anatomical location and beta power corresponded with the contact selected by the clinician to apply DBS at 6 months after surgery. Using a simple-ranking method, with cross-validation, the probability that these factors predicted the clinician-chosen contact was as follows: ERNA 81%, anatomy 72%, beta oscillations 52%. ERNA performed significantly better than anatomy and beta oscillations and combining data using machine learning algorithms did not improve model performance.

6.2.2 Clinical implications

Use of ERNA to assist DBS programming

This work supports the use of ERNA power to assist in identifying the ideal contact to apply DBS. The existing practice of contact selection is arduous, prone to error and highly dependent on clinician expertise. Aids to inform on the ideal contact to apply stimulation and expedite programming are required. With the increasing availability of commercial stimulation and sensing systems (Alpha-Omega, 2020; Medtronic, 2020), ERNA signals could be measured intra-operatively, rapidly processed and made available to clinicians for use. However, the reliability of ERNA was diminished when ERNA power was small, often coinciding with little variation in power measurements across the four contacts on the DBS lead. In these cases, refinements in ERNA recording and analysis or exploration of other ERNA metrics could improve its clinical validity (Section 6.2.3).

Use of ERNA to assist electrode implantation

This study also supports the use of ERNA in intra-operative navigation and target localisation with stimulation of areas measuring larger ERNA power producing greater motor benefit with DBS. Intra-operative ERNA recordings could offer instantaneous information on lead location relative to the STN. For example, the absence of ERNA may provide supportive evidence that the lead is outside the surgical target. The relative size of ERNA power across the contacts may inform on lead depth and guide adjustments during surgery.

Comparison of ERNA and LFPs in assisting DBS programming

Beta oscillations and to a lesser extent, HFO also correlated with the degree of motor benefit with DBS. Beta band power has been assessed as a method to aid contact selection in patients with PD (Ince *et al.*, 2010; Tinkhauser *et al.*, 2018). In a small cohort of four patients (four hemispheres) with PD implanted with STN DBS, the contact pair (in bipolar configuration) measuring the greatest beta power corresponded with the clinician-chosen location on programming two days after implantation (Ince *et al.*, 2010). However, the accuracy of contact selection as determined by clinical evaluation in the acute post-operative phase is likely confounded by the therapeutic lesioning effect of electrode implantation (Maltête *et al.*, 2008). A study of a larger cohort of 12 patients chronically implanted with STN DBS, reported comparable results to our findings (Tinkhauser *et al.*, 2018). In 19 hemispheres, the most clinically effective contact, as determined by improvement in upper limb rigidity, corresponded with the first-ranked contact according to beta power in 12/19 of hemispheres and the second-ranked beta contact in 5/19 hemispheres. Notably, this study was performed in patients

implanted with directional leads and a similar protocol with ERNA recordings would be required for an ideal comparison (Section 6.2.3).

However, unlike ERNA, the first-ranked contact according to beta power produced an acute motor benefit that was significantly lower than the maximal available and corresponded less frequently with the clinician-chosen contact for chronic DBS. Furthermore, the clinical application of beta has been limited by its small amplitude, low-signal-to noise ratio and vulnerability to poor recording quality (Little *et al.*, 2012; Quinn *et al.*, 2015; Steiner *et al.*, 2017). Conversely, ERNA is far larger in amplitude (hundreds of μV) with a high signal-to-noise ratio, and a characteristic time locked, oscillatory decay morphology that renders it easily identifiable and less susceptible to artefact interference (Figure 4.1).

Comparison of ERNA and anatomy in assisting DBS programming

The proximity of contacts to the nominated, ideal anatomical location also predicted the degree of motor benefit from DBS. Accordingly, there is emerging work aimed towards automating post-operative lead localization to guide contact selection during programming (Horn and Kühn, 2015; Anderson *et al.*, 2018; Petersen *et al.*, 2018).

Like beta, contacts selected by anatomical location delivered an acute DBS benefit that was significantly lower than the maximal available and the benefit afforded by the clinician-chosen contact. Moreover, despite clinicians having access to the anatomical location of electrodes during DBS programming, the clinician-chosen contact coincided less frequently with the first-ranked contact according to anatomy compared to ERNA. It should be noted that though the dorsal STN is the postulated ideal location to apply DBS, there is significant heterogeneity amongst DBS experts on the precise location to deliver stimulation in the STN (Hamel *et al.*, 2017). However, despite using a variety of techniques to identify the ideal anatomical location to apply DBS (red-nucleus based targeting, advanced imaging pipeline using the MNI space), ERNA continued to outperform anatomy. Perhaps refining anatomical data with advanced structural imaging techniques such as diffusion tractography could improve the predictive value of anatomy (Vanegas-Arroyave *et al.*, 2016; Anderson *et al.*, 2018).

Another consideration is that whilst anatomy informs on structural networks, neuronal activity such as ERNA may reflect the functional networks intrinsic to the therapeutic mechanisms of DBS (McIntyre and Hahn, 2010). Both are independently predictive of the motor benefit with

DBS, with functional connectivity perhaps demonstrating a stronger correlation with clinical outcomes (Horn *et al.*, 2017c).

6.2.3 Future direction

ERNA recordings in directional leads

These studies support the use of ERNA power to identify the ideal contact to apply DBS in traditional omnidirectional, quadripolar leads. A significant challenge in new devices is the greater number of available contacts on directional DBS leads. To establish the utility of ERNA in directional leads, future studies are required to evaluate the recordability of ERNA on segments and the correlation of these measurements with the motor benefit from DBS. Interpretation of the relative size and distribution of ERNA power across the different levels and segments on the directional lead could also guide position shifts during surgery in both the vertical and horizontal planes.

Exploration of ERNA features

ERNA power alone did not always identify the ideal contact to apply DBS for maximal clinical benefit. Different analysis of ERNA could identify a better metric to improve its predictive value.

The measurement and application of ERNA power could be refined. First, ERNA power was recorded at unstimulated contacts, due to artefact at the stimulated contact. Modifying recording technique could allow for measurement of ERNA power at the stimulated contact. Second, ERNA power was recorded at arbitrary DBS settings of 3.375 mA, 60 µs and 130 Hz over a 16-millisecond period. Adjustments in stimulation parameters and recording duration may improve the clinical reliability of ERNA power. Third, combining ERNA power with other information may be helpful. Indeed, the addition of HFO data to ERNA data increased the correlation between neuronal signals and acute motor benefit with DBS. Though the addition of anatomy and beta power contact ranking data did not enhance the predictive model, other information about these factors may prove more relevant. For example, beta burst duration (Tinkhauser *et al.*, 2017a), subthalamic beta span (Zaidel *et al.*, 2010), phase amplitude coupling (van Wijk *et al.*, 2016; Tinkhauser *et al.*, 2017a) or diffusion tractography

(Vanegas-Arroyave *et al.*, 2016) information could be used together with ERNA data to guide contact selection.

Furthermore, additional ERNA waveform features including latency, frequency and rate of oscillation decay could also inform on the ideal location to apply DBS.

ERNA as a biomarker for closed loop DBS

ERNA fulfils many of the requirements for a feasible biomarker to automate DBS (Section 1.5) It is reliably recordable in the STN of patients with PD; 2) It has a large amplitude and high signal-to-noise ratio; 3) ERNA frequency and amplitude modulates with DBS (Sinclair *et al.*, 2019b).

The correlation between ERNA power and motor outcomes in these studies, though promising, were established based on historical intra-operative recordings. ERNA signals could be recorded in mobile patients using new stimulation and sensing neurostimulators (Medtronic, 2020) during voluntary movement. Temporal correlations between the ERNA waveform and the clinical state of the patients would need to be explored to determine the best ERNA characteristic (e.g. amplitude, latency, frequency) for feedback systems.

The role of ERNA in DBS mechanisms

The relevance of ERNA to the neural networks modulated by DBS remains unclear. Though ERNA power, beta power and anatomical location were all similarly predictive of acute DBS benefit, the addition of beta and anatomy data to ERNA data did not significantly strengthen the predictive model. ERNA may occupy a neural network that overlaps with, though is non-identical to beta and anatomical networks. The presence or absence of ERNA in other structures in the cortico-basal-ganglia-thalamic loop including the GPi, thalamus and cortex could inform on the generation and distribution of ERNA and provide greater insight into the therapeutic mechanisms of DBS.

6.3 Conclusion

The efficacy of DBS in PD is now well established. Coinciding with the rapid growth of DBS is the increase in the burden of therapy for patients, clinicians, and the healthcare system. Device servicing and maintenance, including clinician programming and battery replacements, are necessary for the duration of the patient's life. Hardware related complications are also common, often requiring additional surgeries involving the intracranial electrodes. The development of a neurophysiological biomarker could address the limitations of existing DBS systems to reduce the burden of service delivery. ERNA is a large amplitude, DBS evoked potential with a characteristic oscillatory decay morphology. ERNA power localises to anatomically favourable regions to apply stimulation in the STN, predicts acute motor benefit with DBS and selects contacts that correspond closely with long-term, expert clinician programming. As the paradigm of DBS mechanisms shifts from the traditional 'rate model' of local inhibition to one of widespread network modulation, there is increasing interest in the role of the neuronal signals that occupy these networks. ERNA offers new insights into the therapeutic mechanisms of DBS and could be rapidly translated for clinical use to guide surgical navigation and assist in contact selection to optimise DBS efficacy for individual patients.

7 References

ABS.Stat datasets. [cited 9th February 2021]; Available from: http://stat.data.abs.gov.au/

Abbott RD, Ross GW, White LR, Sanderson WT, Burchfiel CM, Kashon M, *et al.* Environmental, life-style, and physical precursors of clinical Parkinson's disease: recent findings from the Honolulu-Asia Aging Study. Journal of neurology 2003; 250(3): iii30-iii9.

ABS. Health Service Usage and Health Related Actions, Australia, 2014-15 Australian Bureau of Statistics; 2017.

Aharon-Peretz J, Rosenbaum H, Gershoni-Baruch R. Mutations in the Glucocerebrosidase Gene and Parkinson's Disease in Ashkenazi Jews. New England Journal of Medicine 2004; 351(19): 1972-7.

Ahlskog JE, Muenter MD. Frequency of levodopa-related dyskinesias and motor fluctuations as estimated from the cumulative literature. Movement Disorders 2001; 16(3): 448-58.

Akram H, Sotiropoulos SN, Jbabdi S, Georgiev D, Mahlknecht P, Hyam J, *et al.* Subthalamic deep brain stimulation sweet spots and hyperdirect cortical connectivity in Parkinson's disease. Neuroimage 2017; 158: 332-45.

Albin RL, Young AB, Penney JB. The functional anatomy of basal ganglia disorders. 1989.

Alpha-Omega. Neuro Omega™. 2020 [cited 10-7-2020]; Available from: https://www.alphaomega-eng.com/neuro-omegatm.html

Alvarez L, Macias R, Lopez G, Alvarez E, Pavon N, Rodriguez-Oroz M, *et al.* Bilateral subthalamotomy in Parkinson's disease: initial and long-term response. Brain : a journal of neurology 2005; 128(3): 570-83.

Anderson DN, Osting B, Vorwerk J, Dorval AD, Butson CR. Optimized programming algorithm for cylindrical and directional deep brain stimulation electrodes. Journal of neural engineering 2018; 15(2): 026005.

Andrade-Souza YM, Schwalb JM, Hamani C, Eltahawy H, Hoque T, Saint-Cyr J, *et al.* Comparison of three methods of targeting the subthalamic nucleus for chronic stimulation in Parkinson's disease. Neurosurgery 2005; 56(2 Suppl): 360-8; discussion -8.

APRA. Private health insurance statistical trends. Australian Prudential Regulation Authority 2019(September 2019).

Arlotti M, Marceglia S, Foffani G, Volkmann J, Lozano AM, Moro E, *et al.* Eight-hours adaptive deep brain stimulation in patients with Parkinson disease. Neurology 2018; 90(11): e971-e6.

Ashby P, Paradiso G, Saint-Cyr J, Chen R, Lang A, Lozano A. Potentials recorded at the scalp by stimulation near the human subthalamic nucleus. Clinical Neurophysiology 2001; 112(3): 431-7.

Ashkan K, Blomstedt P, Zrinzo L, Tisch S, Yousry T, Limousin-Dowsey P, *et al.* Variability of the subthalamic nucleus: the case for direct MRI guided targeting. British journal of neurosurgery 2007; 21(2): 197-200.

Ashkan K, Rogers P, Bergman H, Ughratdar I. Insights into the mechanisms of deep brain stimulation. Nature Reviews Neurology 2017; 13(9): 548.

Avants BB, Epstein CL, Grossman M, Gee JC. Symmetric diffeomorphic image registration with cross-correlation: evaluating automated labeling of elderly and neurodegenerative brain. Medical image analysis 2008; 12(1): 26-41.

Aviles-Olmos I, Kefalopoulou Z, Tripoliti E, Candelario J, Akram H, Martinez-Torres I, *et al.* Long-term outcome of subthalamic nucleus deep brain stimulation for Parkinson's disease using an MRI-guided and MRI-verified approach. J Neurol Neurosurg Psychiatry 2014: jnnp-2013-306907.

Baayen RH, Davidson DJ, Bates DM. Mixed-effects modeling with crossed random effects for subjects and items. Journal of memory and language 2008; 59(4): 390-412.

Baker KB, Montgomery EB, Jr., Rezai AR, Burgess R, Luders HO. Subthalamic nucleus deep brain stimulus evoked potentials: physiological and therapeutic implications. Movement Disorders 2002; 17(5): 969-83.

Baker SN. Oscillatory interactions between sensorimotor cortex and the periphery. Current opinion in neurobiology 2007; 17(6): 649-55.

Bang Henriksen M, Johnsen EL, Sunde N, Vase A, Gjelstrup MC, Ostergaard K. Surviving 10 years with deep brain stimulation for Parkinson's disease--a follow-up of 79 patients. Eur J Neurol 2016; 23(1): 53-61.

Barbe MT, Reker P, Hamacher S, Franklin J, Kraus D, Dembek TA, *et al.* DBS of the PSA and the VIM in essential tremor: A randomized, double-blind, crossover trial. Neurology 2018; 91(6): e543-e50.

Bates D, Sarkar D, Bates MD, Matrix L. The lme4 package. R package version 2007; 2(1): 74.

Baunez C, Dias C, Cador M, Amalric M. The subthalamic nucleus exerts opposite control on cocaine and'natural'rewards. Nature neuroscience 2005; 8(4): 484-9.

Beach TG, Adler CH, Sue LI, Vedders L, Lue L, White III CL, *et al.* Multi-organ distribution of phosphorylated α-synuclein histopathology in subjects with Lewy body disorders. Acta neuropathologica 2010; 119(6): 689-702.

Beavan MS, Schapira AH. Glucocerebrosidase mutations and the pathogenesis of Parkinson disease. Annals of medicine 2013; 45(8): 511-21.

Bejjani B-P, Dormont D, Pidoux B, Yelnik J, Damier P, Arnulf I, *et al.* Bilateral subthalamic stimulation for Parkinson's disease by using three-dimensional stereotactic magnetic resonance imaging and electrophysiological guidance. Journal of neurosurgery 2000; 92(4): 615-25.

Benabid A-L, Pollak P, Louveau A, Henry S, De Rougemont J. Combined (thalamotomy and stimulation) stereotactic surgery of the VIM thalamic nucleus for bilateral Parkinson disease. Stereotactic and functional neurosurgery 1987; 50(1-6): 344-6.

Benabid AL, Pollak P, Hoffmann D, Gervason C, Hommel M, Perret J, *et al.* Long-term suppression of tremor by chronic stimulation of the ventral intermediate thalamic nucleus. The Lancet 1991; 337(8738): 403-6.

Bergman H, Wichmann T, DeLong MR. Reversal of experimental parkinsonism by lesions of the subthalamic nucleus. Science (New York, NY) 1990; 249(4975): 1436-8.

Bergman H, Wichmann T, Karmon B, DeLong M. The primate subthalamic nucleus. II. Neuronal activity in the MPTP model of parkinsonism. Journal of neurophysiology 1994; 72(2): 507-20.

Bernheimer H, Birkmayer W, Hornykiewicz O, Jellinger K, Seitelberger F. Brain dopamine and the syndromes of Parkinson and Huntington. Clinical, morphological and neurochemical correlations. J Neurol Sci 1973; 20(4): 415-55.

Betarbet R, Sherer TB, MacKenzie G, Garcia-Osuna M, Panov AV, Greenamyre JT. Chronic systemic pesticide exposure reproduces features of Parkinson's disease. Nature neuroscience 2000; 3(12): 1301-6.

Bevan MD. Chapter 14 - The Subthalamic Nucleus. In: Steiner H, Tseng KY, editors. Handbook of Behavioral Neuroscience: Elsevier; 2017. p. 277-91.

Births Deaths and Marriages Victoria. Legal requirements for doctors. 2019 14/06/2019 [cited 2019 16/07/2019]; Available from: https://www.bdm.vic.gov.au/service-partnersmedical-practitioners/legal-requirements-for-doctors

Bjerknes S, Skogseid IM, Sæhle T, Dietrichs E, Toft M. Surgical site infections after deep brain stimulation surgery: frequency, characteristics and management in a 10-year period. PloS one 2014; 9(8): e105288-e.

Blasberg F, Wojtecki L, Elben S, Slotty PJ, Vesper J, Schnitzler A, *et al.* Comparison of Awake vs. Asleep Surgery for Subthalamic Deep Brain Stimulation in Parkinson's Disease. Neuromodulation: Technology at the Neural Interface 2018; 21(6): 541-7.

Blomstedt P, Hariz M. Hardware-related complications of deep brain stimulation: a ten year experience. Acta neurochirurgica 2005; 147(10): 1061-4.

Blume J, Schlaier J, Rothenfußer E, Anthofer J, Zeman F, Brawanski A, *et al.* Intraoperative clinical testing overestimates the therapeutic window of the permanent DBS electrode in the subthalamic nucleus. Acta neurochirurgica 2017; 159(9): 1721-6.

Bonifati V, Rizzu P, Van Baren MJ, Schaap O, Breedveld GJ, Krieger E, *et al.* Mutations in the DJ-1 gene associated with autosomal recessive early-onset parkinsonism. Science (New York, NY) 2003; 299(5604): 256-9.

Boon P, Vonck K, De Herdt V, Van Dycke A, Goethals M, Goossens L, *et al.* Deep brain stimulation in patients with refractory temporal lobe epilepsy. Epilepsia 2007; 48(8): 1551-60.

Boser BE, Guyon IM, Vapnik VN. A training algorithm for optimal margin classifiers. Proceedings of the fifth annual workshop on Computational learning theory. Pittsburgh, Pennsylvania, USA: Association for Computing Machinery; 1992. p. 144–52.

Bour LJ, Contarino MF, Foncke EM, de Bie RM, van den Munckhof P, Speelman JD, *et al.* Long-term experience with intraoperative microrecording during DBS neurosurgery in STN and GPi. Acta neurochirurgica 2010; 152(12): 2069-77.

Braak H, Del Tredici K. Invited Article: Nervous system pathology in sporadic Parkinson disease. Neurology 2008; 70(20): 1916-25.

Braak H, Del Tredici K, Rüb U, de Vos RA, Steur ENJ, Braak E. Staging of brain pathology related to sporadic Parkinson's disease. Neurobiology of aging 2003; 24(2): 197-211.

Breiman L. Random Forests. Machine Learning 2001; 45(1): 5-32.

Bronstein JM, Tagliati M, Alterman RL, Lozano AM, Volkmann J, Stefani A, *et al.* Deep brain stimulation for Parkinson disease: an expert consensus and review of key issues. Archives of neurology 2011; 68(2): 165-.

Bronte-Stewart H, Barberini C, Koop MM, Hill BC, Henderson JM, Wingeier B. The STN beta-band profile in Parkinson's disease is stationary and shows prolonged attenuation after deep brain stimulation. Experimental neurology 2009; 215(1): 20-8.

Brown P, Oliviero A, Mazzone P, Insola A, Tonali P, Di Lazzaro V. Dopamine dependency of oscillations between subthalamic nucleus and pallidum in Parkinson's disease. Journal of Neuroscience 2001; 21(3): 1033-8.

Brown P, Williams D. Basal ganglia local field potential activity: character and functional significance in the human. Clinical neurophysiology 2005; 116(11): 2510-9.

Buzsáki G, Anastassiou CA, Koch C. The origin of extracellular fields and currents—EEG, ECoG, LFP and spikes. Nature reviews neuroscience 2012; 13(6): 407-20.

Canning CG, Sherrington C, Lord SR, Close JC, Heritier S, Heller GZ, *et al.* Exercise for falls prevention in Parkinson disease: a randomized controlled trial. Neurology 2015; 84(3): 304-12.

Castrioto A, Lozano AM, Poon Y-Y, Lang AE, Fallis M, Moro E. Ten-year outcome of subthalamic stimulation in Parkinson disease: a blinded evaluation. Archives of neurology 2011; 68(12): 1550-6.

Charles P, Van Blercom N, Krack P, Lee S, Xie J, Besson G, *et al.* Predictors of effective bilateral subthalamic nucleus stimulation for PD. Neurology 2002; 59(6): 932-4.

Chaturvedi A, Luján JL, McIntyre CC. Artificial neural network based characterization of the volume of tissue activated during deep brain stimulation. Journal of neural engineering 2013; 10(5): 056023.

Chen CC, Brucke C, Kempf F, Kupsch A, Lu CS, Lee ST, *et al.* Deep brain stimulation of the subthalamic nucleus: a two-edged sword. Curr Biol 2006a; 16(22): R952-3.

Chen CC, Hsu YT, Chan HL, Chiou SM, Tu PH, Lee ST, *et al.* Complexity of subthalamic 13–35 Hz oscillatory activity directly correlates with clinical impairment in patients with Parkinson's disease. Experimental neurology 2010; 224(1): 234-40.

Chen CC, Pogosyan A, Zrinzo LU, Tisch S, Limousin P, Ashkan K, *et al.* Intra-operative recordings of local field potentials can help localize the subthalamic nucleus in Parkinson's disease surgery. Exp Neurol 2006b; 198(1): 214-21.

Cilia R, Akpalu A, Sarfo FS, Cham M, Amboni M, Cereda E, *et al.* The modern pre-levodopa era of Parkinson's disease: insights into motor complications from sub-Saharan Africa. Brain : a journal of neurology 2014; 137(10): 2731-42.

Collins DL, Zijdenbos AP, Baaré WF, Evans AC. ANIMAL+ INSECT: improved cortical structure segmentation. Biennial International Conference on Information Processing in Medical Imaging; 1999: Springer; 1999. p. 210-23.

Contarino MF, Marinus J, van Hilten JJ. Does deep brain stimulation of the subthalamic nucleus prolong survival in Parkinson's Disease? Movement Disorders 2018; 33(6): 947-9.

Cooley JW, Tukey JW. An algorithm for the machine calculation of complex Fourier series. Mathematics of computation 1965; 19(90): 297-301.

Cubo E, Rajalingam R, Fasano A, Munhoz RP, Lang A, Calvo S, *et al.* A 21-year retrospective study of the Toronto Western Hospital deep brain stimulation cohort. Movement Disorders 2018; 33(5): 850-2.

Dams J, Balzer-Geldsetzer M, Siebert U, Deuschl G, Schuepbach WM, Krack P, *et al.* Cost-effectiveness of neurostimulation in Parkinson's disease with early motor complications. Mov Disord 2016; 31(8): 1183-91.

Dang TTH, Rowell D, Connelly LB. Cost-Effectiveness of Deep Brain Stimulation With Movement Disorders: A Systematic Review. Movement Disorders Clinical Practice 2019; 6(5): 348-58.

Daniluk S, Davies KG, Ellias SA, Novak P, Nazzaro JM. Assessment of the variability in the anatomical position and size of the subthalamic nucleus among patients with advanced Parkinson’s disease using magnetic resonance imaging. Acta neurochirurgica 2010; 152(2): 201-10.

Danish S, Moyer J, Finkel L, Baltuch G, Jaggi J, Priori A, *et al.* High-frequency oscillations (> 200 Hz) in the human non-parkinsonian subthalamic nucleus. Brain research bulletin 2007; 74(1-3): 84-90.

de Lau LML, Breteler MMB. Epidemiology of Parkinson's disease. The Lancet Neurology 2006; 5(6): 525-35.

Dejean C, Hyland B, Arbuthnott G. Cortical effects of subthalamic stimulation correlate with behavioral recovery from dopamine antagonist induced akinesia. Cereb Cortex 2009; 19(5): 1055-63.

Deleu D, Jacob P, Chand P, Sarre S, Colwell A. Effects of caffeine on levodopa pharmacokinetics and pharmacodynamics in Parkinson disease. Neurology 2006; 67(5): 897-9.

Deloitte. Living with Parkinsons update 2014. 2014.

DeLong MR. Primate models of movement disorders of basal ganglia origin. Trends in neurosciences 1990; 13(7): 281-5.

Dembek TA, Reker P, Visser-Vandewalle V, Wirths J, Treuer H, Klehr M, *et al.* Directional DBS increases side-effect thresholds—A prospective, double-blind trial. Movement Disorders 2017.

Dembek TA, Roediger J, Horn A, Reker P, Oehrn C, Dafsari HS, *et al.* Probabilistic Sweetspots Predict Motor Outcome for DBS in Parkinson's Disease. Annals of neurology 2019.

Deng H, Yue JK, Wang DD. Trends in safety and cost of deep brain stimulation for treatment of movement disorders in the United States: 2002–2014. British Journal of Neurosurgery 2020: 1-8.

Deuschl G, Agid Y. Subthalamic neurostimulation for Parkinson's disease with early fluctuations: balancing the risks and benefits. The Lancet Neurology 2013; 12(10): 1025-34.

Deuschl G, Schade-Brittinger C, Krack P, Volkmann J, Schäfer H, Bötzel K, *et al.* A Randomized Trial of Deep-Brain Stimulation for Parkinson's Disease. New England Journal of Medicine 2006; 355(9): 896-908.

Devergnas A, Wichmann T. Cortical potentials evoked by deep brain stimulation in the subthalamic area. Front Syst Neurosci 2011; 5: 30.

Dewey RB, O'Suilleabhain PE. Treatment of drug-induced psychosis with quetiapine and clozapine in Parkinson's disease. Neurology 2000; 55(11): 1753-4.

Dickson DW, Braak H, Duda JE, Duyckaerts C, Gasser T, Halliday GM, *et al.* Neuropathological assessment of Parkinson's disease: refining the diagnostic criteria. The Lancet Neurology 2009; 8(12): 1150-7.

Doshi PK. Long-term surgical and hardware-related complications of deep brain stimulation. Stereotactic and functional neurosurgery 2011; 89(2): 89-95.

Dreiseitl S, Ohno-Machado L. Logistic regression and artificial neural network classification models: a methodology review. Journal of biomedical informatics 2002; 35(5-6): 352-9.

Engel AK, Fries P. Beta-band oscillations—signalling the status quo? Current opinion in neurobiology 2010; 20(2): 156-65.

Eusebio A, Pogosyan A, Wang S, Averbeck B, Gaynor LD, Cantiniaux S, *et al.* Resonance in subthalamo-cortical circuits in Parkinson's disease. Brain : a journal of neurology 2009; 132(Pt 8): 2139-50.

Eusebio A, Thevathasan W, Doyle Gaynor L, Pogosyan A, Bye E, Foltynie T, *et al.* Deep brain stimulation can suppress pathological synchronisation in parkinsonian patients. Journal of Neurology, Neurosurgery & Psychiatry 2011; 82(5): 569-73.

Evans A, Lawrence AD, Potts J, MacGregor L, Katzenschlager R, Shaw K, *et al.* Relationship between impulsive sensation seeking traits, smoking, alcohol and caffeine intake, and Parkinson's disease. Journal of Neurology, Neurosurgery & Psychiatry 2006; 77(3): 317-21.

Evans JR, Mason SL, Williams-Gray CH, Foltynie T, Brayne C, Robbins TW, *et al.* The natural history of treated Parkinson's disease in an incident, community based cohort. Journal of Neurology, Neurosurgery & Psychiatry 2011; 82(10): 1112-8.

Ewert S, Plettig P, Li N, Chakravarty MM, Collins DL, Herrington TM, *et al.* Toward defining deep brain stimulation targets in MNI space: A subcortical atlas based on multimodal MRI, histology and structural connectivity. NeuroImage 2018; 170: 271-82.

Fahn S. Unified Parkinson's disease rating scale. Recent developments in Parkinson's disease 1987; 2: 153-64.

Fahn S. Description of Parkinson's disease as a clinical syndrome. Ann N Y Acad Sci 2003; 991: 1-14.

Falowski SM, Ooi YC, Bakay RA. Long-Term Evaluation of Changes in Operative Technique and Hardware-Related Complications With Deep Brain Stimulation. Neuromodulation 2015; 18(8): 670-7.

Fasano A, Romito LM, Daniele A, Piano C, Zinno M, Bentivoglio AR, *et al.* Motor and cognitive outcome in patients with Parkinson's disease 8 years after subthalamic implants. Brain : a journal of neurology 2010; 133(9): 2664-76.

Fearnley JM, Lees AJ. Ageing and Parkinson's disease: substantia nigra regional selectivity. Brain : a journal of neurology 1991; 114 (Pt 5): 2283-301.

Fedorov A, Beichel R, Kalpathy-Cramer J, Finet J, Fillion-Robin J-C, Pujol S, *et al.* 3D Slicer as an image computing platform for the Quantitative Imaging Network. Magnetic resonance imaging 2012; 30(9): 1323-41.

Feingold J, Gibson DJ, DePasquale B, Graybiel AM. Bursts of beta oscillation differentiate postperformance activity in the striatum and motor cortex of monkeys performing movement tasks. Proceedings of the National Academy of Sciences 2015; 112(44): 13687-92.

Fenoy AJ, Simpson Jr RK. Management of device-related wound complications in deep brain stimulation surgery. Journal of neurosurgery 2012; 116(6): 1324-32.

Fernández-García C, Foffani G, Dileone M, Catalán-Alonso M, González-Hidalgo M, Barcía J, *et al.* Directional local field potential recordings for symptom-specific optimization of deep brain stimulation. Movement disorders: official journal of the Movement Disorder Society 2017; 32(4): 626.

Fernández-Pajarín G, Sesar A, Ares B, Relova J, Arán E, Gelabert-González M, *et al.* Delayed complications of deep brain stimulation: 16-year experience in 249 patients. Acta neurochirurgica 2017; 159(9): 1713-9.

Fernandez HH, Standaert DG, Hauser RA, Lang AE, Fung VS, Klostermann F, *et al.* Levodopa-carbidopa intestinal gel in advanced Parkinson's disease: Final 12-month, open-label results. Movement Disorders 2015; 30(4): 500-9.

Fine J, Duff J, Chen R, Hutchison W, Lozano AM, Lang AE. Long-term follow-up of unilateral pallidotomy in advanced Parkinson's disease. New England Journal of Medicine 2000; 342(23): 1708-14.

Foffani G, Priori A, Egidi M, Rampini P, Tamma F, Caputo E, *et al.* 300-Hz subthalamic oscillations in Parkinson’s disease. Brain : a journal of neurology 2003; 126(10): 2153-63.

Follett KA, Weaver FM, Stern M, Hur K, Harris CL, Luo P, *et al.* Pallidal versus subthalamic deep-brain stimulation for Parkinson's disease. New England Journal of Medicine 2010; 362(22): 2077-91.

Fonov V, Evans AC, Botteron K, Almli CR, McKinstry RC, Collins DL. Unbiased average age-appropriate atlases for pediatric studies. NeuroImage 2011; 54(1): 313-27.

Fox SH, Katzenschlager R, Lim S-Y, Barton B, de Bie RMA, Seppi K, *et al.* International Parkinson and movement disorder society evidence-based medicine review: Update on treatments for the motor symptoms of Parkinson's disease. Movement Disorders 2018; 33(8): 1248-66.

Fujimoto K, Kita H. Response characteristics of subthalamic neurons to the stimulation of the sensorimotor cortex in the rat. Brain research 1993; 609(1): 185-92.

Fytagoridis A, Heard T, Samuelsson J, Zsigmond P, Jiltsova E, Skyrman S, *et al.* Surgical replacement of implantable pulse generators in deep brain stimulation: adverse events and

risk factors in a multicenter cohort. Stereotactic and functional neurosurgery 2016; 94(4): 235-9.

Gatev P, Darbin O, Wichmann T. Oscillations in the basal ganglia under normal conditions and in movement disorders. Movement Disorders 2006; 21(10): 1566-77.

Gelb DJ, Oliver E, Gilman S. Diagnostic criteria for Parkinson disease. Arch Neurol 1999; 56(1): 33-9.

Geraedts V, van Ham R, Marinus J, van Hilten J, Mosch A, Hoffmann C, *et al.* Intraoperative test stimulation of the subthalamic nucleus aids postoperative programming of chronic stimulation settings in Parkinson's disease. Parkinsonism & related disorders 2019; 65: 62-6.

Giannicola G, Marceglia S, Rossi L, Mrakic-Sposta S, Rampini P, Tamma F, *et al.* The effects of levodopa and ongoing deep brain stimulation on subthalamic beta oscillations in Parkinson's disease. Experimental neurology 2010; 226(1): 120-7.

Gibb W, Lees A. The relevance of the Lewy body to the pathogenesis of idiopathic Parkinson's disease. Journal of Neurology, Neurosurgery & Psychiatry 1988a; 51(6): 745-52.

Gibb WR, Lees AJ. The relevance of the Lewy body to the pathogenesis of idiopathic Parkinson's disease. J Neurol Neurosurg Psychiatry 1988b; 51(6): 745-52.

Gmel GE, Hamilton TJ, Obradovic M, Gorman RB, Single PS, Chenery HJ, *et al.* A new biomarker for subthalamic deep brain stimulation for patients with advanced Parkinson's disease--a pilot study. J Neural Eng 2015; 12(6): 066013.

Goetz CG, Poewe W, Rascol O, Sampaio C, Stebbins GT, Counsell C, *et al.* Movement Disorder Society Task Force report on the Hoehn and Yahr staging scale: Status and recommendations The Movement Disorder Society Task Force on rating scales for Parkinson's disease. Movement Disorders 2004; 19(9): 1020-8.

Goetz CG, Tilley BC, Shaftman SR, Stebbins GT, Fahn S, Martinez-Martin P, *et al.* Movement Disorder Society-sponsored revision of the Unified Parkinson's Disease Rating Scale (MDS-UPDRS): Scale presentation and clinimetric testing results. Movement Disorders 2008; 23(15): 2129-70.

Goodman R, Kim B, McClelland S, Senatus P, Winfield L, Pullman S, *et al.* Operative techniques and morbidity with subthalamic nucleus deep brain stimulation in 100 consecutive patients with advanced Parkinson’s disease. Journal of Neurology, Neurosurgery & Psychiatry 2006; 77(1): 12-7.

Gorgulho A, Juillard C, Uslan DZ, Tajik K, Aurasteh P, Behnke E, *et al.* Infection following deep brain stimulator implantation performed in the conventional versus magnetic resonance imaging–equipped operating room. Journal of neurosurgery 2009; 110(2): 239-46.

Group PMC. Long-term effectiveness of dopamine agonists and monoamine oxidase B inhibitors compared with levodopa as initial treatment for Parkinson's disease (PD MED): a large, open-label, pragmatic randomised trial. The Lancet 2014; 384(9949): 1196-205.

Halpern CH, McGill KR, Baltuch GH, Jaggi JL. Longevity analysis of currently available deep brain stimulation devices. Stereotactic and functional neurosurgery 2011; 89(1): 1-5.

Hamada I, DeLong MR. Excitotoxic acid lesions of the primate subthalamic nucleus result in reduced pallidal neuronal activity during active holding. Journal of neurophysiology 1992a; 68(5): 1859-66.

Hamada I, DeLong MR. Excitotoxic acid lesions of the primate subthalamic nucleus result in transient dyskinesias of the contralateral limbs. Journal of neurophysiology 1992b; 68(5): 1850-8.

Hamel W, Fietzek U, Morsnowski A, Schrader B, Herzog J, Weinert D, *et al.* Deep brain stimulation of the subthalamic nucleus in Parkinson's disease: evaluation of active electrode contacts. Journal of Neurology, Neurosurgery & Psychiatry 2003; 74(8): 1036-46.

Hamel W, Koppen JA, Alesch F, Antonini A, Barcia JA, Bergman H, *et al.* Targeting of the Subthalamic Nucleus for Deep Brain Stimulation: A Survey Among Parkinson Disease Specialists. World Neurosurgery 2017; 99: 41-6.

Hammond C, Bergman H, Brown P. Pathological synchronization in Parkinson's disease: networks, models and treatments. Trends in neurosciences 2007; 30(7): 357-64.

Hardaway FA, Raslan AM, Burchiel KJ. Deep Brain Stimulation-Related Infections: Analysis of Rates, Timing, and Seasonality. Neurosurgery 2017; 83(3): 540-7.

Hariz M. My 25 Stimulating Years with DBS in Parkinson's Disease. Journal of Parkinson's disease 2017; 7(s1): S33-S41.

Harnack D, Meissner W, Jira JA, Winter C, Morgenstern R, Kupsch A. Placebo-controlled chronic high-frequency stimulation of the subthalamic nucleus preserves dopaminergic nigral neurons in a rat model of progressive Parkinsonism. Experimental neurology 2008; 210(1): 257-60.

Hashimoto T, Elder CM, Okun MS, Patrick SK, Vitek JL. Stimulation of the subthalamic nucleus changes the firing pattern of pallidal neurons. Journal of neuroscience 2003; 23(5): 1916-23.

Haynes WI, Haber SN. The organization of prefrontal-subthalamic inputs in primates provides an anatomical substrate for both functional specificity and integration: implications for Basal Ganglia models and deep brain stimulation. The Journal of neuroscience : the official journal of the Society for Neuroscience 2013; 33(11): 4804-14.

Healy DG, Falchi M, O'Sullivan SS, Bonifati V, Durr A, Bressman S, *et al.* Phenotype, genotype, and worldwide genetic penetrance of LRRK2-associated Parkinson's disease: a case-control study. The Lancet Neurology 2008; 7(7): 583-90.

Helmers A-K, Lübbing I, Birkenfeld F, Witt K, Synowitz M, Mehdorn HM, *et al.* Complications of impulse generator exchange surgery for deep brain stimulation: a single-center, retrospective study. World neurosurgery 2018; 113: e108-e12.

Hely MA, Morris JG, Reid WG, Trafficante R. Sydney multicenter study of Parkinson's disease: Non-L-dopa–responsive problems dominate at 15 years. Movement Disorders 2005; 20(2): 190-9.

Hely MA, Morris JG, Traficante R, Reid WG, O'Sullivan DJ, Williamson PM. The Sydney multicentre study of Parkinson's disease: progression and mortality at 10 years. Journal of Neurology, Neurosurgery & Psychiatry 1999; 67(3): 300-7.

Hely MA, Reid WG, Adena MA, Halliday GM, Morris JG. The Sydney multicenter study of Parkinson's disease: the inevitability of dementia at 20 years. Movement disorders 2008; 23(6): 837-44.

Hernán MA, Takkouche B, Caamaño-Isorna F, Gestal-Otero JJ. A meta-analysis of coffee drinking, cigarette smoking, and the risk of Parkinson's disease. Annals of neurology 2002; 52(3): 276-84.

Hershey T, Campbell MC, Videen TO, Lugar HM, Weaver PM, Hartlein J, *et al.* Mapping Go–No-Go performance within the subthalamic nucleus region. Brain : a journal of neurology 2010; 133(12): 3625-34.

Herzog J, Fietzek U, Hamel W, Morsnowski A, Steigerwald F, Schrader B, *et al.* Most effective stimulation site in subthalamic deep brain stimulation for Parkinson's disease. Movement Disorders 2004; 19(9): 1050-4.

Hitti FL, Ramayya AG, McShane BJ, Yang AI, Vaughan KA, Baltuch GH. Long-term outcomes following deep brain stimulation for Parkinson's disease. Journal of neurosurgery 2019; 132(1): 205-10.

Ho AL, Ali R, Connolly ID, Henderson JM, Dhall R, Stein SC, *et al.* Awake versus asleep deep brain stimulation for Parkinson's disease: a critical comparison and meta-analysis. J Neurol Neurosurg Psychiatry 2018; 89(7): 687-91.

Hoehn MM, Yahr MD. Parkinsonism onset, progression, and mortality. Neurology 1967; 17(5): 427-.

Horn A. The impact of modern-day neuroimaging on the field of deep brain stimulation. Current opinion in neurology 2019; 32(4): 511-20.

Horn A, Kühn AA. Lead-DBS: a toolbox for deep brain stimulation electrode localizations and visualizations. Neuroimage 2015; 107: 127-35.

Horn A, Kühn AA, Merkl A, Shih L, Alterman R, Fox M. Probabilistic conversion of neurosurgical DBS electrode coordinates into MNI space. Neuroimage 2017a; 150: 395-404.

Horn A, Li N, Dembek TA, Kappel A, Boulay C, Ewert S, *et al.* Lead-DBS v2: Towards a comprehensive pipeline for deep brain stimulation imaging. NeuroImage 2019; 184: 293-316.

Horn A, Neumann WJ, Degen K, Schneider GH, Kühn AA. Toward an electrophysiological "sweet spot" for deep brain stimulation in the subthalamic nucleus. Human brain mapping 2017b; 38(7): 3377-90.

Horn A, Reich M, Vorwerk J, Li N, Wenzel G, Fang Q, *et al.* Connectivity Predicts deep brain stimulation outcome in Parkinson disease. Annals of neurology 2017c; 82(1): 67-78.

Houshmand L, Cummings KS, Chou KL, Patil PG. Evaluating indirect subthalamic nucleus targeting with validated 3-Tesla magnetic resonance imaging. Stereotactic and functional neurosurgery 2014; 92(6): 337-45.

Hrabovsky D, Balaz M, Bockova M, Feitova V, Novak Z, Chrastina J. Learning curve in anatomo-electrophysiological correlations in subthalamic nucleus stimulation. Turk Neurosurg 2017; 1: 19450-16.0.

Hubsher G, Haider M, Okun M. Amantadine: the journey from fighting flu to treating Parkinson disease. Neurology 2012; 78(14): 1096-9.

Hughes AJ, Bishop S, Kleedorfer B, Turjanski N, Fernandez W, Lees A, *et al.* Subcutaneous apomorphine in Parkinson's disease: response to chronic administration for up to five years. Movement Disorders 1993a; 8(2): 165-70.

Hughes AJ, Daniel SE, Ben-Shlomo Y, Lees AJ. The accuracy of diagnosis of parkinsonian syndromes in a specialist movement disorder service. Brain : a journal of neurology 2002; 125(4): 861-70.

Hughes AJ, Daniel SE, Blankson S, Lees AJ. A clinicopathologic study of 100 cases of Parkinson's disease. Archives of neurology 1993b; 50(2): 140-8.

Hughes AJ, Daniel SE, Lees AJ. Improved accuracy of clinical diagnosis of Lewy body Parkinson’s disease. Neurology 2001; 57(8): 1497-9.

Husch A, Petersen MV, Gemmar P, Goncalves J, Hertel F. PaCER-A fully automated method for electrode trajectory and contact reconstruction in deep brain stimulation. NeuroImage: Clinical 2018; 17: 80-9.

Ikemura M, Saito Y, Sengoku R, Sakiyama Y, Hatsuta H, Kanemaru K, *et al.* Lewy body pathology involves cutaneous nerves. Journal of Neuropathology & Experimental Neurology 2008; 67(10): 945-53.

Ince NF, Gupte A, Wichmann T, Ashe J, Henry T, Bebler M, *et al.* Selection of optimal programming contacts based on local field potential recordings from subthalamic nucleus in patients with Parkinson's disease. Neurosurgery 2010; 67(2): 390-7.

Isoda M, Hikosaka O. Role for subthalamic nucleus neurons in switching from automatic to controlled eye movement. Journal of Neuroscience 2008; 28(28): 7209-18.

Jankovic J. Motor fluctuations and dyskinesias in Parkinson's disease: clinical manifestations. Movement Disorders 2005; 20(S11).

Jankovic J. Parkinson’s disease: clinical features and diagnosis. Journal of Neurology, Neurosurgery & Psychiatry 2008; 79(4): 368-76.

Jankovic J, McDermott M, Carter J, Gauthier S, Goetz C, Golbe L, *et al.* Variable expression of Parkinson's disease A base-line analysis of the DAT ATOP cohort. Neurology 1990; 40(10): 1529-.

Jitkritsadakul O, Bhidayasiri R, Kalia SK, Hodaie M, Lozano AM, Fasano A. Systematic review of hardware-related complications of Deep Brain Stimulation: Do new indications pose an increased risk? Brain Stimulation 2017; 10(5): 967-76.

Joint C, Nandi D, Parkin S, Gregory R, Aziz T. Hardware-related problems of deep brain stimulation. Movement Disorders 2002; 17(S3).

Katzenschlager R, Hughes A, Evans A, Manson AJ, Hoffman M, Swinn L, *et al.* Continuous subcutaneous apomorphine therapy improves dyskinesias in Parkinson's disease: a prospective study using single-dose challenges. Movement Disorders 2005; 20(2): 151-7.

Katzenschlager R, Poewe W, Rascol O, Trenkwalder C, Deuschl G, Chaudhuri KR, *et al.* Apomorphine subcutaneous infusion in patients with Parkinson's disease with persistent motor fluctuations (TOLEDO): a multicentre, double-blind, randomised, placebo-controlled trial. The Lancet Neurology 2018; 17(9): 749-59.

Katzenschlager R, Sampaio C, Costa J, Lees A. Anticholinergics for symptomatic management of Parkinson s disease. Cochrane Database of Systematic Reviews 2002(3).

Kempster PA, O'sullivan SS, Holton JL, Revesz T, Lees AJ. Relationships between age and late progression of Parkinson's disease: a clinico-pathological study. Brain : a journal of neurology 2010; 133(6): 1755-62.

Kent AR, Grill WM. Neural origin of evoked potentials during thalamic deep brain stimulation. Journal of neurophysiology 2013; 110(4): 826-43.

Kent AR, Swan BD, Brocker DT, Turner DA, Gross RE, Grill WM. Measurement of evoked potentials during thalamic deep brain stimulation. Brain stimulation 2015; 8(1): 42-56.

Khawaldeh S, Tinkhauser G, Shah SA, Peterman K, Debove I, Nguyen TK, *et al.* Subthalamic nucleus activity dynamics and limb movement prediction in Parkinson's disease. Brain : a journal of neurology 2020; 143(2): 582-96.

Kitada T, Asakawa S, Hattori N, Matsumine H, Yamamura Y, Minoshima S, *et al.* Mutations in the parkin gene cause autosomal recessive juvenile parkinsonism. Nature 1998; 392(6676): 605.

Krauss JK, Lipsman N, Aziz T, Boutet A, Brown P, Chang JW, *et al.* Technology of deep brain stimulation: current status and future directions. Nature Reviews Neurology 2020: 1-13.

Kühn AA, Kupsch A, Schneider GH, Brown P. Reduction in subthalamic 8–35 Hz oscillatory activity correlates with clinical improvement in Parkinson's disease. European Journal of Neuroscience 2006; 23(7): 1956-60.

Kühn AA, Trottenberg T, Kivi A, Kupsch A, Schneider G-H, Brown P. The relationship between local field potential and neuronal discharge in the subthalamic nucleus of patients with Parkinson's disease. Experimental neurology 2005; 194(1): 212-20.

Kühn AA, Tsui A, Aziz T, Ray N, Brücke C, Kupsch A, *et al.* Pathological synchronisation in the subthalamic nucleus of patients with Parkinson's disease relates to both bradykinesia and rigidity. Experimental neurology 2009; 215(2): 380-7.

Kuncel AM, Grill WM. Selection of stimulus parameters for deep brain stimulation. Clinical neurophysiology 2004; 115(11): 2431-41.

Kupsch A, Benecke R, Müller J, Trottenberg T, Schneider G-H, Poewe W, *et al.* Pallidal deep-brain stimulation in primary generalized or segmental dystonia. New England Journal of Medicine 2006; 355(19): 1978-90.

Lardeux S, Pernaud R, Paleressompoulle D, Baunez C. Beyond the reward pathway: coding reward magnitude and error in the rat subthalamic nucleus. Journal of neurophysiology 2009; 102(4): 2526-37.

Lee M, Marsden C. Movement disorders following lesions of the thalamus or subthalamic region. Movement Disorders 1994; 9(5): 493-507.

Lees A, Katzenschlager R, Head J, Ben–Shlomo Y. Ten-year follow-up of three different initial treatments in de-novo PD A randomized trial. Neurology 2001; 57(9): 1687-94.

Lewis S, Foltynie T, Blackwell A, Robbins T, Owen A, Barker R. Heterogeneity of Parkinson's disease in the early clinical stages using a data driven approach. Journal of Neurology, Neurosurgery & Psychiatry 2005; 76(3): 343-8.

Lewy F. Handbuch der Neurologie. Handbuch Der Neurologie 1912; 3.

Lilleeng B, Brønnick K, Toft M, Dietrichs E, Larsen J. Progression and survival in Parkinson's disease with subthalamic nucleus stimulation. Acta Neurologica Scandinavica 2014; 130(5): 292-8.

Limousin P, Brown P, Marsden J, Defebvre L, Rothwell J. Evoked potentials from subthalamic nucleus, internal pallidum and thalamic stimulation in parkinsonian and postural tremor patients. JOURNAL OF PHYSIOLOGY-LONDON 1998; 509.

Limousin P, Foltynie T. Long-term outcomes of deep brain stimulation in Parkinson disease. Nat Rev Neurol 2019; 15(4): 234-42.

Little S, Brown P. What brain signals are suitable for feedback control of deep brain stimulation in Parkinson's disease? Ann N Y Acad Sci 2012; 1265: 9-24.

Little S, Brown P. The functional role of beta oscillations in Parkinson's disease. Parkinsonism & related disorders 2014; 20: S44-S8.

Little S, Brown P. Debugging Adaptive Deep Brain Stimulation for Parkinson's Disease. Movement Disorders 2020.

Little S, Pogosyan A, Kuhn A, Brown P. Beta band stability over time correlates with Parkinsonian rigidity and bradykinesia. Experimental neurology 2012; 236(2): 383-8.

Little S, Pogosyan A, Neal S, Zavala B, Zrinzo L, Hariz M, *et al.* Adaptive deep brain stimulation in advanced Parkinson disease. Annals of neurology 2013; 74(3): 449-57.

Little S, Tripoliti E, Beudel M, Pogosyan A, Cagnan H, Herz D, *et al.* Adaptive deep brain stimulation for Parkinson's disease demonstrates reduced speech side effects compared to conventional stimulation in the acute setting. Journal of Neurology, Neurosurgery & Psychiatry 2016; 87(12): 1388-9.

López-Azcárate J, Tainta M, Rodríguez-Oroz MC, Valencia M, González R, Guridi J, *et al.* Coupling between beta and high-frequency activity in the human subthalamic nucleus may be a pathophysiological mechanism in Parkinson's disease. Journal of Neuroscience 2010; 30(19): 6667-77.

Loucif AJ, Woodhall GL, Sehirli US, Stanford IM. Depolarisation and suppression of burst firing activity in the mouse subthalamic nucleus by dopamine D1/D5 receptor activation of a cyclic-nucleotide gated non-specific cation conductance. Neuropharmacology 2008; 55(1): 94-105.

Lozano AM, Lang AE, Galvez-Jimenez N, Miyasaki J, Duff J, Hutchison W, *et al.* Effect of GPi pallidotomy on motor function in Parkinson's disease. The Lancet 1995; 346(8987): 1383-7.

Lu CW, Chou KL, Patil PG. Correspondence of optimal stimulation and beta power varies regionally in STN DBS for Parkinson disease. Parkinsonism & Related Disorders 2020; 78: 124-8.

Lyons KE, Wilkinson SB, Overman J, Pahwa R. Surgical and hardware complications of subthalamic stimulation A series of 160 procedures. Neurology 2004; 63(4): 612-6.

Machado A, Rezai AR, Kopell BH, Gross RE, Sharan AD, Benabid AL. Deep brain stimulation for Parkinson's disease: surgical technique and perioperative management. Movement disorders: official journal of the Movement Disorder Society 2006; 21(S14): S247-S58.

MacKinnon CD, Webb RM, Silberstein P, Tisch S, Asselman P, Limousin P, *et al.* Stimulation through electrodes implanted near the subthalamic nucleus activates projections to motor areas of cerebral cortex in patients with Parkinson's disease. Eur J Neurosci 2005; 21(5): 1394-402.

Macleod AD, Grieve JW, Counsell CE. A systematic review of loss of independence in Parkinson's disease. J Neurol 2016; 263(1): 1-10.

Mahlknecht P, Akram H, Georgiev D, Tripoliti E, Candelario J, Zacharia A, *et al.* Pyramidal tract activation due to subthalamic deep brain stimulation in Parkinson's disease. Movement Disorders 2017; 32(8): 1174-82.

Mallet L, Schüpbach M, N'Diaye K, Remy P, Bardinet E, Czernecki V, *et al.* Stimulation of subterritories of the subthalamic nucleus reveals its role in the integration of the emotional and motor aspects of behavior. Proceedings of the National Academy of Sciences 2007; 104(25): 10661-6.

Mallet N, Pogosyan A, Sharott A, Csicsvari J, Bolam JP, Brown P, *et al.* Disrupted dopamine transmission and the emergence of exaggerated beta oscillations in subthalamic nucleus and cerebral cortex. Journal of Neuroscience 2008; 28(18): 4795-806.

Maltête D, Derrey S, Chastan N, Debono B, Gérardin E, Fréger P, *et al.* Microsubthalamotomy: an immediate predictor of long-term subthalamic stimulation efficacy in Parkinson disease. Movement disorders: official journal of the Movement Disorder Society 2008; 23(7): 1047-50.

Manson AJ, Turner K, Lees AJ. Apomorphine monotherapy in the treatment of refractory motor complications of Parkinson's disease: Long-term follow-up study of 64 patients. Movement Disorders 2002; 17(6): 1235-41.

Marceglia S, Foffani G, Bianchi A, Baselli G, Tamma F, Egidi M, *et al.* Dopamine-dependent non-linear correlation between subthalamic rhythms in Parkinson's disease. The Journal of physiology 2006; 571(3): 579-91.

Markesbery WR, Jicha GA, Liu H, Schmitt FA. Lewy body pathology in normal elderly subjects. Journal of Neuropathology & Experimental Neurology 2009; 68(7): 816-22.

Marmor O, Valsky D, Joshua M, Bick AS, Arkadir D, Tamir I, *et al.* Local vs. volume conductance activity of field potentials in the human subthalamic nucleus. Journal of Neurophysiology 2017; 117(6): 2140-51.

Marras C, McDermott M, Rochon P, Tanner C, Naglie G, Rudolph A, *et al.* Survival in Parkinson disease Thirteen-year follow-up of the DATATOP cohort. Neurology 2005; 64(1): 87-93.

Marras C, Rochon P, Lang AE. Predicting motor decline and disability in Parkinson disease: a systematic review. Archives of neurology 2002; 59(11): 1724-8.

Martinez-Martin P, Reddy P, Katzenschlager R, Antonini A, Todorova A, Odin P, *et al.* EuroInf: a multicenter comparative observational study of apomorphine and levodopa infusion in Parkinson's disease. Mov Disord 2015; 30(4): 510-6.

Matsumoto K, Shichijo F, Fukami T. Long-term follow-up review of cases of Parkinson's disease after unilateral or bilateral thalamotomy. Journal of neurosurgery 1984; 60(5): 1033-44.

Matsumura M, Kojima J, Gardiner TW, Hikosaka O. Visual and oculomotor functions of monkey subthalamic nucleus. Journal of Neurophysiology 1992; 67(6): 1615-32.

Maurice N, Deniau J-M, Glowinski J, Thierry A-M. Relationships between the prefrontal cortex and the basal ganglia in the rat: physiology of the corticosubthalamic circuits. Journal of Neuroscience 1998; 18(22): 9539-46.

Mayberg HS, Lozano AM, Voon V, McNeely HE, Seminowicz D, Hamani C, *et al.* Deep brain stimulation for treatment-resistant depression. Neuron 2005; 45(5): 651-60.

Mazzoni P, Hristova A, Krakauer JW. Why don't we move faster? Parkinson's disease, movement vigor, and implicit motivation. Journal of neuroscience 2007; 27(27): 7105-16.

McCulloch CE, Neuhaus JM. Generalized linear mixed models. Encyclopedia of biostatistics 2005; 4.

McIntyre CC, Hahn PJ. Network perspectives on the mechanisms of deep brain stimulation. Neurobiol Dis 2010; 38(3): 329-37.

McIntyre CC, Mori S, Sherman DL, Thakor NV, Vitek JL. Electric field and stimulating influence generated by deep brain stimulation of the subthalamic nucleus. Clinical neurophysiology 2004; 115(3): 589-95.

McNeill A, Duran R, Hughes DA, Mehta A, Schapira AH. A clinical and family history study of Parkinson's disease in heterozygous glucocerebrosidase mutation carriers. J Neurol Neurosurg Psychiatry 2012; 83(8): 853-4.

Medtronic. Percept™ PC Neurostimulator. 2020 [cited 10-7-2020]; Available from: https://www.medtronic.com/us-en/healthcare-professionals/products/neurological/deep-brain-stimulation-systems/percept-pc.html

Mehanna R, Machado AG, Connett JE, Alsaloum F, Cooper SE. Intraoperative microstimulation predicts outcome of postoperative macrostimulation in subthalamic nucleus deep brain stimulation for Parkinson's disease. Neuromodulation: Technology at the Neural Interface 2017; 20(5): 456-63.

Meidahl AC, Moll CK, van Wijk BC, Gulberti A, Tinkhauser G, Westphal M, *et al.* Synchronised spiking activity underlies phase amplitude coupling in the subthalamic nucleus of Parkinson's disease patients. Neurobiology of disease 2019; 127: 101-13.

Meidahl AC, Tinkhauser G, Herz DM, Cagnan H, Debarros J, Brown P. Adaptive Deep Brain Stimulation for Movement Disorders: The Long Road to Clinical Therapy. Movement Disorders 2017; 32(6): 810-9.

Mestre TA, Lang AE, Okun MS. Factors influencing the outcome of deep brain stimulation: Placebo, nocebo, lessebo, and lesion effects. Movement Disorders 2016; 31(3): 290-8.

Metman LV, Del Dotto P, Van Den Munckhof P, Fang J, Mouradian M, Chase T. Amantadine as treatment for dyskinesias and motor fluctuations in Parkinson's disease. Neurology 1998; 50(5): 1323-6.

Miettinen J, Rantanen M, Seppa K. Package 'popEpi'. Google Scholar; 2016.

Miller WC, DeLong MR. Altered tonic activity of neurons in the globus pallidus and subthalamic nucleus in the primate MPTP model of parkinsonism. The basal ganglia II: Springer; 1987. p. 415-27.

Millman KJ, Aivazis M. Python for Scientists and Engineers. Computing in Science & Engineering 2011; 13(2): 9-12.

Montgomery Jr EB. Microelectrode targeting of the subthalamic nucleus for deep brain stimulation surgery. Movement Disorders 2012; 27(11): 1387-91.

Montgomery Jr EB, Gale JT, Huang H. Methods for isolating extracellular action potentials and removing stimulus artifacts from microelectrode recordings of neurons requiring minimal operator intervention. Journal of neuroscience methods 2005; 144(1): 107-25.

Moro E, Esselink R, Xie J, Hommel M, Benabid A, Pollak P. The impact on Parkinson's disease of electrical parameter settings in STN stimulation. Neurology 2002; 59(5): 706-13.

Moro E, Poon Y-YW, Lozano AM, Saint-Cyr JA, Lang AE. Subthalamic nucleus stimulation: improvements in outcome with reprogramming. Archives of neurology 2006; 63(9): 1266-72.

MSAC. Deep brain stimulation for symptoms of Parkinson's disease: Medical Services Advisory Committee, Commonwealth of Australia; 2006.

Mulroy E, Robertson N, Macdonald L, Bok A, Simpson M. Patients' Perioperative Experience of Awake Deep-Brain Stimulation for Parkinson Disease. World Neurosurgery 2017; 105: 526-8.

Murthy VN, Fetz EE. Coherent 25-to 35-Hz oscillations in the sensorimotor cortex of awake behaving monkeys. Proceedings of the National Academy of Sciences 1992; 89(12): 5670-4.

Nakamura K, Christine CW, Starr PA, Marks Jr WJ. Effects of unilateral subthalamic and pallidal deep brain stimulation on fine motor functions in Parkinson's disease. Movement disorders 2007; 22(5): 619-26.

Nestor KA, Jones JD, Butson CR, Morishita T, Jacobson IV CE, Peace DA, *et al.* Coordinate-based lead location does not predict Parkinson's disease deep brain stimulation outcome. PloS one 2014; 9(4): e93524.

Neumann J, Bras J, Deas E, O'sullivan SS, Parkkinen L, Lachmann RH, *et al.* Glucocerebrosidase mutations in clinical and pathologically proven Parkinson's disease. Brain : a journal of neurology 2009; 132(7): 1783-94.

Neumann W-J, Turner RS, Blankertz B, Mitchell T, Kühn AA, Richardson RM. Toward electrophysiology-based intelligent adaptive deep brain stimulation for movement disorders. Neurotherapeutics 2019; 16(1): 105-18.

Neumann WJ, Degen K, Schneider GH, Brucke C, Huebl J, Brown P, *et al.* Subthalamic synchronized oscillatory activity correlates with motor impairment in patients with Parkinson's disease. Movement Disorders 2016a; 31(11): 1748-51.

Neumann WJ, Staub F, Horn A, Schanda J, Mueller J, Schneider GH, *et al.* Deep brain recordings using an implanted pulse generator in Parkinson's disease. Neuromodulation: Technology at the Neural Interface 2016b; 19(1): 20-4.

Ngoga D, Mitchell R, Kausar J, Hodson J, Harries A, Pall H. Deep brain stimulation improves survival in severe Parkinson's disease. Journal of Neurology, Neurosurgery & Psychiatry 2014; 85(1): 17-22.

Nini A, Feingold A, Slovin H, Bergman H. Neurons in the globus pallidus do not show correlated activity in the normal monkey, but phase-locked oscillations appear in the MPTP model of parkinsonism. Journal of neurophysiology 1995; 74(4): 1800-5.

Nussbaum RL, Ellis CE. Alzheimer's disease and Parkinson's disease. New England Journal of Medicine 2003; 348(14): 1356-64.

Nutt JG, Wooten GF. Diagnosis and Initial Management of Parkinson's Disease. New England Journal of Medicine 2005; 353(10): 1021-7.

O'Sullivan SS, Evans AH, Lees AJ. Dopamine dysregulation syndrome. CNS drugs 2009; 23(2): 157-70.

Obeso J, Rodriguez-Oroz M, Marin C, Alonso F, Zamarbide I, Lanciego J, *et al.* The origin of motor fluctuations in Parkinson's disease Importance of dopaminergic innervation and basal ganglia circuits. Neurology 2004; 62(1 suppl 1): S17-S30.

Obeso JA, Rodriguez-Oroz MC, Goetz CG, Marin C, Kordower JH, Rodriguez M, *et al.* Missing pieces in the Parkinson's disease puzzle. Nature medicine 2010; 16(6): 653.

Obeso JA, Rodriguez-Oroz MC, Rodriguez M, Lanciego JL, Artieda J, Gonzalo N, *et al.* Pathophysiology of the basal ganglia in Parkinson's disease. Trends in neurosciences 2000; 23: S8-S19.

Odekerken VJ, Boel JA, Geurtsen GJ, Schmand BA, Dekker I, de Haan RJ, *et al.* Neuropsychological outcome after deep brain stimulation for Parkinson disease. Neurology 2015; 84(13): 1355-61.

Odekerken VJ, Boel JA, Schmand BA, de Haan RJ, Figee M, van den Munckhof P, *et al.* GPi vs STN deep brain stimulation for Parkinson disease Three-year follow-up. Neurology 2016; 86(8): 755-61.

Odekerken VJ, van Laar T, Staal MJ, Mosch A, Hoffmann CF, Nijssen PC, *et al.* Subthalamic nucleus versus globus pallidus bilateral deep brain stimulation for advanced Parkinson's disease (NSTAPS study): a randomised controlled trial. The Lancet Neurology 2013; 12(1): 37-44.

Odin P, Ray Chaudhuri K, Slevin JT, Volkmann J, Dietrichs E, Martinez-Martin P, *et al.* Collective physician perspectives on non-oral medication approaches for the management of clinically relevant unresolved issues in Parkinson's disease: Consensus from an international survey and discussion program. Parkinsonism Relat Disord 2015; 21(10): 1133-44.

Oh MY, Abosch A, Kim SH, Lang AE, Lozano AM. Long-term hardware-related complications of deep brain stimulation. Neurosurgery 2002; 50(6): 1268-76.

Okun MS. Deep-brain stimulation for Parkinson's disease. New England Journal of Medicine 2012; 367(16): 1529-38.

Okun MS, Fernandez HH, Wu SS, Kirsch-Darrow L, Bowers D, Bova F, *et al.* Cognition and mood in Parkinson's disease in subthalamic nucleus versus globus pallidus interna deep brain stimulation: the COMPARE trial. Annals of neurology 2009; 65(5): 586-95.

Okun MS, Tagliati M, Pourfar M, et al. Management of referred deep brain stimulation failures: A retrospective analysis from 2 movement disorders centers. Archives of Neurology 2005; 62(8): 1250-5.

Olanow CW, Kieburtz K, Odin P, Espay AJ, Standaert DG, Fernandez HH, *et al.* Continuous intrajejunal infusion of levodopa-carbidopa intestinal gel for patients with advanced Parkinson's disease: a randomised, controlled, double-blind, double-dummy study. The Lancet Neurology 2014; 13(2): 141-9.

Ondo W, Jankovic J, Schwartz K, Almaguer M, Simpson RK. Unilateral thalamic deep brain stimulation for refractory essential tremor and Parkinson's disease tremor. Neurology 1998; 51(4): 1063-9.

Ondo WG, Meilak C, Vuong KD. Predictors of battery life for the Activa® Soletra 7426 Neurostimulator. Parkinsonism & related disorders 2007; 13(4): 240-2.

Orimo S, Uchihara T, Nakamura A, Mori F, Kakita A, Wakabayashi K, *et al.* Axonal α-synuclein aggregates herald centripetal degeneration of cardiac sympathetic nerve in Parkinson's disease. Brain : a journal of neurology 2007; 131(3): 642-50.

Oswal A, Beudel M, Zrinzo L, Limousin P, Hariz M, Foltynie T, *et al.* Deep brain stimulation modulates synchrony within spatially and spectrally distinct resting state networks in Parkinson's disease. Brain : a journal of neurology 2016; 139(5): 1482-96.

Oyama G, Foote KD, Jacobson CE, Velez-Lago F, Go C, Limotai N, *et al.* GPi and STN deep brain stimulation can suppress dyskinesia in Parkinson's disease. Parkinsonism & related disorders 2012; 18(7): 814-8.

Özkurt TE, Butz M, Homburger M, Elben S, Vesper J, Wojtecki L, *et al.* High frequency oscillations in the subthalamic nucleus: a neurophysiological marker of the motor state in Parkinson's disease. Experimental neurology 2011; 229(2): 324-31.

Ozturk M, Kaku H, Jimenez-Shahed J, Viswanathan A, Sheth SA, Kumar S, *et al.* Subthalamic Single Cell and Oscillatory Neural Dynamics of a Dyskinetic Medicated Patient With Parkinson's Disease. Frontiers in Neuroscience 2020; 14(391).

Pahwa R, Factor S, Lyons K, Ondo W, Gronseth G, Bronte-Stewart H, *et al.* Practice Parameter: Treatment of Parkinson disease with motor fluctuations and dyskinesia (an evidence-based review) Report of the Quality Standards Subcommittee of the American Academy of Neurology. Neurology 2006; 66(7): 983-95.

Park J-S, Davis RL, Sue CM. Mitochondrial Dysfunction in Parkinson's Disease: New Mechanistic Insights and Therapeutic Perspectives. Current Neurology and Neuroscience Reports 2018; 18(5): 21.

Parkinson J. An essay on the shaking palsy. 1817. The Journal of neuropsychiatry and clinical neurosciences 2002; 14(2): 223-36; discussion 2.

Patel DM, Walker HC, Brooks R, Omar N, Ditty B, Guthrie BL. Adverse Events Associated With Deep Brain Stimulation for Movement DisordersAnalysis of 510 Consecutive Cases. Operative Neurosurgery 2015; 11(1): 190-9.

Pedregosa F, Varoquaux G, Gramfort A, Michel V, Thirion B, Grisel O, *et al.* Scikit-learn: Machine learning in Python. the Journal of machine Learning research 2011; 12: 2825-30.

Pepper J, Zrinzo L, Mirza B, Foltynie T, Limousin P, Hariz M. The risk of hardware infection in deep brain stimulation surgery is greater at impulse generator replacement than at the primary procedure. Stereotactic and functional neurosurgery 2013; 91(1): 56-65.

Petersen MV, Husch A, Parsons CE, Lund TE, Sunde N, Østergaard K. Using automated electrode localization to guide stimulation management in DBS. Annals of Clinical and Translational Neurology 2018; 5(7): 888-94.

Picillo M, Lozano AM, Kou N, Munhoz RP, Fasano A. Programming deep brain stimulation for Parkinson's disease: the Toronto western hospital algorithms. Brain stimulation 2016; 9(3): 425-37.

Pietz K, Hagell P, Odin P. Subcutaneous apomorphine in late stage Parkinson's disease: a long term follow up. Journal of Neurology, Neurosurgery & Psychiatry 1998; 65(5): 709-16.

Politis M. Neuroimaging in Parkinson disease: from research setting to clinical practice. Nature Reviews Neurology 2014; 10(12): 708-22.

Pollo C, Kaelin-Lang A, Oertel MF, Stieglitz L, Taub E, Fuhr P, *et al.* Directional deep brain stimulation: an intraoperative double-blind pilot study. Brain : a journal of neurology 2014: awu102.

Polymeropoulos MH, Lavedan C, Leroy E, Ide SE, Dehejia A, Dutra A, *et al.* Mutation in the α-synuclein gene identified in families with Parkinson's disease. Science (New York, NY) 1997; 276(5321): 2045-7.

Poortvliet P, Silburn PA, Coyne T, Chenery H. Deep brain stimulation for Parkinson disease in Australia: current scientific and clinical status. Internal medicine journal 2015; 45(2): 134-9.

Postuma RB, Aarsland D, Barone P, Burn DJ, Hawkes CH, Oertel W, *et al.* Identifying prodromal Parkinson's disease: pre-motor disorders in Parkinson's disease. Movement Disorders 2012a; 27(5): 617-26.

Postuma RB, Lang AE, Munhoz RP, Charland K, Pelletier A, Moscovich M, *et al.* Caffeine for treatment of Parkinson disease: a randomized controlled trial. Neurology 2012b; 79(7): 651-8.

Priori A, Foffani G, Pesenti A, Tamma F, Bianchi A, Pellegrini M, *et al.* Rhythm-specific pharmacological modulation of subthalamic activity in Parkinson's disease. Experimental neurology 2004; 189(2): 369-79.

Priori A, Foffani G, Rossi L, Marceglia S. Adaptive deep brain stimulation (aDBS) controlled by local field potential oscillations. Experimental neurology 2013; 245: 77-86.

Quik M. Smoking, nicotine and Parkinson's disease. Trends in neurosciences 2004; 27(9): 561-8.

Quinn EJ, Blumenfeld Z, Velisar A, Koop MM, Shreve LA, Trager MH, *et al.* Beta oscillations in freely moving Parkinson's subjects are attenuated during deep brain stimulation. Movement Disorders 2015; 30(13): 1750-8.

R Development Core Team. R: A language and environment for statistical computing. . Vienna, Austria: R Foundation for Statistical Computing; 2017.

Rajput A, Voll A, Rajput M, Robinson C, Rajput A. Course in Parkinson disease subtypes: a 39-year clinicopathologic study. Neurology 2009; 73(3): 206-12.

Ramirez-Zamora A, Giordano J, Gunduz A, Alcantara J, Cagle JN, Cernera S, *et al.* Proceedings of the Seventh Annual Deep Brain Stimulation Think Tank: Advances in

Neurophysiology, Adaptive DBS, Virtual Reality, Neuroethics and Technology. Frontiers in Human Neuroscience 2020; 14: 54.

Ramirez-Zamora A, Kahn M, Campbell J, DeLaCruz P, Pilitsis JG. Interleaved programming of subthalamic deep brain stimulation to avoid adverse effects and preserve motor benefit in Parkinson's disease. Journal of neurology 2015; 262(3): 578-84.

Rascol O, Goetz C, Koller W, Poewe W, Sampaio C. Treatment interventions for Parkinson's disease: an evidence based assessment. The Lancet 2002; 359(9317): 1589-98.

Ray NJ, Jenkinson N, Wang S, Holland P, Brittain JS, Joint C, *et al.* Local field potential beta activity in the subthalamic nucleus of patients with Parkinson's disease is associated with improvements in bradykinesia after dopamine and deep brain stimulation. Experimental Neurology 2008; 213(1): 108-13.

Reed R. Models of general practitioner services in residential aged care facilities. Australian Family Physician 2015; 44: 176-9.

Richter EO, Hoque T, Halliday W, Lozano AM, Saint-Cyr JA. Determining the position and size of the subthalamic nucleus based on magnetic resonance imaging results in patients with advanced Parkinson disease. Journal of neurosurgery 2004; 100(3): 541-6.

Rizzone MG, Fasano A, Daniele A, Zibetti M, Merola A, Rizzi L, *et al.* Long-term outcome of subthalamic nucleus DBS in Parkinson's disease: from the advanced phase towards the late stage of the disease? Parkinsonism & related disorders 2014; 20(4): 376-81.

Rocha S, Monteiro A, Linhares P, Chamadoira C, Basto MA, Reis C, *et al.* Long-term mortality analysis in Parkinson's disease treated with deep brain stimulation. Parkinson's Disease 2014; 2014.

Rolston JD, Englot DJ, Starr PA, Larson PS. An unexpectedly high rate of revisions and removals in deep brain stimulation surgery: Analysis of multiple databases. Parkinsonism Relat Disord 2016; 33: 72-7.

Rosa M, Arlotti M, Ardolino G, Cogiamanian F, Marceglia S, Di Fonzo A, *et al.* Adaptive deep brain stimulation in a freely moving Parkinsonian patient. Movement Disorders 2015; 30(7): 1003-5.

Rosa M, Arlotti M, Marceglia S, Cogiamanian F, Ardolino G, Di Fonzo A, *et al.* Adaptive deep brain stimulation controls levodopa-induced side effects in Parkinsonian patients. Movement Disorders 2017; 32(4): 628.

Schapira AH, Jenner P. Etiology and pathogenesis of Parkinson's disease. Movement Disorders 2011; 26(6): 1049-55.

Schenkman M, Moore CG, Kohrt WM, Hall DA, Delitto A, Comella CL, *et al.* Effect of high-intensity treadmill exercise on motor symptoms in patients with de novo Parkinson disease: a phase 2 randomized clinical trial. JAMA neurology 2018; 75(2): 219-26.

Schrag A, Ben-Shlomo Y, Brown R, David Marsden C, Quinn N. Young-onset Parkinson's disease revisited—clinical features, natural history, and mortality. Movement disorders: official journal of the Movement Disorder Society 1998; 13(6): 885-94.

Schrag A, Quinn N. Dyskinesias and motor fluctuations in Parkinson's disease: A community-based study. Brain : a journal of neurology 2000; 123(11): 2297-305.

Schuepbach WM, Rau J, Knudsen K, Volkmann J, Krack P, Timmermann L, *et al.* Neurostimulation for Parkinson's disease with early motor complications. New England Journal of Medicine 2013; 368(7): 610-22.

Schüpbach M, Chabardes S, Matthies C, Pollo C, Steigerwald F, Timmermann L, *et al.* Directional leads for deep brain stimulation: Opportunities and challenges. Movement Disorders 2017; 32(10): 1371-5.

Schüpbach MWM, Welter ML, Bonnet AM, Elbaz A, Grossardt BR, Mesnage V, *et al.* Mortality in patients with Parkinson's disease treated by stimulation of the subthalamic nucleus. Movement Disorders 2007; 22(2): 257-61.

Selikhova M, Williams D, Kempster P, Holton J, Revesz T, Lees A. A clinico-pathological study of subtypes in Parkinson's disease. Brain : a journal of neurology 2009; 132(11): 2947-57.

Sem-Jacobsen C. Depth-electrographic observations related to Parkinson's disease. Recording and electrical stimulation in the area around the third ventricle. Journal of neurosurgery 1966; 24(1): Suppl: 388-402.

Sharma M, Ambekar S, Guthikonda B, Wilden J, Nanda A. Regional trends and the impact of various patient and hospital factors on outcomes and costs of hospitalization between academic and nonacademic centers after deep brain stimulation surgery for Parkinson's disease: a United States Nationwide Inpatient Sample analysis from 2006 to 2010. Neurosurgical focus 2013; 35(5): E2.

Shinall MC, Jr, Arya S, Youk A, Varley P, Shah R, Massarweh NN, *et al.* Association of Preoperative Patient Frailty and Operative Stress With Postoperative Mortality. JAMA Surgery 2020; 155(1): e194620-e.

Sidransky E, Nalls MA, Aasly JO, Aharon-Peretz J, Annesi G, Barbosa ER, *et al.* Multicenter analysis of glucocerebrosidase mutations in Parkinson's disease. New England Journal of Medicine 2009; 361(17): 1651-61.

Silberstein P, Pogosyan A, Kühn AA, Hotton G, Tisch S, Kupsch A, *et al.* Cortico-cortical coupling in Parkinson's disease and its modulation by therapy. Brain : a journal of neurology 2005; 128(6): 1277-91.

Sillay KA, Larson PS, Starr PA. Deep brain stimulator hardware-related infections: incidence and management in a large series. Neurosurgery 2008; 62(2): 360-7.

Sinclair NC, Fallon JB, Bulluss KJ, Thevathasan W, McDermott HJ. On the neural basis of deep brain stimulation evoked resonant activity. Biomedical Physics & Engineering Express 2019a.

Sinclair NC, McDermott HJ, Bulluss KJ, Fallon JB, Perera T, Xu SS, *et al.* Subthalamic nucleus deep brain stimulation evokes resonant neural activity. Annals of neurology 2018; 83(5).

Sinclair NC, McDermott HJ, Fallon JB, Perera T, Brown P, Bulluss KJ, *et al.* Deep brain stimulation for Parkinson's disease modulates high-frequency evoked and spontaneous neural activity. Neurobiology of Disease 2019b: 104522.

Singleton AB, Farrer MJ, Bonifati V. The genetics of Parkinson's disease: progress and therapeutic implications. Movement Disorders 2013; 28(1): 14-23.

Sitz A, Hoevels M, Hellerbach A, Gierich A, Luyken K, Dembek TA, *et al.* Determining the orientation angle of directional leads for deep brain stimulation using computed tomography and digital x-ray imaging: A phantom study. Medical physics 2017; 44(9): 4463-73.

Slater KD, Sinclair NC, Nelson TS, Blamey PJ, Mcdermott HJ. neuroBi: a highly configurable neurostimulator for a retinal prosthesis and other applications. IEEE journal of translational engineering in health and medicine 2015; 3: 1-11.

Soares J, Kliem MA, Betarbet R, Greenamyre JT, Yamamoto B, Wichmann T. Role of external pallidal segment in primate parkinsonism: comparison of the effects of 1-methyl-4-phenyl-1, 2, 3, 6-tetrahydropyridine-induced parkinsonism and lesions of the external pallidal segment. Journal of Neuroscience 2004; 24(29): 6417-26.

Spieles-Engemann A, Behbehani M, Collier T, Wohlgenant S, Steece-Collier K, Paumier K, *et al.* Stimulation of the rat subthalamic nucleus is neuroprotective following significant nigral dopamine neuron loss. Neurobiology of disease 2010; 39(1): 105-15.

Spillantini MG, Schmidt ML, Lee VM-Y, Trojanowski JQ, Jakes R, Goedert M. α-Synuclein in Lewy bodies. Nature 1997; 388(6645): 839.

Starr PA. Placement of deep brain stimulators into the subthalamic nucleus or globus pallidus internus: technical approach. Stereotactic and functional neurosurgery 2002; 79(3-4): 118-45.

Steiner LA, Neumann WJ, Staub-Bartelt F, Herz DM, Tan H, Pogosyan A, *et al.* Subthalamic beta dynamics mirror Parkinsonian bradykinesia months after neurostimulator implantation. Movement Disorders 2017; 32(8): 1183-90.

Stroupe KT, Smith B, Weaver FM, Gonzalez B, Huo Z, Cao L, *et al.* Healthcare Utilization and Costs for Patients With Parkinson's Disease After Deep Brain Stimulation. Movement Disorders Clinical Practice 2019; 6(5): 369-78.

Suchowersky O, Reich S, Perlmutter J, Zesiewicz T, Gronseth G, Weiner WJ. Practice Parameter: diagnosis and prognosis of new onset Parkinson disease (an evidence-based review): report of the Quality Standards Subcommittee of the American Academy of Neurology. Neurology 2006; 66(7): 968-75.

Surmeier DJ, Guzman JN, Sanchez-Padilla J. Calcium, cellular aging, and selective neuronal vulnerability in Parkinson's disease. Cell calcium 2010; 47(2): 175-82.

Tabbal SD, Ushe M, Mink JW, Revilla FJ, Wernle AR, Hong M, *et al.* Unilateral subthalamic nucleus stimulation has a measurable ipsilateral effect on rigidity and bradykinesia in Parkinson disease. Experimental neurology 2008; 211(1): 234-42.

Tamir I, Wang D, Chen W, Ostrem JL, Starr PA, de Hemptinne C. Eight cylindrical contact lead recordings in the subthalamic region localize beta oscillations source to the dorsal STN. Neurobiology of Disease 2020; 146: 105090.

Tanner CM, Kamel F, Ross GW, Hoppin JA, Goldman SM, Korell M, *et al.* Rotenone, paraquat, and Parkinson’s disease. Environmental health perspectives 2011; 119(6): 866-72.

Telkes I, Jimenez-Shahed J, Viswanathan A, Abosch A, Ince NF. Prediction of STN-DBS electrode implantation track in Parkinson's disease by using local field potentials. Frontiers in neuroscience 2016; 10: 198.

Telkes I, Sabourin S, Durphy J, Adam O, Sukul V, Raviv N, *et al.* Functional Use of Directional Local Field Potentials in the Subthalamic Nucleus Deep Brain Stimulation. Frontiers in human neuroscience 2020; 14: 145.

Temperli P, Ghika J, Villemure JG, Burkhard PR, Bogousslavsky J, Vingerhoets FJ. How do parkinsonian signs return after discontinuation of subthalamic DBS? Neurology 2003; 60(1): 78-81.

Thompson JA, Lanctin D, Ince NF, Abosch A. Clinical implications of local field potentials for understanding and treating movement disorders. Stereotactic and functional neurosurgery 2014; 92(4): 251-63.

Thrane JF, Sunde NA, Bergholt B, Rosendal F. Increasing infection rate in multiple implanted pulse generator changes in movement disorder patients treated with deep brain stimulation. Stereotactic and functional neurosurgery 2014; 92(6): 360-4.

Timmermann L, Jain R, Chen L, Maarouf M, Barbe MT, Allert N, *et al.* Multiple-source current steering in subthalamic nucleus deep brain stimulation for Parkinson's disease (the VANTAGE study): a non-randomised, prospective, multicentre, open-label study. The Lancet Neurology 2015; 14(7): 693-701.

Tinkhauser G, Pogosyan A, Debove I, Nowacki A, Shah SA, Seidel K, *et al.* Directional local field potentials: A tool to optimize deep brain stimulation. Movement Disorders 2018; 33(1): 159-64.

Tinkhauser G, Pogosyan A, Little S, Beudel M, Herz DM, Tan H, *et al.* The modulatory effect of adaptive deep brain stimulation on beta bursts in Parkinson's disease. Brain : a journal of neurology 2017a.

Tinkhauser G, Pogosyan A, Tan H, Herz DM, Kühn AA, Brown P. Beta burst dynamics in Parkinson’s disease OFF and ON dopaminergic medication. Brain : a journal of neurology 2017b; 140(11): 2968-81.

Tinkhauser G, Shah AS, Fischer P, Peterman K, Debove I, Nygyuen K, *et al.* Electrophysiological differences between Upper and Lower Limb movements in the human subthalamic nucleus. Clinical Neurophysiology 2019.

Tisch S, Rothwell JC, Zrinzo L, Bhatia KP, Hariz M, Limousin P. Cortical evoked potentials from pallidal stimulation in patients with primary generalized dystonia. Movement Disorders 2008; 23(2): 265-73.

Tolleson C, Stroh J, Ehrenfeld J, Neimat J, Konrad P, Phibbs F. The factors involved in deep brain stimulation infection: a large case series. Stereotactic and functional neurosurgery 2014; 92(4): 227-33.

Tomlinson CL, Stowe R, Patel S, Rick C, Gray R, Clarke CE. Systematic review of levodopa dose equivalency reporting in Parkinson's disease. Mov Disord 2010; 25(15): 2649-53.

Torrecillos F, Tinkhauser G, Fischer P, Green AL, Aziz TZ, Foltynie T, *et al.* Modulation of beta bursts in the subthalamic nucleus predicts motor performance. Journal of Neuroscience 2018: 1314-18.

Trager MH, Koop MM, Velisar A, Blumenfeld Z, Nikolau JS, Quinn EJ, *et al.* Subthalamic beta oscillations are attenuated after withdrawal of chronic high frequency neurostimulation in Parkinson's disease. Neurobiology of Disease 2016; 96: 22-30.

Tripoliti E, Zrinzo L, Martinez-Torres I, Tisch S, Frost E, Borrell E, *et al.* Effects of contact location and voltage amplitude on speech and movement in bilateral subthalamic nucleus deep brain stimulation. Movement Disorders 2008; 23(16): 2377-83.

Umemura A, Jaggi J, Hurtig H, Siderowf A, Colcher A, Stern M, *et al.* Deep brain stimulation for movement disorders: morbidity and mortality in 109 patients. Journal of neurosurgery 2003; 98(4): 779-84.

Ungerstedt U, Ljungberg T, Steg G. Behavioral, physiological, and neurochemical changes after 6-hydroxydopamine-induced degeneration of the nigro-striatal dopamine neurons. Advances in neurology 1973; 5: 421-6.

Vabalas A, Gowen E, Poliakoff E, Casson AJ. Machine learning algorithm validation with a limited sample size. PloS one 2019; 14(11): e0224365.

Valente EM, Abou-Sleiman PM, Caputo V, Muqit MM, Harvey K, Gispert S, *et al.* Hereditary early-onset Parkinson's disease caused by mutations in PINK1. Science (New York, NY) 2004; 304(5674): 1158-60.

van der Kolk NM, de Vries NM, Kessels RP, Joosten H, Zwinderman AH, Post B, *et al.* Effectiveness of home-based and remotely supervised aerobic exercise in Parkinson's disease: a double-blind, randomised controlled trial. The Lancet Neurology 2019; 18(11): 998-1008.

van Wijk BC, Beudel M, Jha A, Oswal A, Foltynie T, Hariz MI, *et al.* Subthalamic nucleus phase–amplitude coupling correlates with motor impairment in Parkinson's disease. Clinical Neurophysiology 2016; 127(4): 2010-9.

van Wijk BCM, Pogosyan A, Hariz MI, Akram H, Foltynie T, Limousin P, *et al.* Localization of beta and high-frequency oscillations within the subthalamic nucleus region. NeuroImage Clinical 2017; 16: 175-83.

Vanegas-Arroyave N, Lauro PM, Huang L, Hallett M, Horovitz SG, Zaghloul KA, *et al.* Tractography patterns of subthalamic nucleus deep brain stimulation. Brain : a journal of neurology 2016; 139(4): 1200-10.

Vergani F, Landi A, Pirillo D, Cilia R, Antonini A, Sganzerla EP. Surgical, medical, and hardware adverse events in a series of 141 patients undergoing subthalamic deep brain stimulation for Parkinson disease. World Neurosurgery 2010; 73(4): 338-44.

Vidailhet M, Vercueil L, Houeto J-L, Krystkowiak P, Benabid A-L, Cornu P, *et al.* Bilateral Deep-Brain Stimulation of the Globus Pallidus in Primary Generalized Dystonia. New England Journal of Medicine 2005; 352(5): 459-67.

Videnovic A, Metman LV. Deep brain stimulation for Parkinson's disease: Prevalence of adverse events and need for standardized reporting. Movement Disorders 2008; 23(3): 343-9.

Vitek JL, Jain R, Chen L, Tröster AI, Schrock LE, House PA, *et al.* Subthalamic nucleus deep brain stimulation with a multiple independent constant current-controlled device in Parkinson's disease (INTREPID): a multicentre, double-blind, randomised, sham-controlled study. The Lancet Neurology 2020; 19(6): 491-501.

Voges J, Waerzeggers Y, Maarouf M, Lehrke R, Koulousakis A, Lenartz D, *et al.* Deep-brain stimulation: long-term analysis of complications caused by hardware and surgery—experiences from a single centre. Journal of Neurology, Neurosurgery & Psychiatry 2006; 77(7): 868-72.

Volkmann J, Albanese A, Antonini A, Chaudhuri KR, Clarke CE, De Bie RM, *et al.* Selecting deep brain stimulation or infusion therapies in advanced Parkinson's disease: an evidence-based review. Journal of neurology 2013; 260(11): 2701-14.

Volkmann J, Moro E, Pahwa R. Basic algorithms for the programming of deep brain stimulation in Parkinson's disease. Movement Disorders 2006; 21(S14).

Walker HC, Huang H, Gonzalez CL, Bryant JE, Killen J, Cutter GR, *et al.* Short latency activation of cortex during clinically effective subthalamic deep brain stimulation for Parkinson's disease. Movement Disorders 2012; 27(7): 864-73.

Wallace BA, Ashkan K, Heise CE, Foote KD, Torres N, Mitrofanis J, *et al.* Survival of midbrain dopaminergic cells after lesion or deep brain stimulation of the subthalamic nucleus in MPTP-treated monkeys. Brain : a journal of neurology 2007; 130(8): 2129-45.

Wang J, Hirschmann J, Elben S, Hartmann CJ, Vesper J, Wojtecki L, *et al.* High-frequency oscillations in Parkinson's disease: Spatial distribution and clinical relevance. Movement Disorders 2014; 29(10): 1265-72.

Weaver FM, Follett K, Stern M, Hur K, Harris C, Marks WJ, *et al.* Bilateral deep brain stimulation vs best medical therapy for patients with advanced Parkinson disease: a randomized controlled trial. Jama 2009; 301(1): 63-73.

Weaver FM, Stroupe KT, Smith B, Gonzalez B, Huo Z, Cao L, *et al.* Survival in patients with Parkinson's disease after deep brain stimulation or medical management. Movement Disorders 2017; 32(12): 1756-63.

Weinberger M, Mahant N, Hutchison WD, Lozano AM, Moro E, Hodaie M, *et al.* Beta oscillatory activity in the subthalamic nucleus and its relation to dopaminergic response in Parkinson's disease. Journal of neurophysiology 2006; 96(6): 3248-56.

Weintraub D, Koester J, Potenza MN, Siderowf AD, Stacy M, Voon V, *et al.* Impulse control disorders in Parkinson disease: a cross-sectional study of 3090 patients. Archives of neurology 2010; 67(5): 589-95.

Weintraub D, Siderowf AD, Potenza MN, Goveas J, Morales KH, Duda JE, *et al.* Association of dopamine agonist use with impulse control disorders in Parkinson disease. Archives of neurology 2006; 63(7): 969-73.

Weiss D, Massano J. Approaching adaptive control in neurostimulation for Parkinson disease: Autopilot on. Neurology 2018; 90(11): 497-8.

Wichmann T, Bergman H, DeLong M. The primate subthalamic nucleus. I. Functional properties in intact animals. Journal of neurophysiology 1994; 72(2): 494-506.

Williams A, Gill S, Varma T, Jenkinson C, Quinn N, Mitchell R, *et al.* Deep brain stimulation plus best medical therapy versus best medical therapy alone for advanced Parkinson's disease (PD SURG trial): a randomised, open-label trial. The Lancet Neurology 2010; 9(6): 581-91.

Xu SS, Sinclair NC, Bulluss K, Perera T, Lee W-L, McDermott H, *et al.* Towards guided and automated programming of subthalamic area stimulation in Parkinson's disease. Neuromodulation 2020; Under review.

Yang AI, Vanegas N, Lungu C, Zaghloul KA. Beta-coupled high-frequency activity and beta-locked neuronal spiking in the subthalamic nucleus of Parkinson's disease. Journal of Neuroscience 2014; 34(38): 12816-27.

Young DT. Medtronic Receives CE Mark Approval for the Percept™ PC Neurostimulator DBS System with BrainSense™ Technology. Dublin: Medtronic; 2020.

Zaidel A, Spivak A, Grieb B, Bergman H, Israel Z. Subthalamic span of β oscillations predicts deep brain stimulation efficacy for patients with Parkinson's disease. Brain : a journal of neurology 2010; 133(7): 2007-21.

Zibetti M, Merola A, Rizzi L, Ricchi V, Angrisano S, Azzaro C, *et al.* Beyond nine years of continuous subthalamic nucleus deep brain stimulation in Parkinson's disease. Movement Disorders 2011; 26(13): 2327-34.